PROBING THE MECHANISTIC SPECIFICITIES OF SIALIDASE-CATALYZED HYDROLYSIS REACTIONS

by

Jefferson Chan
B.Sc. University of British Columbia 2006

THESIS SUBMITTED IN PARTIAL FULFILLMENT OF
THE REQUIREMENTS FOR THE DEGREE OF

DOCTOR OF PHILOSOPHY

In the
Department of Chemistry

© Jefferson Chan 2011

SIMON FRASER UNIVERSITY

Spring 2011

All rights reserved. However, in accordance with the *Copyright Act of Canada*, this work may be reproduced, without authorization, under the conditions for *Fair Dealing*. Therefore, limited reproduction of this work for the purposes of private study, research, criticism, review and news reporting is likely to be in accordance with the law, particularly if cited appropriately.

APPROVAL

Name: Jefferson Chan

Degree: Doctor of Philosophy

Title of Thesis: Probing the Mechanistic Specificities of Sialidase-Catalyzed Hydrolysis Reactions

Examining Committee:

Chair: Dr. Corina Andreoiu
Assistant Professor, Department of Chemistry

_____

Dr. Andrew J. Bennet
Senior Supervisor
Professor, Department of Chemistry

_____

Dr. Charles J. Walsby
Supervisor
Associate Professor, Department of Chemistry

_____

Dr. Peter D. Wilson
Supervisor
Associate Professor, Department of Chemistry

_____

Dr. Tim Storr
Internal Examiner
Assistant Professor, Department of Chemistry

_____

Dr. Jeffrey W. Keillor
External Examiner
Professor, Department of Chemistry
University of Ottawa

Date Defended/Approved: April 11, 2011

SFU SIMON FRASER UNIVERSITY
LIBRARY

Declaration of
Partial Copyright Licence

The author, whose copyright is declared on the title page of this work, has granted to Simon Fraser University the right to lend this thesis, project or extended essay to users of the Simon Fraser University Library, and to make partial or single copies only for such users or in response to a request from the library of any other university, or other educational institution, on its own behalf or for one of its users.

The author has further granted permission to Simon Fraser University to keep or make a digital copy for use in its circulating collection (currently available to the public at the "Institutional Repository" link of the SFU Library website <www.lib.sfu.ca> at: <http://ir.lib.sfu.ca/handle/1892/112>) and, without changing the content, to translate the thesis/project or extended essays, if technically possible, to any medium or format for the purpose of preservation of the digital work.

The author has further agreed that permission for multiple copying of this work for scholarly purposes may be granted by either the author or the Dean of Graduate Studies.

It is understood that copying or publication of this work for financial gain shall not be allowed without the author's written permission.

Permission for public performance, or limited permission for private scholarly use, of any multimedia materials forming part of this work, may have been granted by the author. This information may be found on the separately catalogued multimedia material and in the signed Partial Copyright Licence.

While licensing SFU to permit the above uses, the author retains copyright in the thesis, project or extended essays, including the right to change the work for subsequent purposes, including editing and publishing the work in whole or in part, and licensing other parties, as the author may desire.

The original Partial Copyright Licence attesting to these terms, and signed by this author, may be found in the original bound copy of this work, retained in the Simon Fraser University Archive.

Simon Fraser University Library
Burnaby, BC, Canada

ABSTRACT

Sialic acids are a family of 9-carbon keto sugars found throughout nature. The most prevalent example is *N*-acetylneuraminic acid (Neu5Ac). This carbohydrate is commonly found capping the terminal ends of a variety of glycoconjugates and polysaccharides. The family of enzymes that catalyze the hydrolytic cleavage of Neu5Ac containing complexes are known as sialidases. Numerous studies have implicated the involvement of these enzymes in human diseases such as cancer, cholera and influenza. As such, sialidase inhibitors can function as tools to study these conditions or to serve as potential therapeutics.

Rational drug design has emerged as a powerful tool used to develop such compounds. This process involves acquiring a comprehensive mechanistic understanding of the target enzyme. Particularly interesting are features manifested at the enzymatic transition state (TS) which include the extent of bond-formation/cleavage, charge development and geometry. Since sialidases operate via a double displacement mechanism, both glycosylation and deglycosylation TSs must be considered to fully understand this family of enzymes. Thus, a major component and objective of this thesis work was to use established techniques such as enzyme kinetics, mutagenesis and the measurement and analysis of multiple kinetic isotope effects (KIEs) to unravel the mechanism for various sialidases. With regard to KIEs, a novel NMR-based technique was developed and employed to measure competitive enzymatic KIEs on the sialidase-catalyzed hydrolysis reactions.

DEDICATION

To my parents, grandmother, wife and dogs (Buffy and Rex).

I would not be who I am without your love, guidance and support.

ACKNOWLEDGEMENTS

I would like to begin by thanking my supervisor, Professor Andrew Bennet, for providing me with an exceptional learning environment. During my studies at SFU, Professor Bennet gave me numerous opportunities to attend national and international conferences. Without a doubt, these experiences have proven to be extremely important for my development. In addition, Professor Bennet is an amazing teacher, I have learnt more than I could have ever thought possible when I first began this journey. I feel very fortunate because I know I would not have come this far without Professor Bennet as a mentor and friend.

I would also like to extend my sincere thanks to my committee members, Professor Charles Walsby and Professor Peter Wilson for their help and constructive criticism throughout my graduate studies. I have always found the discussions during committee meetings to be very useful. I would also like to thank Professor David Vocadlo for giving me invaluable advice during my postdoctoral application process. Next, I would like to acknowledge and thank Dr. Andrew Lewis for teaching me how to operate the NMR spectrometer. I have gained a tremendous amount of respect for spectroscopy from our work. I also like to thank Professor Vern Schramm and Professor Margo Moore for kindly offering their labs, resources and valuable time to provide me with training in computational chemistry and molecular cloning techniques, respectively. Finally, I would like to acknowledge our collaborators, Professor Rita Gerardy-Schahn, Dr. Warren Wakarchuk, Dr. Michel Gilbert and Professor Garry Taylor for their helpful

suggestions and comments during our work together.

I would like to thank my lab mates, past and present, who I have worked together with: Dr. Deepani Indurugalla, Dr. Ivan Hemeon, Dr. Vinay Choytun, Yi Wang, Lydia Cheng, Zoran Cikojevic, Saswati Chakladar, Fahimeh Shidmoossavee, Kobi Khazaei, Gurtej Sandhu, April Lu, Ariel Tang and Viviana Cerda. Research is full of ups and downs but I am thankful to have been able to share these experiences with them. I would like to wish each of them good luck in their future endeavours. I would also like to draw attention to April and Ariel's contributions to my work. Both are intelligent researchers that were always willing to work very long hours to help me with my experiments. I truly appreciate their hard work and friendship.

Next, I would like to thank my closest friends Sterling Wong and Trung La for always being there for me regardless of the situation, time or place. I am very fortunate to have them in my life. I would like to acknowledge and thank Dr. Godwin Choy for being a good friend and for encouraging me to pursue a degree in chemistry.

Finally, I thank my parents, Michael and Queenie Chan, and my grandmother for always loving me. I am extremely grateful that they continue go out of their way to ensure that I live an easier life. Next, I would like to thank my dogs, Buffy and Rex. The old saying is true − "a dog is a man's best friend". Lastly, I would like to thank my wife, Melissa Chan, for supporting me throughout my graduate studies and for encouraging me to be the best I can be.

TABLE OF CONTENTS

LIST OF FIGURES

LIST OF TABLES

GLOSSARY

2,2-DMP	2,2-Dimethoxypropane
4-MU	4-Methylumbelliferone
Å	Ångstrom
°C	Degree Celsius
BSA	Bovine serum albumin
cAMP	Cyclic adenosine monophosphate
CC	Cubic centimetre
CI-MS	Chemical ionization-mass spectroscopy
CMP	Cytidine monophosphate
CMP-Neu5Ac	Cytidine-5′-monophospho-*N*-acetylneuraminic acid sodium salt
CTP	Cytidine triphosphate
Da	Dalton
DANA	5-Acetamido-2,6-anhydro-3,5-dideoxy-D-*glycero*-D-*galacto*-non-2-enoic acid
DCM	Dichloromethane
DEAD	Diethyl azodicarboxylate
DMF	*N,N*-Dimethylformamide
dt	Doublet of triplets
EC	Enzyme commission
EC-MS	Electro spray-mass spectroscopy
FID	Free induction decay
FMU	8-fluoro-7-hydroxy-4-methylcoumarin
Gal	D-Galactose
GalNAc	2-(Acetylamino)-2-deoxy-D-galactose
HEPES	4-(2-Hydroxyethyl)-1-piperazineethanesulfonic acid

h	Hour
J	Spin-spin coupling constant
k_{cat}	Turnover
k_{cat}/K_m	Catalytic efficiency
K_i	Inhibitor constant
KIE	Kinetic Isotope Effect
LC-MS	Liquid chromatography-mass spectrometry
LR-MS	Low resolution mass spectrometry
m	Multiplet
ManNAc	*N*-Acetylmannosamine
MES	2-(*N*-morpholino)ethanesulfonic acid
MHz	Megahertz
min	Minute
mL	Millilitre
mmol	Millimole
MS	Mass spectrometry
MvNA	*Micromonospora viridifaciens* sialidase
Neu5Ac	*N*-Acetylneuraminic acid
Neu5AcαMU	4-Methylumbelliferyl *N*-acetyl-α-D-neuraminic acid
Neu5AcαPNP	4-Nitrophenyl *N*-acetyl-α-D-neuraminic acid
Neu5Gc	*N*-Glycolylneuraminic acid
NMR	Nuclear magnetic resonance
NOE	Nuclear overhauser effect
PPi	Inorganic pyrophosphate
Pyr	Pyridine
R_F	Retention factor
rpm	Revolutions per minute
s	Singlet
sat.	Saturated
SDKIE	Secondary deuterium kinetic isotope effect

S/N	Signal-to-noise
t	Triplet
T_1	Spin-lattice relaxation time
TBAB	Tetrabutylammonium bromide
TcTS	*Trypanosoma cruzi trans*-sialidase
TFA	Trifluoroacetic acid
Tf_2O	Trifluoromethanesulfonic anhydride
THF	Tetrahydrofuran
TLC	Thin layer chromatography
Tris	Tris(hydroxymethyl)aminomethane
TsOH	p-Toluenesulfonic acid
U	Unit of enzyme activity
VcNA	*Vibrio cholerae* sialidase
V_{max}	Maximum reaction rate of an enzyme
ZPE	Zero-point energy

1: GENERAL INTRODUCTION

1.1 Sialic acid

In 1936, Gunnar Blix isolated several novel carbohydrate species from the acid hydrolysis of bovine submaxillary mucin.[1] Ernst Klenk would later independently identify a similar compound, he coined neuraminic acid, obtained from the methanolysis of gangliosides.[2] Two prominent structural features that define this novel monosaccharide family include: i) a hexosamine framework; and ii) an acid group.[1,2] Although the precise structural analysis of these sugars was not possible at the time, it was apparent that they had great biological significance. For instance, Alfred Gottschalk noted that the presence of these sugars on the surface of developing frog eggs had an anti-proteolytic effect.[3] To avoid confusion in the literature when referencing the growing number of sugars belonging to this family, several recommendations were made to the scientific community.[4] The basic unsubstituted compound was to be called neuraminic acid, whereas, the group name for acylated neuraminic acids was 'sialic acid'.[4]

Today the sialic acid family contains more than fifty naturally occurring members.[5] Modifications to the neuraminic acid framework include *N*-acetylation, *N*-glycolylation, *O*-acetylation, *O*-lactylation, *O*-methylation and *O*-sulfonation. The most prominent and frequently studied example is *N*-acetylneuraminic acid (Neu5Ac **1.1**, depicted as the α-anomer in Figure 1-1) which features a carboxylic acid functionality at the C-2 hemiketal anomeric centre, a *N*-acetamido group at C-5 and a glycerol side-chain at C-6. In solution, Neu5Ac is present as an equilibrium mixture consisting of mainly β-

Neu5Ac and α-Neu5Ac (~95:5 ratio) as well as three acyclic species (a ketone, a gem-diol and an enol).[6]

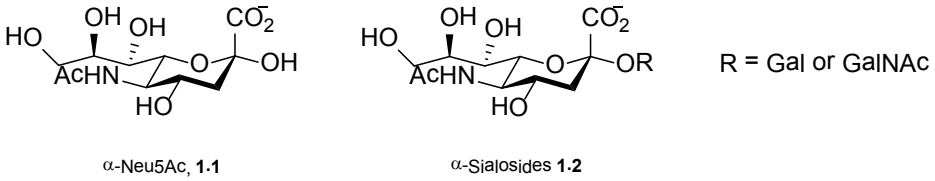

Figure 1-1 Structure of α-Neu5Ac and α-sialosides.

In general, Neu5Ac residues occupy the terminal positions of glycoconjugates by forming 2,3- or 2,6-α-ketosidic linkages to either galactose or *N*-acetylgalactosamine (**1.2**, Figure 1-1).[7] In addition, Neu5Ac homopolymers are known to exist where the sugars are connected via 2,8- or 2,9-α-glycosidic bonds.[8,9] Since these sugars are ubiquitous in nature, it is not surprising that sialylated glycoconjugates play important roles in a vast number of biological processes, which range from mediating the immune response to modulating the pathogenicity of some viruses and bacteria. For instance, sialyl Lewis^x, a Neu5Ac containing antigen, is a ligand for both P- and E-selectins.[10] These cell adhesion molecules are critical in the recruitment of white blood cells to damaged and inflamed tissues. With regard to the infectivity of influenza, a viral carbohydrate-binding protein, hemagglutinin, recognizes and interacts with sialylated host glycoproteins. This key binding event triggers an endocytotic process that internalizes the virus and thus causes infection.[11]

1.2 Sialidases

The family of enzymes that catalyze the hydrolytic cleavage of Neu5Ac containing structures are known as sialidases (or neuraminidases[4], EC 3.2.1.18) and it is comprised of two distinct subgroups. *exo*-Sialidases cleave terminally link Neu5Ac residues[12] whereas *endo*-sialidases[13,14] process the internal linkages of polysialic acid chains. Since this thesis deals exclusively with *exo*-sialidases they shall be referred to as sialidases from here onwards.

1.2.1 Sialidase Homology

Sialidases are present in mammals[15], bacteria[16], fungi[17,18] and viruses such as influenza[19]. Despite their diverse origins, these enzymes share fundamental structural similarities such as a 6-fold β-propeller motif and seven highly conserved amino acid residues that are found in the enzyme active site.[20] These residues include i) an arginine triad that forms an ionic interaction with the anomeric carboxylate of α-sialoside substrates; ii) a structural glutamate; iii) an aspartic acid−glutamate pair; and iv) a tyrosine residue.[21] Of note, the contribution and importance of the triad to catalysis was probed by mutagenesis in which two of the conserved arginines, R152 and R371, from influenza sialidase were substituted with R152K / R152I and R371K, respectively.[22] In each case a correctly folded enzyme was expressed; however, catalysis was either completely abolished or greatly diminished (5-10% of the wild-type activity) for the R152 and R371 mutations, respectively.[22]

1.2.2 Retaining Enzymes

Mechanistically, sialidases are classified as retaining enzymes, that is, the initial

product released, α-Neu5Ac **1.1**, has the same anomeric configuration as that of the substrate **1.2**. Typically, retaining enzymes (i.e., retaining glucosidases) operate via a double displacement mechanism. The first step, glycosylation, involves formation of a covalent enzyme-bound intermediate. During the second step, deglycosylation, this intermediate is hydrolyzed to yield the product. Of note, the transition states for both glycosylation and deglycosylation have been proposed to be similar (Figure 1-2).

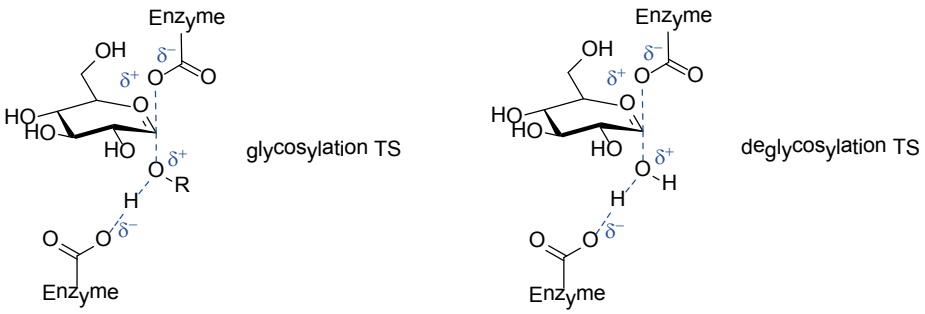

Figure 1-2 Generic transition state structures for the glycosylation and deglycosylation reactions of retaining α-glucosidases.

For many glycosyl hydrolases the nucleophilic species involved in the initial displacement reaction is either a glutamate or aspartate residue. With regard to sialidases, analysis of crystal structures have suggested that the conserved aspartic acid-glutamate pair was too remote from the reaction centre to function as the nucleophile.[23] To account for the observed product stereochemistry, three pathways were proposed (Figure 1-3), they are: i) a transient α-lactone intermediate formed by an intramolecular attack of the anomeric carboxylate **1.3**; ii) an oxacarbenium ion, which is stabilized by the adjacent glutamate-tyrosine pair **1.4**; and iii) a covalent enzyme-bound intermediate generated by an unidentified nucleophile **1.5**.

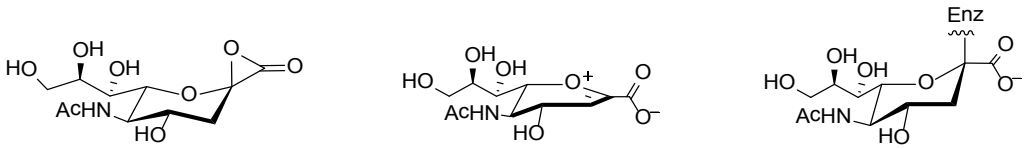

Figure 1-3 Structures for the three possible sialoside intermediates resulting in retention of stereochemistry.

1.2.2.1 Intramolecular Nucleophilic Attack

Results obtained from the non-enzymatic hydrolysis of Neu5AcαPNP led Sinnott and co-workers to propose the nucleophilic involvement of the C-1 carboxylate during cleavage of the glycosidic bond.[24] A similar mechanism for the corresponding enzymatic reaction was suggested based on these observations, which involves an intramolecular attack of the anomeric carboxylate *en route* to generating an α-lactone intermediate, **1.3**. This proposal is unlikely since the strong ionic interactions between the carboxylate and the three conserved arginine residues tightly constrain the carboxylate during catalysis. The average distance for the six closest O-N contacts for sialic acid bound to influenza sialidase is only 3.18 Å which clearly demonstrates the strength of the interactions.[25]

1.2.2.2 Oxacarbenium ion intermediate

The difficulty associated with performing KIE measurements on V_{max} is that reaction rate constants must be determined separately for each isotopomer. As such, larger systematic errors are common for these non-competitive experiments. However, Chong *et al.* measured a small reproducible inverse β-secondary deuterium KIE on the first-order rate constant, V = 0.976 at pH 6.0, for the influenza sialidase-catalyzed hydrolysis of Neu5AcαMU.[26] Based on these results, the authors proposed the involvement of an enzyme stabilized oxacarbenium ion intermediate (Figure 1-3, **1.5**)

which reacts exclusively from the α-face to generate α-Neu5Ac.[26] In addition, a number of theoretical studies have implicated and supported the proposal that an oxacarbenium ion is an intermediate along the reaction pathway for sialidase reactions.[27,28] Of note, a key assumption made during many of these calculations is that 5-acetamido-2,6-anhydro-3,5-dideoxy-D-*glycero*-D-*galacto*-non-2-enoic acid (DANA, **1.6**) is a transition state analogue.[28] To probe whether a compound, such as DANA, is a transition state analogue inhibitor, it is necessary to synthesize a series of inhibitor-substrate pairs that feature a common modification of the parent structure. The corresponding inhibitor potency (K_i) and catalytic efficiency (k_{cat}/K_m) for each pair are determined and plotted. A strong correlation between the two kinetic parameters (i.e., slope that is close to 1) suggests that the modification effects binding to the enzyme equally for both inhibitor and substrate. This is an essential condition for a genuine transition state analogue inhibitor. Of note, no reports have been made which demonstrate a correlation for DANA.[29]

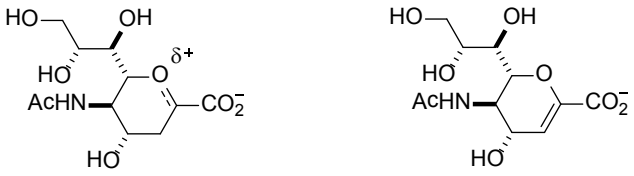

1.5 **1.6**

Figure 1-4 Structures for oxacarbenium ion intermediate and DANA.

1.2.2.3 Covalent Enzyme-Bound Intermediate

Withers and co-workers pioneered a "non-perturbing" fluoro-sugar labelling technique with the aim of identifying the nucleophilic residue involved in glycosyl hydrolase-catalyzed reactions.[30] This method employs glycoside substrates that contain an electronegative fluorine atom adjacent to the reaction centre, which functions to

decelerate the rate of formation of the oxacarbenium ion-like TS during both the glycosylation and deglycosylation steps. To compensate for the rate reduction experienced during glycosylation, highly activated substrates containing good leaving groups such as fluoride or 2,4-dinitrophenolate are used. Typically, this modification causes the deglycosylation step to become rate limiting for the overall catalytic cycle.

With regard to the current discussion of sialidases, Watts *et al.* used 2,3-difluoro sialic acid, **1.7** (Figure 1-4) to trap and characterize the intermediate formed with *Trypanosoma cruzi trans*-sialidase (TcTS).[31] *trans*-Sialidases predominantly catalyze the transfer of terminal α-2,3-linked Neu5Ac residues from galactose on host glycoconjugates to terminal galactose residues of glycoconjugate chains on the external surface of the parasite.[32] However, the transfer reaction, similar to hydrolysis, occurs with retention of stereochemistry. Since the same seven highly conserved active site residues that characterize members of the *exo*-sialidase super-family are present, it is likely the overall mechanism is very similar to that of *exo*-sialidases.

When compound **1.7** was incubated with TcTS, a mass increase of 304 $\pm$ 12 Da was observed by ES/MS analysis. This observation is consistent with the formation of a covalently bound fluoro-Neu5Ac-enzyme intermediate. To identify the point of attachment, samples of 'labelled' and 'unlabelled' enzymes were digested for comparison. Analysis of the peptide fragments by LC-MS demonstrated that the conserved active site tyrosine was covalently modified with compound **1.7**.[31] In addition, when 'labelled' TcTS incubated with **1.8**, transfer of fluoro-sialic acid onto the 3'-position of the acceptor was observed. In contrast, incubation with the 3'-deoxy analogue **1.9** resulted in no transferase activity. These key experiments demonstrate that TcTS operates via a double

displacement mechanism involving transient formation of a covalent intermediate, with the conserved active site tyrosine residue acting as the nucleophile.[31]

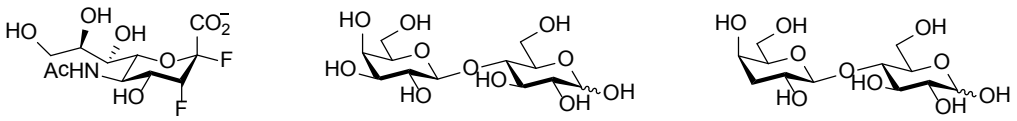

1.7 **1.8** **1.9**

Figure 1-5 Structures of 2,3-difluorosialic acid analogue **1.7**, lactose **1.8**, and 3'-deoxy-lactose **1.9**.

In a separate study, Bennet and co-workers employed mutagenesis to replace the conserved active site tyrosine (Y370) of the *Micromonospora viridifaciens* sialidase with an alanine (Y370A), a glycine (Y370G) and an aspartic acid (Y370D).[33] In each case, an active enzyme was expressed, however, NMR spectroscopic analysis demonstrated the mechanism of these mutant enzymes had changed from retention to inversion of stereochemistry. The authors reasoned that substitution of tyrosine with smaller amino acid residues leads to formation of a 'cavity' that can accommodate one or more water molecules in the presence of bound substrate. As such, the water molecule can i) act as nucleophile during a S_N2-like mechanism to displace the leaving group; or ii) capture a nascent oxacarbenium ion intermediate formed during a S_N1-like pathway.[34]

1.2.3 Rationale for Tyrosine as an Active Site Nucleophile

One proposal has suggested that nature evolved a neutral nucleophile, the active site tyrosine, rather than the more common aspartate or glutamate nucleophiles to avoid potentially unfavorable electrostatic interactions that may arise between the negatively

charged carboxylates of the substrate and aspartate/glutamate residues.[31] However, given that the sialoside carboxylate is constrained by three positively charged arginine residues this explanation is unlikely. A second, more probable explanation suggests that due to the intrinsically greater reactivity of sialosides, a poorer leaving group for the sialosyl-enzyme intermediate is required to give the carbohydrate leaving group enough time to diffuse from the active site to be replaced by a water molecule.[33]

1.2.4 Catalytic Mechanism of Sialidases

The generally accepted mechanistic scheme for sialidases, where E = sialidase.[35] This mechanism involves i) formation of a Michaelis complex where the substrate (αNeu5Ac-OR) binds to the enzyme in a $^2C_5$ chair conformation (k_1); ii) a substrate conformation change to $B_{2,5}$ boat (k_2); iii) cleavage of the glycosidic bond to give an enzyme-bound intermediate (k_3); iv) hydrolysis of the intermediate which generates the sialic acid product (αNeu5Ac-OH) which is bound to the enzyme in a $B_{2,5}$ boat conformation (k_4); v) a product conformational change to a $^2C_5$ chair (k_5); and finally vi) release of the product from the enzyme active site (Figure 1-6).

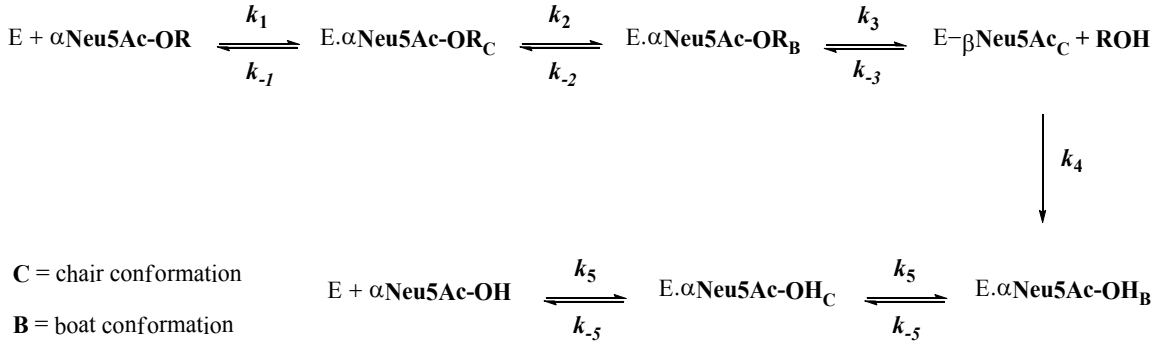

Figure 1-6 Mechanistic scheme for sialidase-catalyzed hydrolysis reactions.

Since all sialidases contain the same conserved active site residues, it is

reasonable to assume that in general, these enzymes operate with the same overall mechanism. As such, the differences in the catalytic specificities are likely due to the relative free energy levels of the various intermediates and transition states.

1.3 Mechanistic Tools

1.3.1 Enzyme Kinetics

In 1913 Michaelis and Menten introduced a central equation (Eq. 1) for describing the reaction rate and specificity for single substrate enzymes.[36] In the equation v_o is the current reaction rate; v_{max} is the maximum reaction rate; K_m, the Michaelis-constant, is the substrate concentration where v_o is half the value of v_{max}; and [S] is the substrate concentration.

Eq. 1

$$v_o = \frac{v_{max}[S]}{K_m + [S]}$$

Since this initial report, enzyme kinetics has been used routinely to study the origins and causes of biological catalysis. There are two kinetic parameters that are important when considering sialidase-catalyzed reactions. They are k_{cat}, the first-order rate constant for the conversion of the Michaelis complex to free enzyme and product, and k_{cat}/K_m, the apparent second-order rate constant for the reaction of free enzyme and free substrate.[36] With regard to k_{cat}/K_m, this term is also a measure of the enzymes' catalytic efficiency (Figure 1-7) and has a theoretical limit that is set by the diffusion-controlled interaction of substrate and enzyme. In addition, the enzyme catalytic proficiency ($k_{cat}/K_m \times 1/k_{uncat}$) must also be considered when studying sialidases since this term relates catalysis to the

corresponding uncatalyzed process.[37]

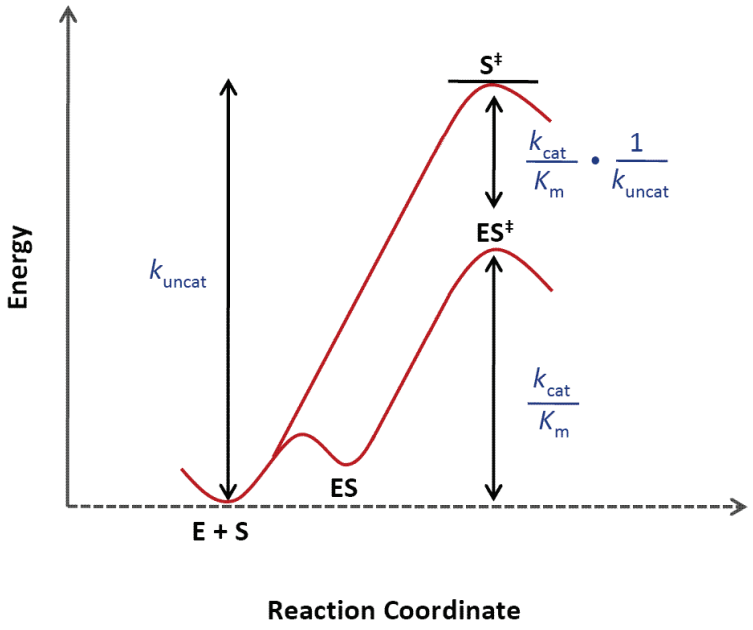

Figure 1-7 Free energy diagram showing catalytic proficiency ($k_{cat}/K_m \times 1/k_{uncat}$) and catalytic efficiency (k_{cat}/K_m).

1.3.2 Brønsted Analysis

One type of Brønsted involves plotting the logarithm of a rate constant against the pK_a value of the leaving group's conjugate acid. The derived slope, β_{lg}, can provide valuable insight with regard to the degree of glycosidic bond cleavage at the transition state. This technique is often used to probe both the k_{cat} and k_{cat}/K_m kinetic parameters, the results of which can provide complementary information regarding the catalytic mechanism. This technique has been used to study a number of sialidases and the results are summarized below (Figure 1-8). For instance, the β_{lg} value on k_{cat}/K_m for *V. cholerae* enzyme is more negative than that for the *M. Viridifaciens* sialidase. This comparison suggests that cleavage of the glycosidic bond during glycosylation is more rate limiting

for *V. cholerae* than for *M. viridifaciens* (k_3, Figure 1-6). In addition, the β_{lg} values for the uncatalyzed hydrolysis reactions of α-sialosides are typically larger (i.e., $\beta_{lg} = -1.32$). Three main factors can account for the smaller values associated with the enzyme-catalyzed process, i) general-acid catalysis diminishes the charge on the leaving group; ii) nucleophilic catalysis reduces the degree of glycosidic bond cleavage at the TS; and iii) a step other than glycosidic bond cleavage is rate-determining (i.e., conformational change).

Enzyme	β_{lg} (k_{cat}/K_m)	β_{lg} (k_{cat})	Reference
Vibrio cholerae	–0.73	–0.25	*Biochem. J.* **1993**, *254*, 653.
Influenza A (N2)	–0.46	–0.11	*JACS* **1994**, *116*, 5572.
S. typhimurium	–0.80	–0.53	*JACS* **1994**, *116*, 5572.
M. viridifaciens	–0.30	0.02	*Biochemistry* **2003**, *42*, 12682.

Figure 1-8 Brønsted β_{lg} values for various sialidases.

1.3.3 Kinetic Isotope Effects (KIEs)

The measurement and analysis of KIEs can be used to probe the mechanism of chemical transformations as well as enzyme-catalyzed processes. Valuable transition state details can be obtained with this technique, these include: i) whether a reaction is concerted or step-wise; ii) the extent of covalent bond cleavage and formation; iii) degree of charge development; and iv) geometry at the transition state.[38,39]

Substitution of a light isotope with a heavy isotope at or adjacent to the position

of bond cleavage or formation can result in a change in the observed reaction rate. Typically, isotopically labelled materials have a lower zero-point energy (ZPE) than their unlabelled counterparts. This results in a difference in ZPE for the reactants and for the transition state. If the ZPE difference is greater for the reactants, a normal KIE (KIE > 1) will be observed (Figure 1−9). In contrast, if the ZPE difference is larger at the transition state, then an inverse KIE (KIE < 1) will result.

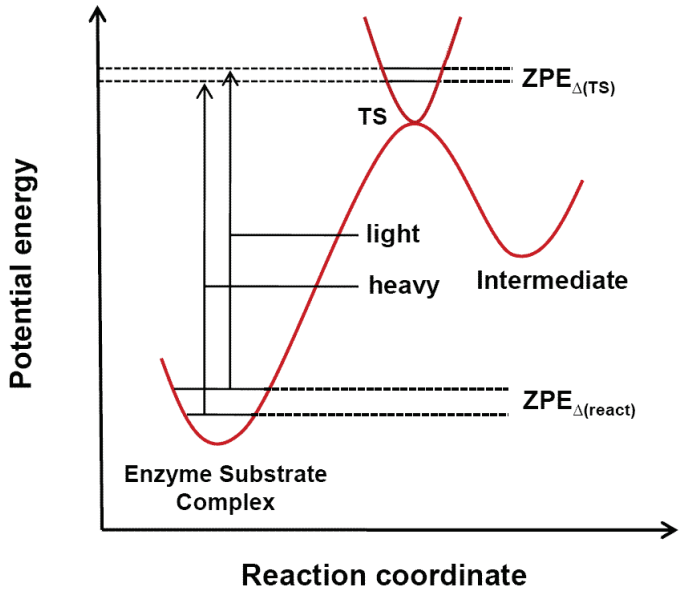

Figure 1-9 Differential zero point energy differences in activation energy between heavy and light isotopomers.

1.3.4 Nomenclature

KIEs can be measured on both k_{cat} and k_{cat}/K_m. Since V_{max} is the product of k_{cat} and $[E]_o$, the enzyme concentration, these two kinetic parameters can be rewritten as V and V/K, respectively. As such, an ^{18}O KIE (k_{16O}/k_{18O}) measured on V will be referenced as ^{18}V in this thesis. Similarly, a ^{13}C KIE (k_{12C}/k_{13C}) measured on the V/K will be written as $^{13}V/K$.

1.3.4.1 Primary KIEs

A primary KIEs occurs when an isotopic substitution is at a position that is undergoing bond-cleavage or formation at the TS. These effects are most significant when the relative isotopic mass change is largest (i.e., deuterium substitution). In contrast, heavy-atom primary KIEs, such as a ^{13}C substitution, are much smaller and hence more difficult to determine accurately.

1.3.4.2 Secondary KIEs

Secondary KIEs are produced when the isotopic substitution is at a position not directly involved in covalent bond changes at the TS. In general, only deuterium and not heavy-atom substitutions will result in measurable non-unity KIEs. Secondary deuterium KIEs (SDKIE) can be classified as either α or β depending on whether the position of substitution is at or adjacent to the reaction centre, respectively. Of note, α-SDKIE are associated with reaction centre re-hybridization, whereas, β-SDKIE arise from changes in hyper-conjugation.

1.3.4.3 Solvent KIEs

A solvent KIE is observed if a change in reaction rates occurs when a non-deuterated solvent (i.e., water) is replaced with its deuterated analogue (i.e., deuterium oxide). There are two main mechanisms, a primary and a secondary effect, that can account for the observed rate change.[39] A primary isotope effect results when a proton/deuterium from the solvent is undergoing transfer at the transition state. In contrast, a secondary isotope effect occurs in instances where the transition state is stabilized to different extents by the deuterated solvent. As such, the activation energy

will differ leading to the observed KIE. Typically, secondary effects are much smaller than the corresponding primary effects.

2: A DIRECT NMR METHOD FOR THE MEASUREMENT OF COMPETITIVE KINETIC ISOTOPE EFFECTS

2.1 Introduction

The measurement and analysis of kinetic isotope effects (KIE) is an invaluable tool used by researchers to gain insight into fundamental chemical and biological reactions. The TS features that can be probed by these experiments include i) extent of charge development; ii) degree of covalent bond formation and cleavage; and iii) geometry. Accordingly, this information can be used to aid in the design of tight-binding TS analogue inhibitors. A notable example designed using this approach is the drug candidate Immucillin-H, a potent picomolar inhibitor of purine nucleoside phosphorylase.[40]

The most accurate methods for determining KIEs are based on competitive techniques in which both the labelled and unlabelled isomer (isotopomer) are present in the same reaction vessel. This eliminates many systematic errors, such as variable temperature, differences in concentration, and the presence of inhibitors or activators, that would otherwise exist with non-competitive techniques.[39] Of note, irrespective of concentration, KIEs measured with competitive methods report only on the second-order rate constant k_{cat}/K_m in enzyme-catalyzed reactions.[39]

Existing competitive methods for determining KIEs include the use of radio isotope labelling,[39] MS,[39,41] NMR spectroscopy[42,43] and polarimetry.[44] Each method has limitations that prevent universal applicability. For instance, the use of radioisotopes

requires the handling and chemical synthesis of radioactive reactants and limits measurements to readily available radioisotopes. With regard to polarimetry, this technique is restricted to reactions in which a large observable optical rotation change is present between the reactants and products. In addition, polarimetry is incompatible with systems that are not translucent. The most widely used NMR technique involves reacting large quantities, typically grams, of unlabelled material until a high percent of conversion has been established. After subsequent reisolation of unreacted starting material, ^{13}C NMR spectroscopy is employed to analyze the isotopic fractionation patterns. Of note, all isotope effects derived from this method are relative to a position where the KIE is assumed to be 1.0. Since gram quantities of material are typically required for the experiments, it is unsuitable for studying many enzymatic systems, especially those with complex substrates. Furthermore, the protocol cannot be used to measure ^{18}O-KIEs, as it is limited to the detection of NMR-active nuclei.[42, 43] Most modern methodologies, including scintillation counting, isotope ratio MS and NMR spectroscopy, determine KIEs through measurements taken at a single time point rather than continuous measurements taken throughout the reaction.

Herein we report the development of a sensitive, NMR-based protocol for the measurement of heavy-atom KIEs, one that enables KIE values to be determined using data collected continuously throughout the reaction time course. In addition, high-precision ring oxygen, anomeric carbon and leaving group oxygen KIE measurements are reported for the *V. cholerae* sialidase-catalyzed hydrolysis of sialyllactoside substrates.

2.2 Development of Methodology

The current technique involves combining singly and doubly labelled compounds directly in a NMR tube to monitor the isotopic ratio for an atom of interest by quantitative ^{13}C-NMR spectroscopy. Particularly, a NMR active nucleus is used to probe the isotopic composition at an adjacent atom. For instance, both ^{13}C and ^{18}O KIEs can be determined experimentally using this protocol when the adjacent ^{13}C atom is used as the probe nucleus (Figure 2-1).

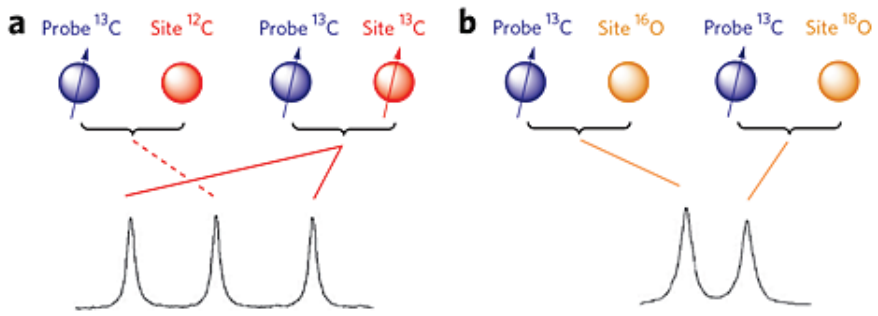

Figure 2-1 Direct NMR spectroscopic measurement of a) ^{13}C and b) ^{18}O KIEs.

Measurement of ^{13}C KIEs ($^{13}V/K$) is possible with this technique when the adjacent nuclei for the "light" and "heavy" isotopomers are ^{12}C and ^{13}C, respectively (Figure 2-1a). As such, the different one-bond coupling constants are used to distinguish between the isotopomers. In these experiments, the singly labelled isotopomer will appear as a singlet, whereas the doubly labelled material will appear as a doublet. In contrast, when the adjacent isotopic nuclei are both NMR inactive (i.e., ^{16}O and ^{18}O, Figure 2-1b), ^{18}O KIEs ($^{18}V/K$) can be measured based on a chemical shift perturbation caused by bonding to different isotopes. Each experiment typically requires only milligram quantities of material since the protocol employs probe nuclei that are either i)

present at high natural abundance (i.e., ^{1}H, ^{19}F, ^{31}P); or ii) are isotopically enriched (i.e., ^{13}C). Consequently, this procedure can avoid using gram quantities of substrate as is the case with natural abundance NMR-based techniques.[43] Additional advantages of using minute levels of substrates are that i) the reaction can be monitored directly in a NMR tube; and ii) the fraction of reaction can be determined without the reisolation of unreacted starting material by simply adding an innocuous internal standard such as ^{13}C-alanine.[42,43] Data acquisition begins when reactants are added and can continue uninterrupted until the signal-to-noise ratio deteriorates to an unsatisfactory level, typically when the reaction approaches 80−90% completion. As such, the derived KIEs are calculated from multiple data points obtained during the entire reaction as opposed to single time point.

During the development of this technique, it was imperative to ensure that the KIEs measured are intrinsic and fully expressed. As such, we selected *V. cholerae* sialidase (VcNA) to serve as the model enzyme since it has been established by Brønsted analysis that the rate-determining chemical step for k_{cat}/K_m is cleavage of the glycosidic bond.[45] Furthermore, the leaving group heavy-atom KIE has been reported using Neu5AcαPNP as the substrate. Despite containing an activated leaving group that may alter the TS, a direct comparison with the corresponding ^{18}O KIE obtained using the current technique can still provide valuable mechanistic information. The isotopically labelled natural substrate analogues used to measure the ring oxygen, anomeric carbon and leaving group oxygen KIEs for the VcNA-catalyzed hydrolysis reaction are summarized below (Figure 2-2).

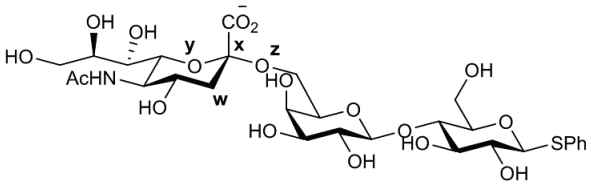

Neu5Acα2,6LacβSPh (2.1)

KIE	Compound	Position(s) Labelled
Endocyclic oxygen	2.1 a 2.1 b	x = ^{13}C y = ^{18}O, x = ^{13}C
Anomeric carbon	2.1 c 2.1 d	w = ^{13}C x, w = ^{13}C
Leaving group oxygen	2.1 a 2.1 e	x = ^{13}C x = ^{13}C, z = ^{18}O

Figure 2-2 Labelled Neu5Acα2,6LacβSPh **2.1a-e** used in KIE measurements.

2.3 Substrate Synthesis

Neu5Acα2,6LacβSPh **2.1** and the requisite singly and doubly labelled isotopologues **2.1 a-e** were prepared chemoenzymatically from the appropriately labelled precursors LacβSPh **2.2**, ManNAc **2.3** and pyruvate (Figure 2-2). LacβSPh was prepared in three-steps from D-lactose in an overall yield of 50%.[46] ^{13}C-labelled sodium pyruvates (99.9 atom%) were purchased from Cambridge Isotopes, and ^{13}C-labelled sialic acids, used in the preparation of labelled 2,3-sialyl lactosides, were purchased from Omicron Biochemicals Inc. [$^{18}O_2$]-Benzoic acid was used to introduce the ^{18}O atom for all ^{18}O labelled precursors. Labelled ^{18}O-3-ManNAc[47] was synthesized using a published procedure (Figure 2-3). Labelled ^{18}O-6'-LacβSPh was accessed in six-steps beginning from **2.2** in 37% yield overall (Figure 2-4).

2.3.1 Synthesis of [$^{18}O_2$]-Benzoic acid

A flame-dried Schlenk flask (25 mL) was charged with α,α,α-trichlorotoluene (1.6 mL, 11 mmol), 2,4,6-trimethylpyridine (10.0 mL, 76 mmol) and (^{18}O)-H_2O (0.5 mL, 25 mmol; Marshall isotopes, 95.1 atom% O-18, batch no. 020414nw). After sealing the flask the mixture was stirred at 130 °C for 18 h, after which it was cooled to room temperature. The resulting mixture was diluted with dichloromethane (25 mL) followed by the addition of sat. aqueous sodium bicarbonate (25 mL). Upon separation, the aqueous layer was washed with ether (5 × 25 mL) and the pH was then adjusted to ~2 by the addition of 10% sulfuric acid. Subsequent extraction of the aqueous layer with dichloromethane (3 × 50 mL) gave, after drying the organic layer (sodium sulfate) and concentration under reduced pressure, labelled benzoic acid as a white solid (1.30 g, 93% yield). Based on the observed intensities of the isotopic peak distribution for the M^+H^+

molecular ion peaks in a CI-MS, the isotopic composition of this material was calculated, using the method of Brauman,[48] to be [$^{18}O_2$] 84.5%, [$^{18}O_1$] 14.1%, and [$^{18}O_0$] 1.4%. mp = 121-122 °C. ^{1}H NMR (600 MHz, $CDCl_3$) δ 8.21–8.11 (m, 2H), 7.65 (t, J = 7.4, 1H), 7.52 (t, J = 7.8, 2H). ^{13}C NMR (151 MHz, $CDCl_3$) δ 171.7, 133.8, 130.2, 129.2, 128.5.

2.3.2 Synthesis of ^{18}O-3-ManNAc

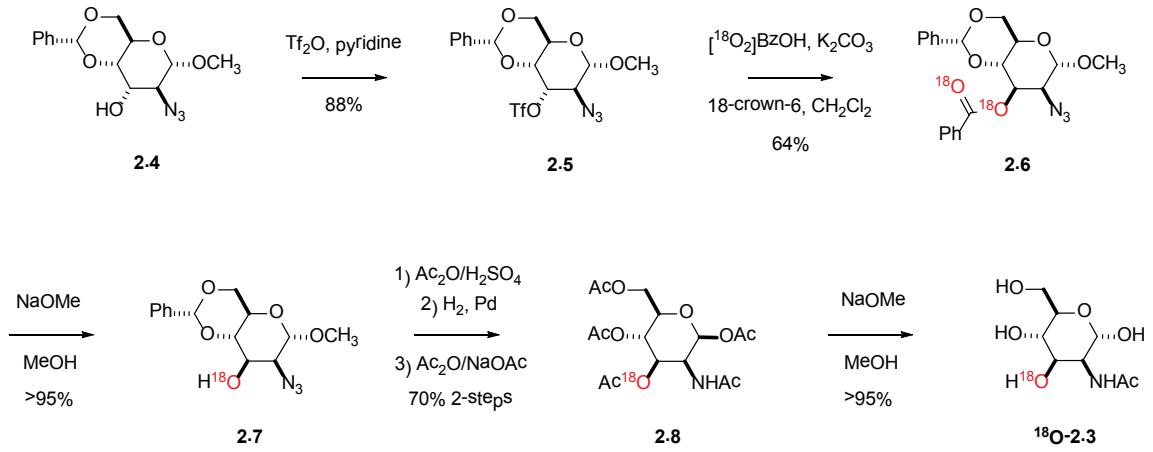

Figure 2-3 Synthetic route to ^{18}O-3-ManNAc.

Preparation of **^{18}O-2.3** involved activating the 3-OH group of the D-gulose intermediate **2.4** with trifluoromethanesulfonic anhydride to give compound **2.5** in 88% yield. Nucleophilic substitution of the triflate with ^{18}O-labelled potassium benzoate afforded compound **2.6** in 64% yield. Of note, a 3,4-elimination reaction produces an alkene side product (~15%) which was removed via column chromatography.[47] Zemplín conditions were employed to hydrolyze the benzoate ester to give compound **2.7** quantitatively. Cleavages of the 4,6-O-benzylidene and methyl acetal functionalities were achieved under acidic conditions. The liberated hydroxyl groups were acetylated *in*

situ with acetic anhydride. Without purification, the resultant peracetylated 2-azido mannoside was subjected to hydrogenation conditions. This was followed by treatment with acetic anhydride and sodium acetate to give compound **2.8** in 70% yield over three-steps. Finally, the desired compound **^{18}O-2.3** was obtained under standard Zemplín deacetylation conditions quantitatively (Figure 2-3).

Methyl 2-azido-2-deoxy-4,6-*O*-benzylidene-α-D-mannopyranoside (2.5). A solution of compound **2.4** (5.0 g, 16 mmol) in pyridine (40 mL) and dichloromethane (100 mL) was cooled to 0 °C in an ice-bath. Trifluoromethanesulfonic anhydride (3.42 mL, 20 mmol) was added drop-wise and the resultant solution was stirred at room temperature for 1 hr. The solution was washed successively with water (100 mL), 10% sulfuric acid (100 mL × 2) and brine (100 mL). The organic layer was dried (sodium sulfate) and concentrated to give a crude syrup which was used without further purification (6.2 g, 88% yield). Data in accord with Reference 47.

Methyl 2-azido-2-deoxy-3-benzoyl-4,6-*O*-benzylidene-α-D-(3-^{18}O)mannopyranoside (2.6). A flame-dried flask was charged with compound **2.5** (1.88 g, 4.3 mmol), [$^{18}O_2$]-benzoic acid (673 mg, 5.3 mmol), potassium carbonate (885 mg, 6.4 mmol), 18-crown-6 (1.69 g, 6.4 mmol) and dichloromethane (60 mL). The resultant mixture was stirred at room temperature for 48 hrs. The volatiles were removed under reduced pressure and the resultant crude solid was purified via flash chromatography (1:5 v/v ethyl acetate/hexanes) to afford the desired product as a white solid (1.1 g, 64% yield). In addition, a 3,4-elimination compound was isolated as a side-product (~15% yield). Data for both compound **2.6** and the elimination product in accord with Reference 47.

Methyl 2-azido-2-deoxy-4,6-O-benzylidene-α-D-(3-^{18}O)mannopyranoside (2.7). A

solution of compound **2.6** (1.0 g, 2.41 mmol) in methanol (25 mL) was treated with a freshly prepared solution of sodium methoxide (~0.5 M, 10 mL). The resultant mixture was stirred at room temperature for 1 hr. Amberlite IR-120 resin (H^+ form) was added to neutralize the reaction. After filtration, the filtrate was concentrated under reduced pressure to afford a syrupy residue (1.28g, >95% yield). ^{1}H NMR spectroscopy demonstrated that the crude product was >95% pure. As such, this material was used without further purification. Data in accord with Reference 47.

1,3,4,6-Tetra-*O*-acetyl-2-acetamido-2-deoxy-α-D-(3-^{18}O)mannopyranose (2.8). A solution of compound **2.7** (750 mg, 2.3 mmol) in 5% sulfuric acid in acetic anhydride (20 mL) was stirred for 1.5 hr at 0 °C. The solution was diluted with ethyl acetate (100 mL) and washed with sat. aqueous sodium bicarbonate (100 mL), water (100 mL) and brine (100 mL). Upon separation, the organic layer was dried (sodium sulfate) and concentrated. The resultant solid residue was dissolved in methanol (25 mL) and treated with 10% palladium on activated carbon. This mixture was stirred at room temperature for 24 hr while maintaining a hydrogen atmosphere with a balloon. The catalyst was removed by filtration through a celite pad which was rinsed with copious amounts of methanol. The filtrate was concentrated under reduced pressure to afford a syrupy residue which was dissolved in acetic anhydride (10 mL), cooled to 0 °C and treated with a catalytic amount of sodium acetate. The mixture was stirred at 0 °C for 1 hr and then co-evaporated with toluene. The resultant compound was purified via flash chromatography (1:1 v/v ethyl acetate/hexanes) to give the desired product as a white solid (6.25 mg, 70% yield over two-steps). Data in accord with Reference 47.

2-Acetamido-2-deoxy-D-(3-^{18}O)mannose (^{18}O-2.3). A solution of compound **2.8** (500

mg, 1.3 mmol) in methanol (20 mL) was treated with a freshly prepared solution of sodium methoxide (~0.5 M, 5 mL). The resultant mixture was stirred at room temperature for 1 hr. Amberlite IR-120 resin (H^+ form) was added to neutralize the reaction. After filtration, the filtrate was concentrated under reduced pressure to afford the desired compound as a glassy solid (275 mg, >95% yield). This material was used directly in the subsequent enzymatic synthesis without further purification. Data in accord with Reference 47.

2.3.3 Synthesis of ^{18}O-6'-LacβSPh

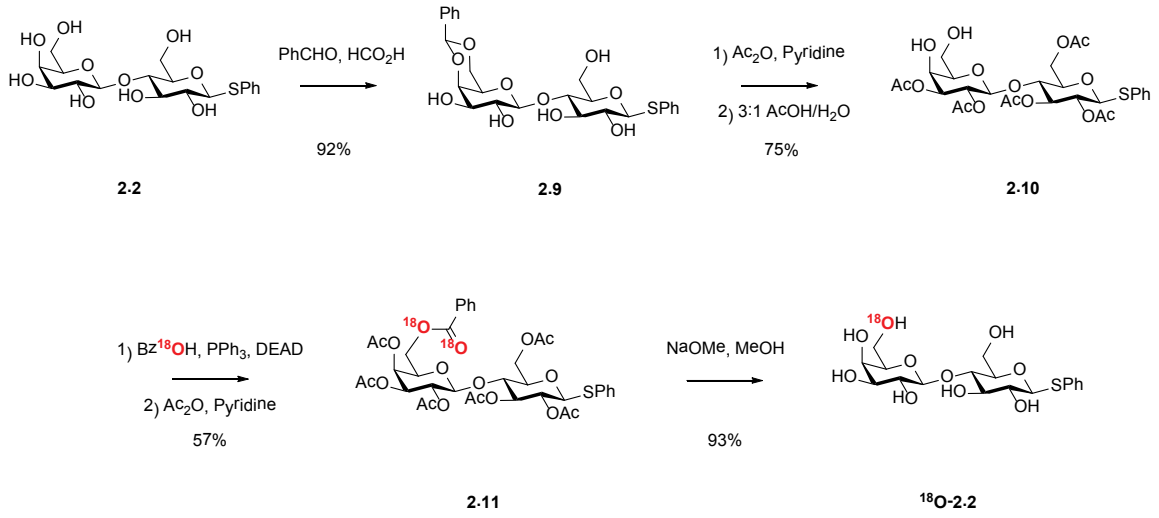

Figure 2-4 Synthetic route to ^{18}O-6'-LacβSPh.

The synthetic route used to access **^{18}O-2.2** began with the selective reaction of the 4'- and 6'-hydroxyl groups of the unlabelled lactoside with a benzylidene protecting group to give compound **2.9** in 92% yield. Acetylation of the remaining hydroxyl groups and subsequent acid-catalyzed hydrolysis of the benzylidene moiety liberated the 4'- and

6'-OH groups to afford compound **2.10** in 75% yield over two-steps. A Mitsunobu reaction was employed to selectively introduce the ^{18}O atom in the 6'-position. The ensuing acetylation of the 4'-OH facilitated purification via column chromatography to give compound **2.11** in 57% over two-steps. Finally, Zemplín deacetylation was used to obtain compound **^{18}O-2.2** in 93% yield.

Phenyl (4,6-*O*-benzylidene-β-D-galactopyranosyl)-(1→4)-1-thio-β-D-glucopyranoside (2.9): Formic acid (4.0 mL, 106 mmol) was added to a suspension of phenyl 1-thio-β-lactoside **2.2** (4.0 g, 9.2 mmol) in benzaldehyde (4.0 mL, 39 mmol). The resultant mixture was stirred at room temperature for 45 min and then it was poured into ether (50 mL). The precipitate was collected via filtration and rinsed with ether (50 mL) to afford the desired product as a white solid (4.4 g, 92% yield). ^{1}H NMR (600 MHz, CH_3OD) δ 7.63–7.50 (m, 4H), 7.41–7.22 (m, 6H), 5.65 (s, 1H), 4.66–4.60 (m, 1H), 4.50 (s, 1H), 4.30–4.10 (m, 3H), 3.92 (s, 2H), 3.75–3.38 (m, 7H). ^{13}C NMR (151 MHz, CH_3OD) δ 131.6, 128.5, 127.6, 127.0, 126.0, 103.4, 100.9, 87.8, 79.1, 78.1, 76.4, 76.0, 72.1, 70.3, 68.8, 60.4.

Phenyl (2,3-di-*O*-acetyl-β-D-galactopyranosyl)-(1→4)-2,3,6-tri-*O*-acetyl-1-thio-β-D-glucoside (2.10): A solution of compound **2.9** (2.25 g, 4.3 mmol) in pyridine (20 mL) was cooled in an ice-bath and treated with acetic anhydride (5.1 mL, 54 mmol). The reaction mixture was stirred at room temperature overnight, diluted with dichloromethane (50 mL) and poured into cold water (100 mL). After separation, the organic layer was washed successively with 10% sulfuric acid (2 × 50 mL), sat. aqueous sodium bicarbonate (2 × 50 mL) and brine (50 mL). Upon drying (sodium sulfate) and concentration, the residue was treated with acetic acid–water (3:1, 20 mL) and heated to

90 °C for 1 hr. The reaction mixture was concentrated under reduced pressure and the crude residue was purified via flash chromatography (1:19 v/v methanol/dichloromethane) to afford the desired product as a white solid (2.08 g, 75% yield over two-steps). mp = 208-210 °C. ^{1}H NMR (600 MHz, $CDCl_3$) δ 7.53–7.46 (m, *J* = 2.4, 7.2, 2H), 7.36–7.30 (m, 3H), 5.30–5.17 (m, 2H), 4.99 – 4.88 (m, 2H), 4.71 (d, *J* = 10.0, 1H), 4.59 (d, *J* = 11.8, 1H), 4.53 (d, *J* = 7.9, 1H), 4.14–4.06 (m, 2H), 3.99–3.90 (m, *J* = 5.5, 11.2, 1H), 3.88–3.78 (m, 2H), 3.73–3.67 (m, *J* = 6.0, 1H), 3.57 (t, *J* = 5.0, 1H), 2.80 (d, *J* = 3.7, 1H), 2.51 (dd, *J* = 4.7, 7.9, 1H), 2.12 (d, *J* = 5.2, 3H), 2.11 (s, 3H), 2.10 (s, 3H), 2.09 (d, *J* = 12.3, 3H), 2.07 (s, 3H). ^{13}C NMR (151 MHz, $CDCl_3$) δ 170.5, 170.5, 170.1, 169.6, 169.4, 133.0, 131.8, 128.9, 128.3, 100.9, 85.4, 76.7, 76.1, 74.4, 74.3, 73.33, 70.30, 69.6, 68.2, 62.5, 62.4, 20.94, 20.89, 20.83, 20.82, 20.7. Anal. calcd for $C_{28}H_{36}O_{15}S$: C, 52.17; H, 5.63. Found: C, 51.98; H, 5.62.

Phenyl (2,3,4-tri-*O*-acetyl-6-*O*-[^{18}O 0;1]-benzoyl-[6-^{18}O 0;1]-β-D-galactopyranosyl)-(1→4)-2,3,6-tri-*O*-acetyl-1-thio-β-D-glucopyranoside (2.11): A flame-dried flask was charged with compound **2.10** (197.5 mg, 0.31 mmol), benzoic acid (65.2 mg, 0.53 mmol), [$^{18}O_2$]-benzoic acid (75.7 mg, 0.59 mmol), triphenylphosphine (288.5 mg, 1.1 mmol) and anhydrous THF (30 mL). The reaction mixture was cooled in an ice-bath and treated with a 40% solution of diethyl azodicarboxylate in toluene (526 μL, 1.1 mmol). After stirring at room temperature for 28 h, the solvent was removed under reduced pressure. The resultant residue was dissolved in pyridine (10 mL) and treated with acetic anhydride (0.5 mL, 5.3 mmol). The reaction progress was monitored by TLC, R_F = 0.28 (1:4 v/v acetone/toluene). Upon completion, the reaction mixture was diluted with dichloromethane (25 mL) and washed successively with water (20 mL), 10% sulfuric

acid (20 mL), sat. aqueous sodium bicarbonate (20 mL) and brine (20 mL). After drying (sodium sulfate), the reaction mixture was concentrated to give a syrupy residue which was purified via flash chromatography (1:4 v/v acetone/toluene) to afford the desired product as a white solid (140.1 mg, 57% yield over two-steps). mp = 81-82 °C. ^{1}H NMR (600 MHz, $CDCl_3$) δ 8.03 (d, *J* = 8.4, 2H), 7.65–7.57 (m, 1H), 7.53–7.45 (m, 4H), 7.37–7.30 (m, 3H), 5.48 (d, *J* = 3.4, 1H), 5.27 (t, *J* = 9.2, 1H), 5.17 (dd, *J* = 7.9, 10.4, 1H), 5.02 (dd, *J* = 3.5, 10.4, 1H), 4.92 (t, *J* = 9.7, 1H), 4.69 (d, *J* = 10.1, 1H), 4.57 (d, *J* = 11.8, 1H), 4.52 (d, *J* = 7.9, 1H), 4.46 (dd, *J* = 6.5, 11.3, 1H), 4.32 (dd, *J* = 7.3, 11.0, 1H), 4.12 (dd, *J* = 5.6, 12.0, 1H), 4.01 (t, *J* = 6.8, 1H), 3.78 (t, *J* = 9.6, 1H), 3.71–3.64 (m, 1H), 2.21 (s, 3H), 2.12 (d, *J* = 1.5, 6H), 2.10 (s, 3H), 2.07 (s, 3H), 1.99 (s, 3H). ^{13}C NMR (151 MHz, $CDCl_3$) δ 170.3, 170.14, 170.07, 169.9, 169.6, 169.1, 169.0, 133.6, 133.0, 129.7, 128.9, 128.7, 128.3, 101.2, 85.4, 77.2, 77.0, 76.8, 76.7, 76.3, 73.8, 71.0, 70.8, 70.2, 69.1, 66.8, 62.1, 20.85, 20.82, 20.81, 20.70, 20.66, 20.5. ESI-MS: 812.3 $[(M+NH_4)^+]$. Anal. calcd for $C_{37}H_{42}O_{17}S$: C, 56.20; H, 5.35. Found: C, 55.61; H, 5.36.

Phenyl [6-^{18}O 0;1]-β-D-galactopyranosyl-(1→4)-1-thio-β-D-glucopyranoside (^{16}O/^{18}O-2.2): A solution of freshly prepared sodium methoxide (0.5 M, 25 mL) was added to compound **2.11** (100.7 mg, 0.13 mmol) and stirred at room temperature overnight. Amberlite IR-120$^+$ resin (H+ form) was added to neutralize the reaction. The suspension was then stirred for 15 min and then filtered. The filtrate was concentrated under reduced pressure afford the desired product as a white solid (52 mg, 93% yield). mp = 195-196 °C. ^{1}H NMR (600 MHz, D_2O) δ 7.57–7.47 (m, 2H, Ar-H), 7.34 (m, 3H, Ar-H), 4.76 (d, *J* = 10 Hz, 1H, 1'-H), 4.38 (d, *J* = 8 Hz, 1H, 1-H), 3.92–3.81 (m, 2H), 3.80–3.52 (m, 8H), 3.52–3.42 (m, 1H), 3.39–3.30 (m, 1H). ^{13}C NMR (151 MHz, D_2O) δ

132.3, 131.4, 131.2, 129.0, 128.8, 127.7, 102.4, 86.6, 78.2, 77.4, 75.3, 74.9, 72.0, 71.0, 70.5, 68.1, 60.5, 59.6. ESI-MS: 436.4 [$(M+H)^+$].

2.3.4 Preparation and Purification of Neu5Acα2,6LacβSPh 2.1

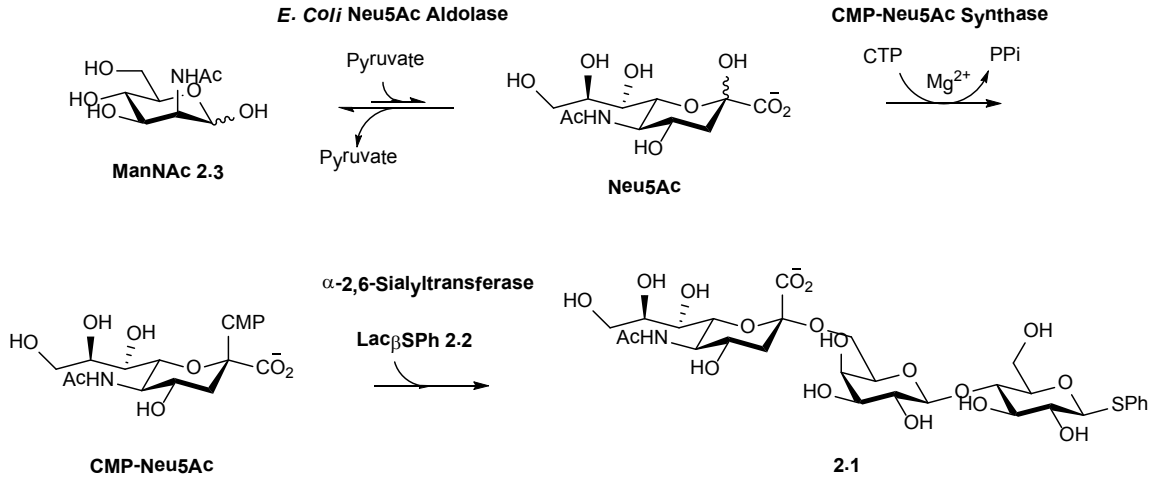

Figure 2-5 Enzyme mediated synthesis of Neu5Acα2,6LacβSPh.

A 15 mL autoclaved falcon tube was charged with *N*-acetyl-D-mannosamine (42.0 mg, 190 μmol), sodium pyruvate (20.9 mg, 190 μmol), water (2 mL) and *E. coli* Neu5Ac aldolase (1 mg). The reaction vessel was incubated and shaken at 37 °C for 3 h. Subsequently cytidine 5'-triphosphate disodium salt (150.2 mg, 285 μmol), tris (1.0 M, 2.0 mL), magnesium chloride (1.0 M, 0.85 mL), dithiothreitol (1.0 M, 1.5 μL) and CMP-Neu5Ac synthase (78 U/mL, 0.35 mL) were added to this reaction mixture. After a further incubation at 37 °C for approximately 1.5 h, the reaction mixture was centrifuged (10 min @ 2500 rpm). The supernatant was separated from the pellet and transferred to a new 15 mL autoclaved falcon tube, after which LacβSPh (82.5 mg, 190 μmol) and α-2,6-

sialyl transferase (0.25 mL, 9.9 U/ml) were added to this solution and the resultant mixture was incubated at 37 °C overnight. Formation of Neu5Acα2,6LacβSPh **2.1** was monitored by TLC, R_F = 0.30 (1:4 v/v water/acetonitrile). When the reaction was complete the mixture was loaded onto a reversed-phased C18 sep-pak cartridge (20 cc, 5 gram), which was eluted successively with water (~50 mL) and acetonitrile-water (1:19, ~120 mL). The fractions containing product were pooled and lyophilized to afford the desired material as a white solid (yields ranged from 40–60%). mp = 166-167 °C. ^{1}H NMR (600 MHz, D_2O) δ 7.57–7.48 (m, 2H), 7.41–7.29 (m, 3H), 4.75 (d, *J* = 11.2 Hz, 1H), 4.35 (d, *J* = 7.9 Hz, 1H), 3.95–3.41 (m, 19H), 3.36 (t, *J* = 9.3 Hz, 1H), 2.62 (dd, *J* = 21.9, 17.2 Hz, 1H), 1.96 (s, 3H), 1.72–1.57 (m, 1H). ^{13}C NMR (151 MHz, D_2O) δ 174.4 (×2), 173.2, 172.8, 131.3, 128.8, 127.7, 102.7, 99.7, 86.4, 78.8, 78.0, 75.5, 73.2, 72.0, 71.9, 71.3, 70.8, 70.3, 68.0, 67.9, 63.1, 62.1, 59.8, 58.8, 51.3, 39.7, 39.4, 21.6.

2.4 NMR Experiments

2.4.1 Acquisition of NMR Spectra

Spectra were acquired on a Bruker AVANCE II digital spectrometer equipped with a digital DRU receiver operating at 600.33 MHz for ^{1}H and 150.90 MHz for ^{13}C. The NMR spectrometer was equipped with a Bruker 5 mm QNP cryoprobe. This direct-detect probe for ^{13}C has cold (20 K) ^{13}C, ^{1}H and ^{2}H coils, and the ^{13}C and ^{1}H preamplifier channels are both cooled to 77 K. Samples were run in 600 MHz-grade 5 mm diameter NMR tubes with a 3 mm coaxial tube insert (Wilmad, Figure 2.6) containing 99.9% deuterium oxide, which was used to lock the spectrometer frequency. The sample temperature was maintained at 298 K using a Bruker BVT-3000 and a Bruker BCU-05 air controller to control a heated flow of air (800 L/h) over the NMR tubes. To overcome radiation damping problems that are associated with cryoprobes, sample temperatures were calibrated using 99%-deuterated methanol.[49]

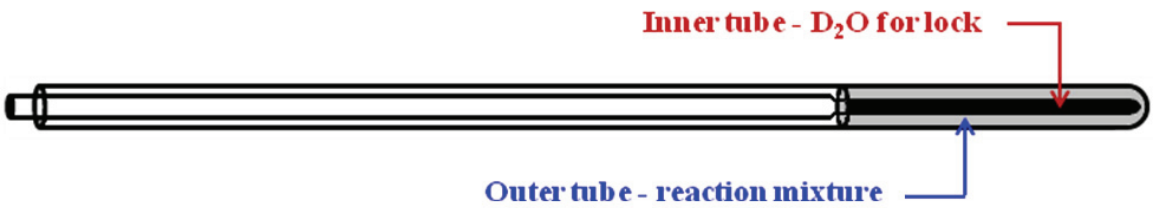

Figure 2-6 Coaxial insert used in NMR experiments.

Automated shimming of the magnetic field using the ^{2}H lock signal (e.g. gradient shimming) was not possible because the deuterated solvent was only present in the central tube. Therefore, samples were manually shimmed by adjusting the various shim currents in order to optimize the ^{1}H NMR spectrum, which was automatically Fourier transformed in real-time every 3 seconds during this procedure.

In a typical experiment, (2,3-^{13}C)-Neu5Acα2,6LacβSPh (~2 mg), (3-^{13}C)-Neu5Acα2,6LacβSPh (~1 mg) and (2-^{13}C)-D-alanine (~0.2 mg) were dissolved in 50 mM sodium acetate buffer (435 μL, pH 5.5). *Vibrio cholerae* sialidase (15 μL) was added and the resultant reaction mixture was transferred into the outer tube. The inner tube containing deuterium oxide was then inserted into the outer tube. The position of the inner tube was adjusted such that the deuterium oxide volume height matched that of the reaction mixture. The ^{13}C-labelled alanine was added as both the internal intensity and the chemical shift (peak set to 50.70 ppm) standards. Pulse lengths were measured with the alanine peak on-resonance and the amplifier power adjusted to yield π/2 pulses of 11.50 μs. The ^{13}C T1 values of the sialyl lactosides were measured using a standard inversion-recovery pulse sequence[50] with a recycle delay set to 31.5 s. T1 values for C3 of the 2,3-sialyl lactoside, and C2 and C3 of the 2,6-sialyl lactoside were determined to be 201 ms, 4.78 s and 214 ms, respectively. The time delay set between acquisition scans were ≥6.5 *T*1 (≥99.85% relaxed).

Quantitative, proton-decoupled ^{13}C NMR spectra were acquired using an inverse-gated pulse sequence[50] to eliminate NOE enhancements. The spectral width was 240 ppm; transmitter frequency was set to 100 ppm. For the experiments in which the anomeric carbon (^{13}C-2) signal was monitored, four dummy scans followed by 32 scans (each consisting of 131072 complex points, acquisition time of 3.5 s) were accumulated with a recycle delay of 31.5 s between scans (21.0 min per spectrum). In cases where the methylene carbon (^{13}C-3) signal was monitored 4 dummy scans, 256 scans and recycle delay of 1.5 s were used (14.5 min per spectrum). Proton decoupling was performed using the WALTZ-16 decoupling sequence[51] (^{1}H pulses of 100 μs, ^{1}H transmitter set to

4.00 ppm). Three repeat spectra were acquired on each sample before addition of enzyme and then a series of spectra were acquired (21.0 or 14.5 min per spectrum, no delay between spectra) after enzyme addition. Note that the magnetic field was re-shimmed and the probe re-tuned after adding the enzyme to achieve optimal (symmetric) peak shapes because the sample volume had increased. During the time course of the experiment the S/N for each spectrum declines and thus several consecutive FIDs could be summed together using the *Topspin* program from Bruker to compensate for this deterioration in data quality. Data acquisition continued until the quantity of unreacted substrate reached ~0.2 mg, at which point increasing S/N values by summing spectra became too costly in terms of NMR spectrometer time. Thus, as the quantity of initial substrates varied in each reaction, the fraction of reaction (F_1) at which data acquisition was stopped generally ranged from 0.75–0.85. Fourier transformation of the FIDs was performed with two-fold zero-filling and application of an exponential line broadening between 0.2–1.0 Hz.

2.4.2 NMR Spectra Fitting

Spectra were manually phased and baseline corrected using Bruker *Topspin* software prior to fitting. The resulting series of quantitative ^{13}C spectra were deconvoluted using procedures coded in a *Mathematica*[52] notebook written by Dr. Darren Brouwer. An initial, automated deconvolution over the chemical shift range of interest (39–52 ppm) was performed by reading in the phased, baseline-corrected spectrum of the sample before addition of the enzyme. From this analysis the peak positions, peak widths at half-height and optimal combination of Lorentzian and Gaussian peaks were determined that best matched the specific sample's resonances. The procedure was repeated on a spectrum selected from the midpoint of the enzyme reaction as the

shimming changes could result in slightly different peaks shapes (and consequently a different ratio of Lorentzian and Gaussian peak shapes). Experimental spectra were fit using the least-squares "NonlinearRegress" function in *Mathematica*. Starting from the initial parameters (with peak positions, peak widths and Lorentzian / Gaussian ratio fixed at the appropriate values), only the peak heights were allowed to vary when performing the "least-squares" fit to the experimental spectrum. For the 2,6-sialyl lactoside substrates the number of peaks that were included in the fitting algorithm were: (i) oxygen-18 KIE measurements 3 peaks, which included the alanine α-carbon resonance, and (ii) carbon-13 KIE experiments, 4 peaks (1 doublet and 2 singlets). Whereas, for the 2,3-sialyl lactoside carbon-13 KIE measurements, 7 peaks were fit (three for the remaining substrate, three for the β-sialic acid product, and the alanine reference singlet). Normalization was achieved by dividing peak areas for reactants by that found for alanine in the same spectrum. This procedure removed effects of variations between individual spectra (such as number of scans etc.). The resultant fraction of reaction (F_1) and individual peak areas were calculated and this data was input into "Prism-4", and a non-linear least squares fit to equation 2.1[39] was performed, where F_1 is the fraction of reaction for the light isotopomer, k_1/k_2 is the KIE, and R and R_0 are the concentration ratios of heavy to light isotopomers at times = t and 0, respectively. All errors quoted in this chapter are standard errors.

Eq. 2.1

$$\frac{R}{R_0} = (1 - F_1)^{(k_2/k_1) - 1}$$

2.5 Results and Discussion

2.5.1 Anomeric ^{13}C KIEs

Presented in Figure **2-7** is a representative stacked plot of three ^{13}C NMR spectra collected during the *V. cholerae* sialidase-catalyzed reaction. The spectra displays the sialosyl C-3 signals of a ~1:2 mixture of singly (**2.1c**, $w = {}^{13}C$) and doubly (**2.1d**, $w = x = {}^{13}C$) labelled Neu5Acα2,6LacβSPh. The peak intensities for the singly labelled C-3 signals were adjusted to the same intensity. In addition, a dotted line is added to serve as a visual aid when comparing the relatively peak intensities corresponding to the "light" and "heavy" isotopomers as the reaction progresses. The NMR resonances for the initially formed α-Neu5Ac product[53,54] and the thermodynamically more stable β-anomer[55] are centred at 40.75 and 39.45 ppm, respectively. The derived anomeric ^{13}C-KIEs for the sialidase-catalyzed hydrolysis of Neu5Acα2,6LacβSPh obtained from Eq. 2.1 are 1.0169(14), 1.0167(15) and 1.0164(12) (standard error in parentheses, relating to the last two significant figures). In contrast to existing methods that sample the isotopic ratio at a single point, typically at a high fraction of reaction, the current protocol obtains a high level of accuracy and precision by accumulating data throughout the time-course of the reaction. Fits of experimental spectra before the addition of enzyme ($F_1 = 0.00$) and at a high fraction of reaction ($F_1 = 0.79$) are shown below (Figure 2-8). Plots of the fits to Eq. 2.1 for the experimental data from three separate runs are displayed in Figure 2-9.

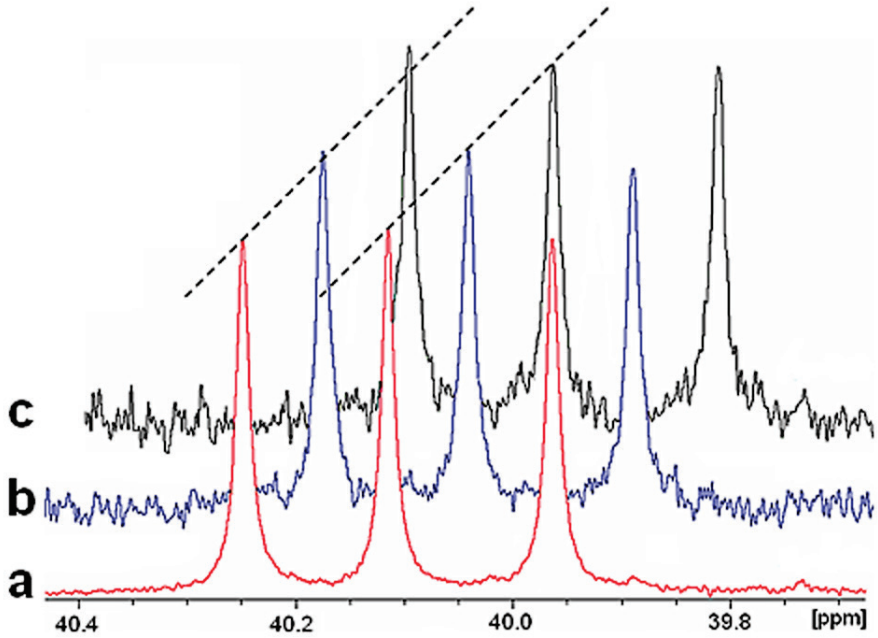

Figure 2-7 ^{13}C NMR spectra of the sialosyl C-3 atom from an approximate 1:2 mixture of singly (**2.1c**, w = ^{13}C) and doubly (**2.1d**, x = w = ^{13}C) labelled Neu5Acα2,6LacβSPh. (a) Fraction of reaction $F_1 = 0.00$, (b) $F_1 = 0.63$, (c) $F_1 = 0.79$.

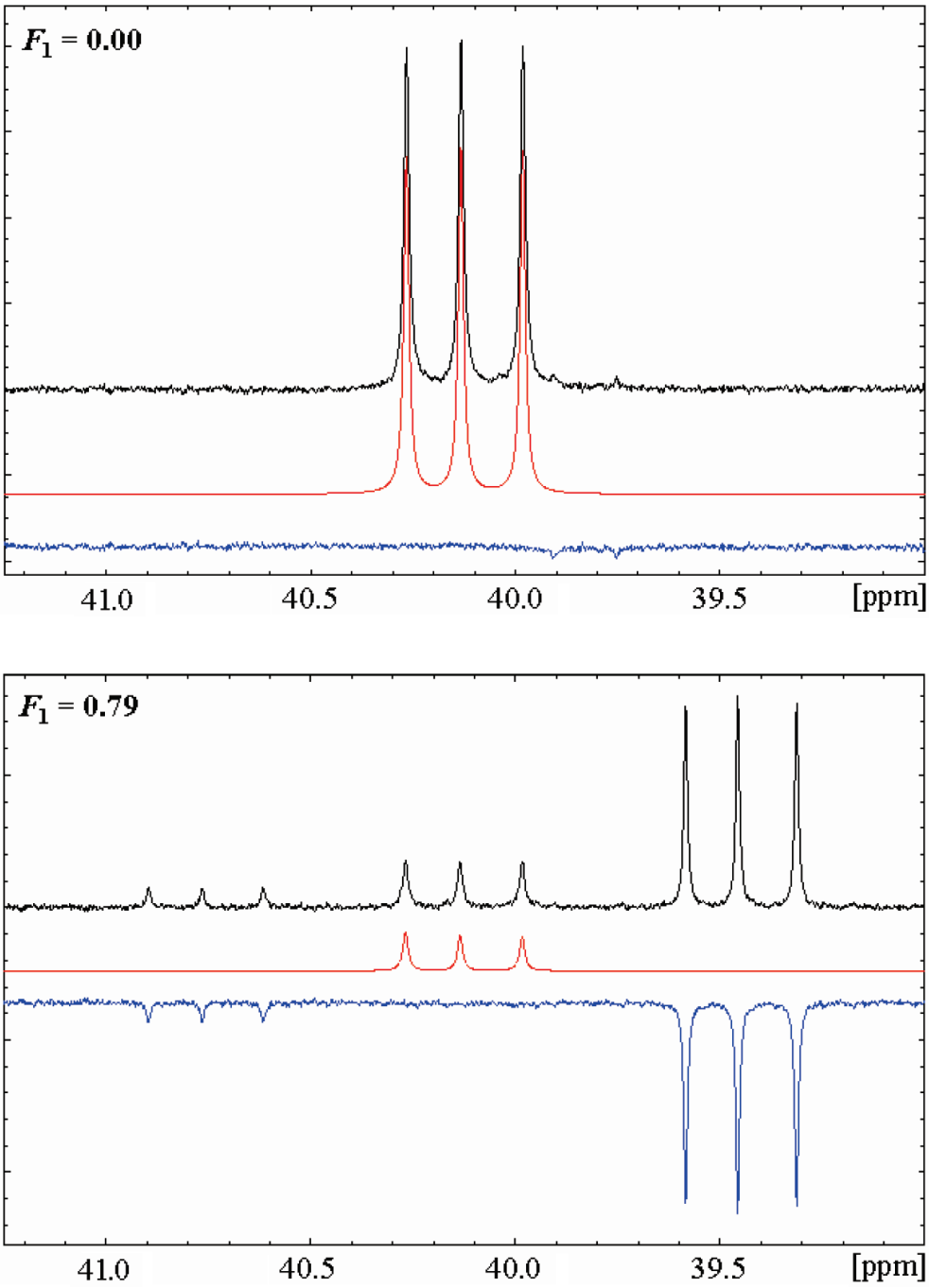

Figure 2-8 Fit of the experimental spectra for *V. cholerae* sialidase-catalyzed hydrolysis of **2.1c** (w = ^{13}C) and **2.1d** (w = x = ^{13}C) using the least-squares "NonlinearRegress" function in Mathematica. Experimental spectra in black; calculated spectra in red; and difference spectra in blue.

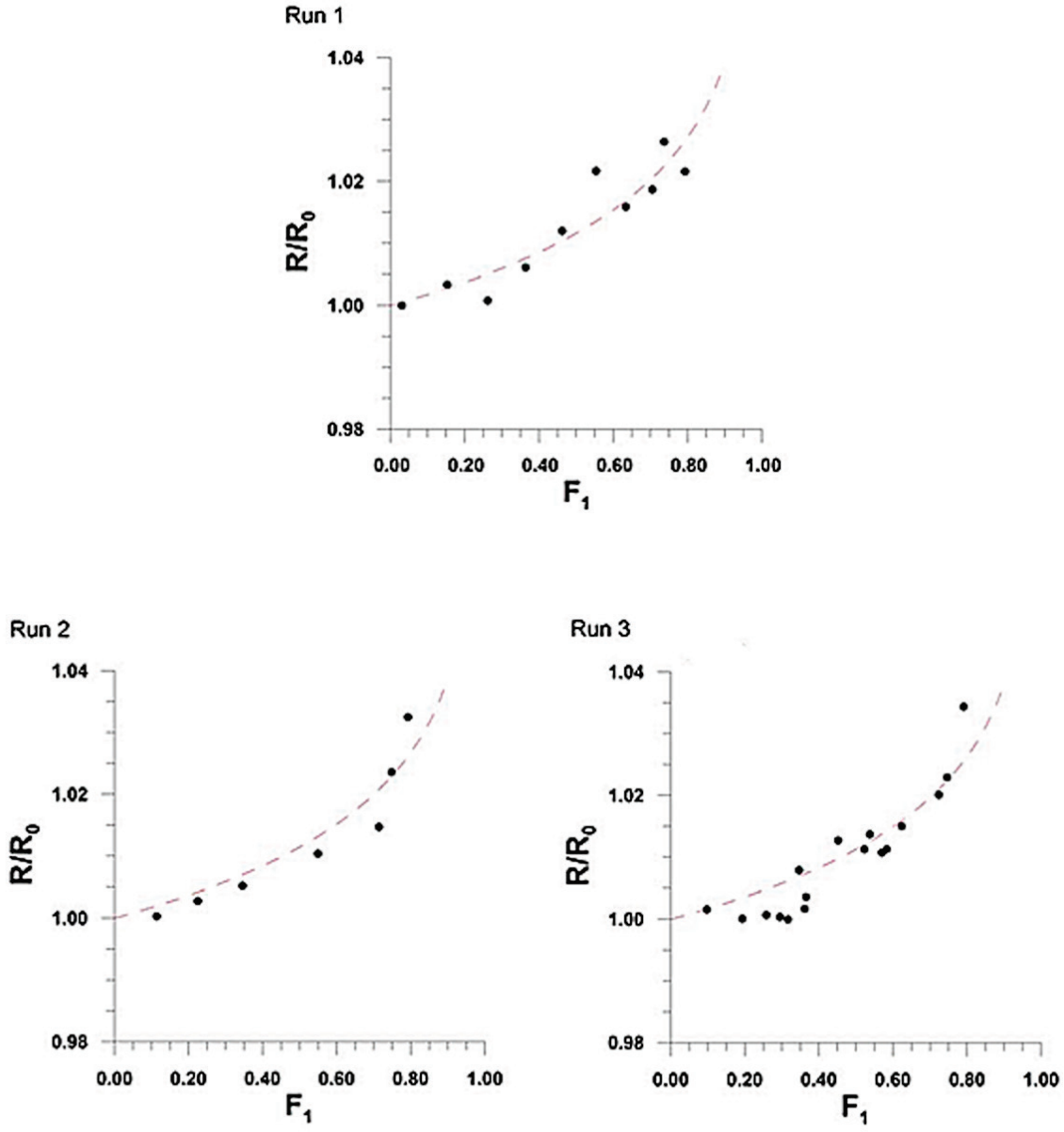

Figure 2-9 Plots of fits for the experimental data of the *V. cholerae S*ialidase-catalyzed hydrolysis of singly (**2.1c**, w = ^{13}C) and doubly (**2.1d**, w = x = ^{13}C) labelled Neu5Acα2,6LacβSPh to eq. 2.1. The best fit line is shown in each plot.

2.5.2 Leaving Group and Ring ^{18}O KIEs

Presented in Figure 2-10 is a representative stacked plot of three ^{13}C NMR spectra collected during progress of the *V. cholerae* sialidase-catalyzed reaction. The spectra displays the sialosyl C-2 signals of a ~1:1 mixture of singly (**2.1a**, *x* = ^{13}C) and doubly (**2.1e**, *x* = ^{13}C, z = ^{18}O) labelled Neu5Acα2,6LacβSPh. The results indicate that the upfield resonance of the doubly labelled substrate (^{13}C–^{18}O) increases in relative intensity during the hydrolysis reactions. The corresponding derived leaving group ^{18}O-KIEs are 1.0400(14), 1.0388(17) and 1.0393(38) for runs 1, 2 and 3, respectively. Plots of the fits to Eq. 2.1 for the experimental data from three separate runs are shown in Figure 2-11.

Shown in Figure 2-12 are representative stacked plot of three ^{13}C NMR spectra from a competitive hydrolysis reaction between singly labelled (**2.1a**, x = ^{13}C) and double labelled (**2.1b**, y = ^{18}O, x = ^{13}C) Neu5Acα2,6LacβSPh. In contrast, the downfield resonance increases in relative intensity which is consistent with an inverse KIE. The derived ^{18}O-KIE values for three runs are 0.9747(17), 0.9749(31) and 0.9743(25). Plots of the fits to Eq. 2.1 for the experimental data from three separate runs are shown in Figure 2-13. Mathematica fits for both the leaving group and ring oxygen experiments are not shown.

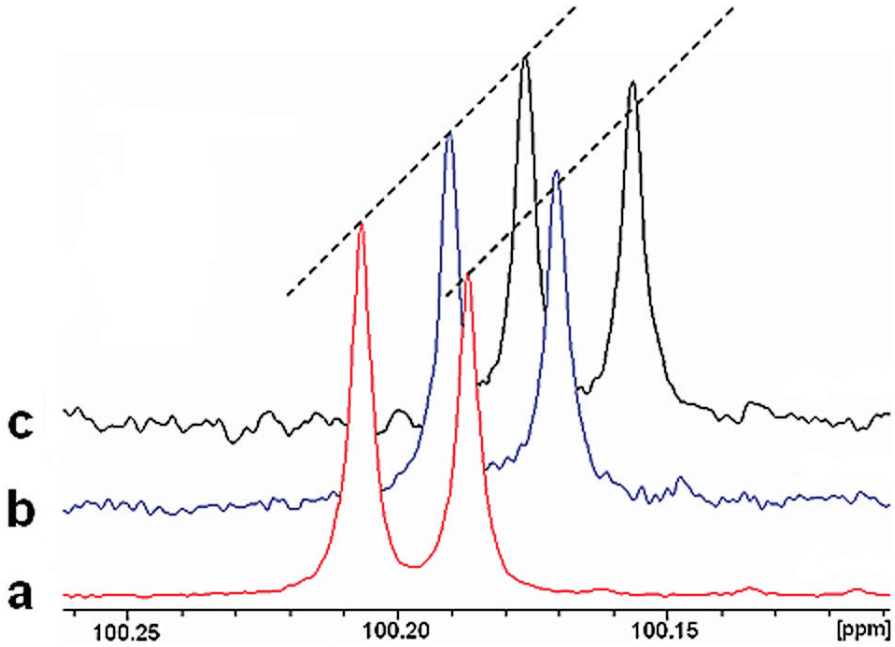

Figure 2-10 ^{13}C NMR spectra of the sialosyl C-2 atom from an approximate 1:1 mixture of singly (**2.1a**, x = ^{13}C) and doubly (**2.1e**, x = ^{13}C, z = ^{18}O) labelled Neu5Acα2,6LacβSPh. (a) Fraction of reaction $F_1 = 0.00$, (b) $F_1 = 0.65$, (c) $F_1 = 0.77$

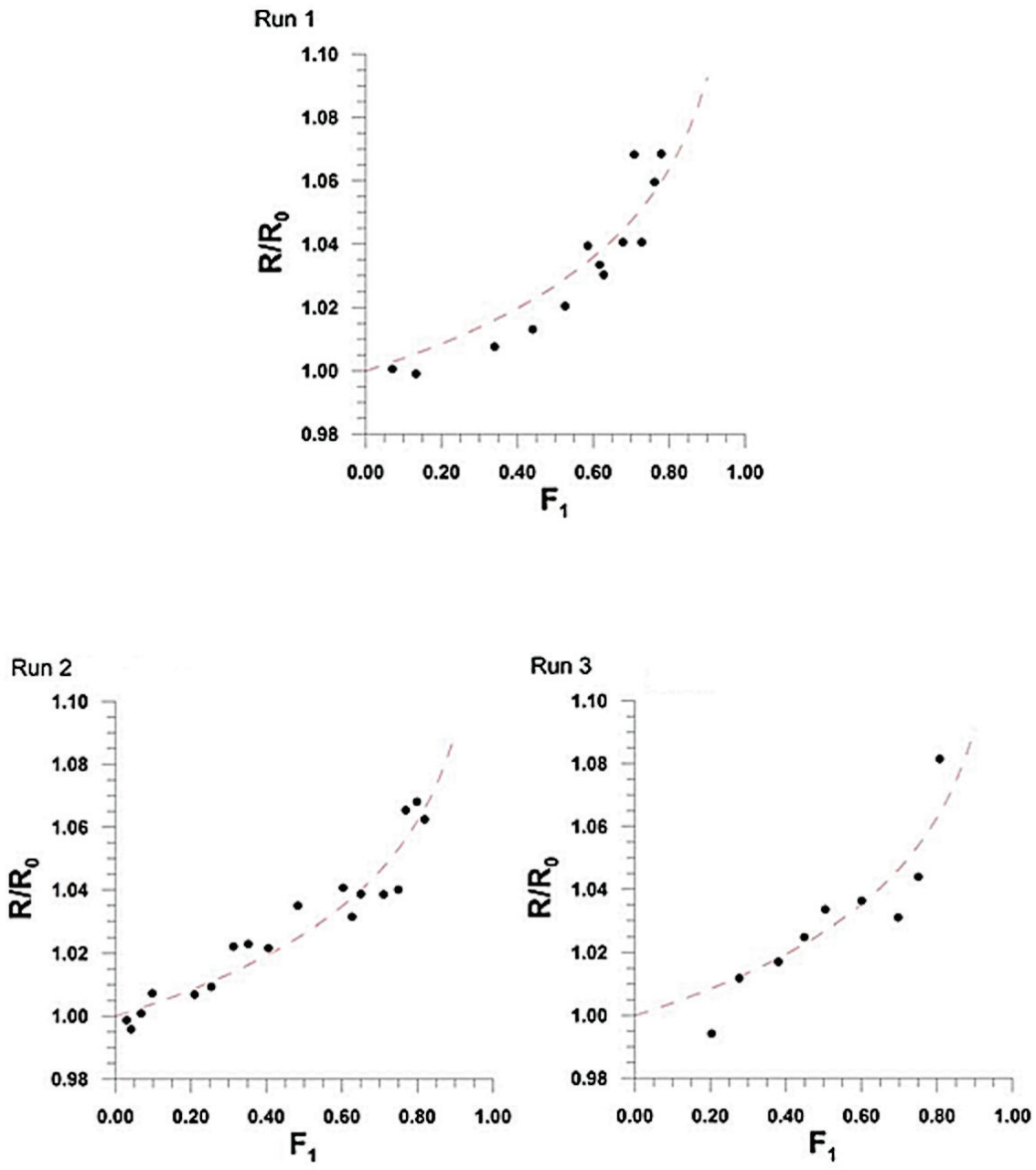

Figure 2-11 Plots of fits for the experimental data of the *V. cholerae* Sialidase-catalyzed hydrolysis of singly (**2.1a**, x = ^{13}C) and doubly (**2.1e**, x = ^{13}C, z = ^{18}O) labelled Neu5Acα2,6LacβSPh to Eq. 2.1. The best-fit line is shown in each plot.

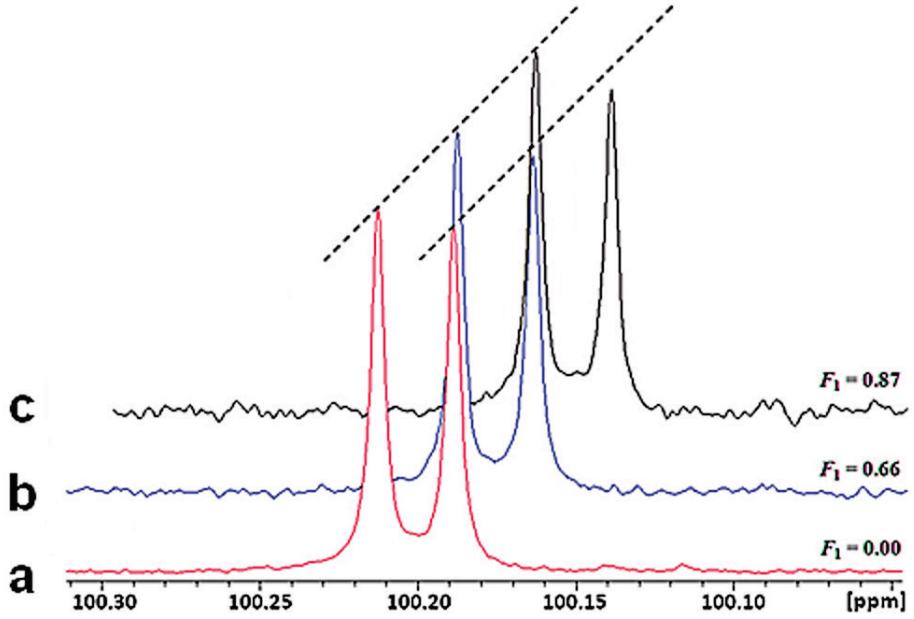

Figure 2-12 ^{13}C NMR spectra of the sialosyl C-2 atom from an approximate 1:1 mixture of singly (**2.1a**, x = ^{13}C) and doubly (**2.1b**, y = ^{18}O, x = ^{13}C) labelled Neu5Acα2,6LacβSPh.

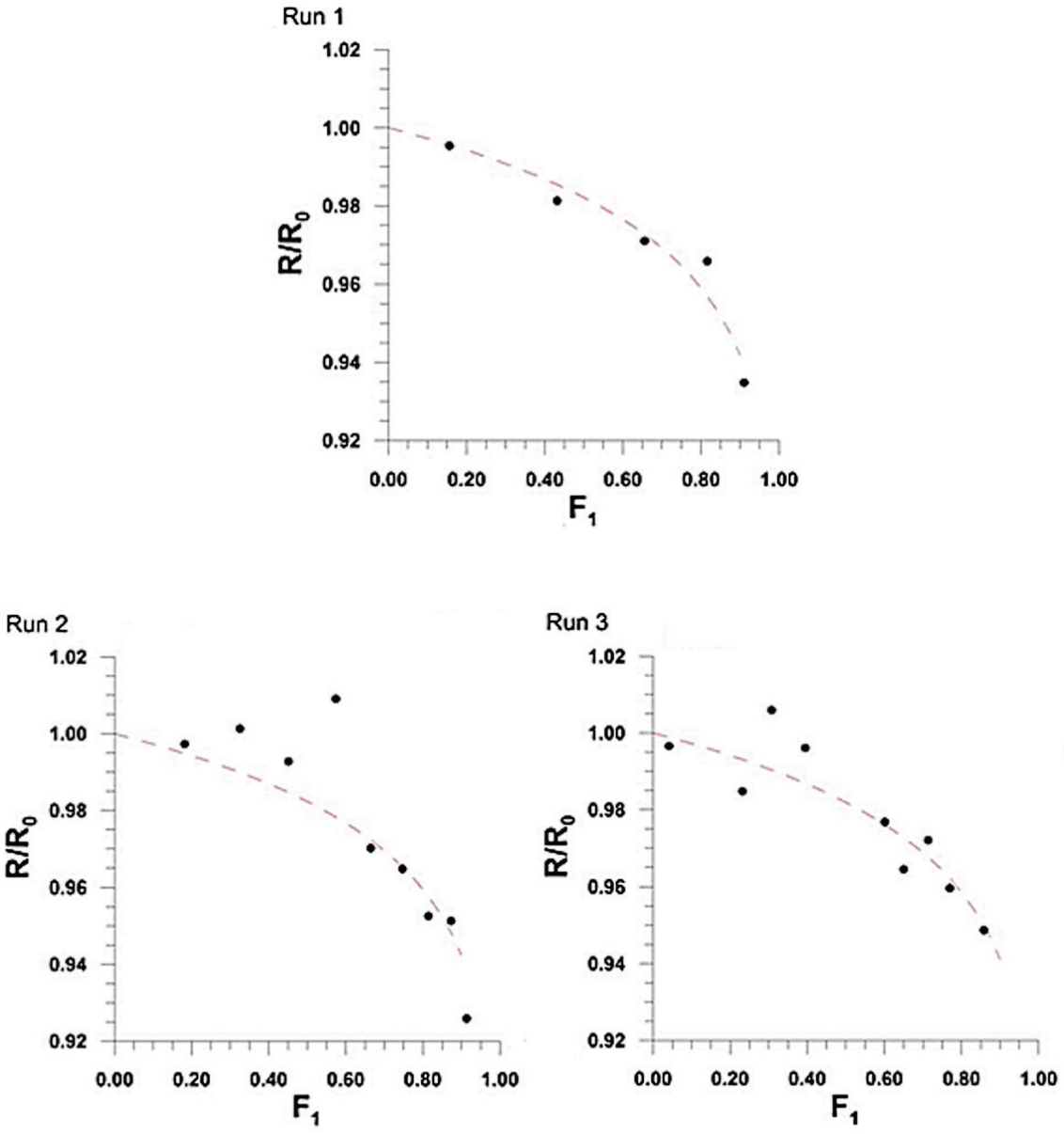

Figure 2-13 Plots of fits for the experimental data of the *V. cholerae* Sialidase-catalyzed hydrolysis of singly (**2.1a**, x = ^{13}C) and doubly (**2.1e**, x = ^{13}C, z = ^{18}O) labelled Neu5Acα2,6LacβSPh to Eq. 2.1. The best-fit line is shown in each plot.

2.5.3 Interpretation of KIE Data

V. cholerae sialidase is a retaining enzyme which operates via a double displacement mechanism.[56] β_{lg} analysis of this enzyme has demonstrated that glycosylation, the first chemical step in the catalytic pathway, is rate-limiting.[45] The sizable leaving group ^{18}O-KIE on k_{cat}/K_m (k_{16}/k_{18} = 1.046) for the *V. cholerae* sialidase-catalyzed hydrolysis of Neu5AcαPNP is consistent with extensive C−O bond cleavage and minimal proton donation to the leaving group oxygen atom.[45] In the current study, the derived leaving group ^{18}O-KIE (^{18}V = 1.039) for Neu5Acα2,6LacβSPh is similar in magnitude thus suggesting that the extent of C-O cleavage and proton transfer is comparable for both substrates. This finding is surprising since the corresponding lactoside is a poorer leaving group than 4-nitrophenol based on the ~6.5 p*K*a unit difference in their acidities. With regard to the anomeric ^{13}C-KIE (^{13}V = 1.017) presented in this study, we are unable unambiguously to determine whether glycosylation operates via a S_N2 or a S_N1 process since this value is bracketed by KIEs typical for both mechanisms. Finally, the size of the inverse ^{18}O-KIE associated with the ring oxygen atom requires that charge is delocalized onto the oxygen atom at the TS.

The reaction coordinate presented in Figure 2-14 for the sialidase-catalyzed glycosylation reaction is consistent with the present KIEs. An enzyme:substrate complex[35] positions the sialoside substrate in a $^4S_2$ skew-boat conformation, which passes through a $^4H_5$ half-chair TS conformation during glycosidic bond cleavage to yield a $^2C_5$ chair conformation for the enzyme bound intermediate.[57] It is worth mentioning that the present data does not allow us to determine whether the active site glutamate is assisting the tyrosine nucleophile to attack at the TS. Further studies in the form of mutagenesis and complementary kinetics should help to address this issue.

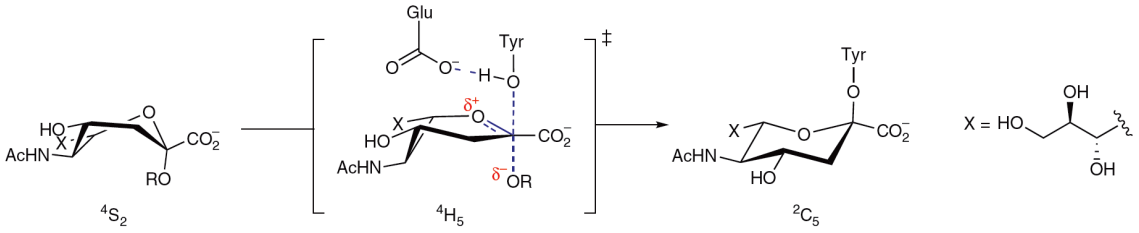

Figure 2-14 Proposed glycosylation TS that is consistent with derived KIEs.

2.5.4 Conclusions

We have developed a novel NMR-based methodology which allows for the determination of accurate and precise competitive KIEs. Compared to existing methods, the current technique possesses a number of key advantages: i) data is collected continuously throughout the entire reaction as opposed to most competitive techniques that rely on single-point determinations; ii) the technique can be used to measure KIEs for NMR inactive nuclei such as ^{18}O; iii) it is unnecessary to assign an internal reference atom for which the KIE is assumed to be unity, as is the case for current NMR and radioisotope methods; iv) the KIE can also be calculated using the product isotopomer ratio;[39] vi) other probe nuclei, including ^{1}H, ^{15}N, ^{19}F and ^{31}P, can be used; and vii) is compatible with enzyme-catalyzed reactions since only milligram quantities of labelled substrates are required.

2.6 Supplementary Data

Run No.	Fraction of Reaction (F_1)	R/R_0
1	0.0304	1.0000
1	0.1529	1.0034
1	0.2618	1.0008
1	0.3639	1.0061
1	0.4623	1.0120
1	0.5539	1.0217
1	0.6337	1.0159
1	0.7049	1.0187
1	0.7364	1.0264
1	0.7926	1.0216
2	0.1136	1.0003
2	0.2248	1.0028
2	0.3458	1.0052
2	0.5491	1.0104
2	0.7141	1.0147
2	0.7480	1.0236
2	0.7922	1.0325
3	0.0968	1.0016
3	0.1926	1.0001
3	0.2572	1.0007
3	0.2949	1.0004
3	0.3166	1.0000
3	0.3466	1.0079

3	0.3655	1.0036
3	0.3611	1.0017
3	0.4519	1.0127
3	0.5225	1.0113
3	0.5372	1.0137
3	0.5695	1.0107
3	0.5833	1.0113
3	0.6235	1.0150
3	0.7234	1.0201
3	0.7455	1.0229
3	0.7910	1.0344

Table 1 Data From the VcNA-Catalyzed Hydrolysis of a Mixture of **2.1c** and **2.1d** at 298 K in 50 mM Sodium Acetate Buffer (pH 5.5)

Run No.	Fraction of Reaction (F_1)	R/R_0
1	0.0704	1.0006
1	0.1325	0.9991
1	0.3396	1.0077
1	0.4398	1.0132
1	0.5251	1.0205
1	0.5853	1.0394
1	0.6169	1.0334
1	0.6267	1.0303
1	0.6781	1.0406
1	0.7074	1.0683
1	0.7275	1.0406
1	0.7616	1.0596
1	0.7789	1.0685

2	0.0297	0.9987
2	0.0414	0.9959
2	0.0679	1.0009
2	0.0976	1.0073
2	0.2093	1.0069
2	0.2535	1.0094
2	0.3123	1.0222
2	0.3516	1.0230
2	0.4049	1.0217
2	0.4828	1.0350
2	0.6028	1.0407
2	0.6260	1.0315
2	0.6497	1.0387
2	0.7099	1.0386
2	0.7491	1.0401
2	0.7684	1.0654
2	0.7982	1.0681
2	0.8190	1.0625
3	0.2033	0.9942
3	0.2762	1.0119
3	0.3801	1.0171
3	0.4488	1.0249
3	0.5037	1.0336
3	0.5999	1.0363
3	0.6968	1.0310
3	0.7500	1.0440
3	0.8071	1.0815

Table 2 Data From the VcNA-Catalyzed Hydrolysis of a Mixture of **2.1a** and **2.1e** at 298 K in 50 mM Sodium Acetate Buffer (pH 5.5)

Run No.	Fraction of Reaction (F_1)	R/R_0
1	0.1556	0.9954
1	0.4315	0.9813
1	0.6557	0.9710
1	0.8161	0.9658
1	0.9102	0.9348
2	0.1818	0.9973
2	0.3250	1.0013
2	0.4509	0.9928
2	0.5734	1.0091
2	0.6647	0.9702
2	0.7471	0.9648
2	0.8140	0.9526
2	0.8725	0.9514
2	0.9131	0.9259
3	0.0410	0.9966
3	0.2314	0.9848
3	0.3074	1.0060
3	0.3943	0.9961
3	0.6005	0.9768
3	0.6496	0.9645
3	0.7130	0.9721
3	0.7692	0.9597
3	0.8582	0.9487

Table 3 Data From the VcNA-Catalyzed Hydrolysis of a Mixture of **2.1a** and **2.1b** at 298 K in 50 mM Sodium Acetate Buffer (pH 5.5)

3: TRANSITION STATE ANALYSIS OF *VIBRIO CHOLERAE* SIALIDASE-CATALYZED HYDROLYSES WITH NATURAL SUBSTRATE ANALOGUES

3.1 Introduction

Vibrio cholerae, a gram-negative bacterium, is responsible for cholera, an illness characterized by acute diarrhea which can result in death due to severe dehydration.[58] The first well documented cholera epidemic occurred in India nearly 200 years ago[59] but has since been eradicated from most developed countries. Nonetheless, cholera continues to be a serious health concern in many third-world nations. Its presence and impact are especially evident after a natural disaster (i.e., 2010 Haitian earthquake)[60,61] which is typically associated with a breakdown of water and sanitation infrastructure. Upon infection, *V. cholerae* aggressively secretes an enterotoxin which binds to the GM_1 ganglioside of enterocyte microvilli.[62] This critical interaction leads to internalization of the toxin and triggers a cyclic adenosine monophosphate (cAMP) mediated disruption of the sodium and chloride channels resulting in profuse diarrhea.[62]

In addition, members of the O1 serogroup are known to produce an 83 kDa *exo*-sialidase[63] (EC 3.2.1.18; VcNA) which has been shown to process higher order gangliosides to yield GM_1.[64] Subsequent studies have established a synergistic relationship between VcNA and the *V. cholerae* toxin in which VcNA activity enhances toxin binding.[65] X-ray crystallography has revealed VcNA folds into a central catalytic domain flanked by two carbohydrate-binding modules (CBM)[63], one of which displays an

unprecedented affinity for α-sialic acid motifs.[66] It is believed that this CBM is involved in directing *V. cholerae* to the small intestine where epithelial cells are rich in sialic acid.[67] Due to its role in pathogenesis, VcNA has been identified as a potential target for drug development.

One approach to drug discovery is to gain a detailed mechanistic understanding of the target enzyme by performing kinetic isotope effect (KIE) measurements. Key transition state (TS) features such as geometry, charge development and the degree of bond cleavage and formation can serve as a blue-print for designing tight-binding TS analogue inhibitors.[40] With regard to VcNA, the first KIE measurements were detailed by Guo and Sinnott using, an activated substrate, *p*-nitrophenyl α-sialoside **3.1** as the reporter molecule.[45] The authors measured four heavy-atom KIEs on the kinetic parameters *V*/*K* and *V*. This includes three β-secondary ^{2}H-KIEs and a leaving group ^{18}O-KIE.[45] Activated substrates alter the free energy profiles for enzyme-catalyzed reactions, and as such can involve TSs and/or rate-limiting steps that are different from those of natural substrates. Therefore, it is better to probe the VcNA hydrolysis TS using natural substrate analogues. The determination of a ^{13}C-KIE, a ring-oxygen ^{18}O-KIE and a leaving group ^{18}O-KIE were reported for Neu5Acα2,6βSPh (see Chapter 2 of this thesis).[68] In this chapter additional ^{13}C-KIE, ^{18}O-KIEs and β-secondary ^{2}H-KIEs are reported to assist fully characterization of the enzymatic TS for hydrolysis of 2,3- and 2,6- natural substrate analogues.

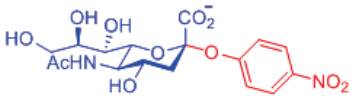

Neu5AcαPNP 3.1

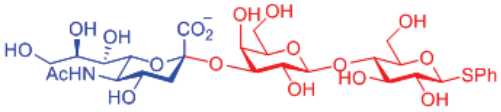

Neu5Acα2,3LacβSPh 3.2

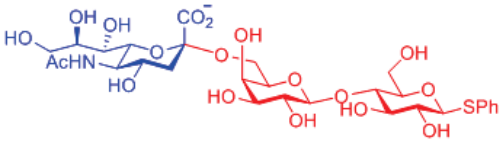

Neu5Acα2,6LacβSPh 3.3

Figure 3-1 α-Sialosides used to measure KIEs for VcNA-catalyzed hydrolysis reactions.

3.2 Substrate Synthesis

The chemoenzymatic synthesis and purification of Neu5Acα2,3βSPh **3.2** was identical to the procedure described in Chapter 2 for the preparation of Neu5Acα2,6βSPh **3.3**. The isotopomers required in this present study are summarized below (Figure 3-2). The requisite labelled [C3-^{13}C]-deuterated Neu5Ac was prepared from [C3-^{13}C]-Neu5Ac using an established protocol.[24] 3'-^{18}O-1-Thiolactoside **3.4** was prepared from the unlabelled thiolactoside and full experimental details are given below.

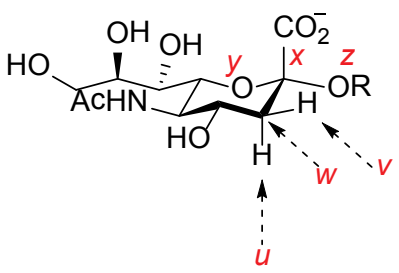

3.2. R = -3LacβSPh

3.2a. X = ^{13}C
3.2b. X = ^{13}C, Y = ^{18}O
3.2c. X = ^{13}C, Z = ^{18}O
3.2d. W = ^{13}C
3.2e. W = ^{13}C, U = ^{2}H
3.2f. W = ^{13}C, V = ^{2}H
3.2g. X = W = ^{13}C

3.3. R = -6LacβSPh

3.3a. W = ^{13}C
3.3b. W = ^{13}C, U = ^{2}H
3.3c. W = ^{13}C, V = ^{2}H

Figure 3-2 Requisite panel of isotopically labelled **3.2** and **3.3** used in the measurement of VcNA KIEs.

3.2.1 Synthesis of 3'-^{18}O-1-thiolactoside

A sequence involving selective isopropylidenation, acetylation and isopropylidene deprotection of unlabelled 1-thiolactoside **3.2** was used to isolate the 3'- and 4'-OH groups for further derivatization. Compound **3.7** was subsequently treated with ethyl orthoacetate to generate the corresponding orthoester moiety *in situ*. Upon addition of $H_2{}^{18}O$, the intermediate was hydrolyzed to yield compound **3.8** where the 4'-*O*-acetyl carbonyl oxygen atom was selectively labelled. The 3'-OH was then activated with trifluoromethanesulfonic anhydride and displaced with sodium nitrite to afford compound

3.9, which features the corresponding D-gulose configuration. Next, compound **3.10** was generated by 3'-OH triflation which facilitates an intramolecular transfer of the acetyl group. Finally, standard Zemplín conditions were used to afford compound **3.4** in 24% overall yield in nine steps (Figure 3-3).

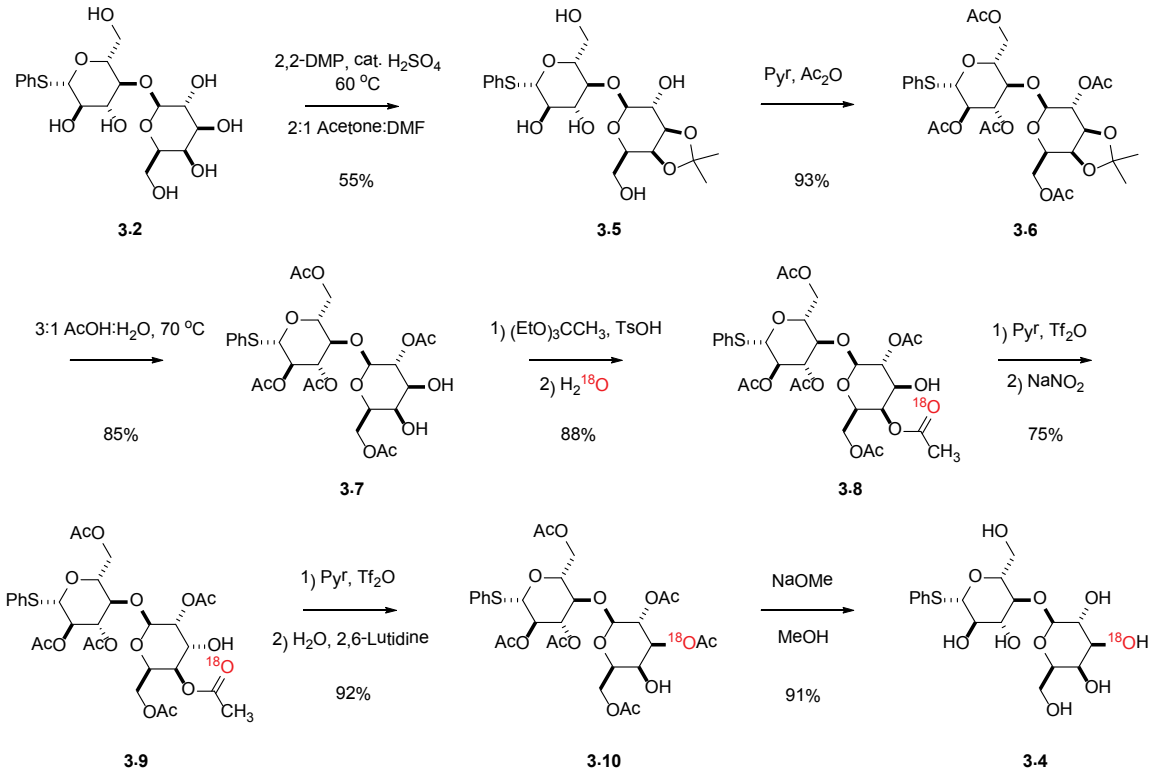

Figure 3-3 Synthesis of 3'-^{18}O-1-thiolactoside.

Phenyl (3,4-*O*-isopropylidene-β-D-galactopyranosyl)-(1→4)-1-thio-β-D-glucopyranoside (3.5): A solution of compound **3.2** (3.50 g, 8.06 mmol), 2,2-dimethoxypropane (1.7 mL, 14 mmol), anhydrous DMF (31 mL) and acetone (65 mL) was treated with conc. sulfuric acid (90 µL, 1.7 mmol). The reaction mixture was stirred

at 60 °C until TLC analysis showed the reaction to be complete, R_F = 0.33 (1:9 v/v methanol/dichloromethane). Upon removal of the volatiles under reduced pressure, the crude residue was washed with ether (2 × 50 mL) and purified via flash chromatography (1:9 v/v methanol/dichloromethane) to afford the desired product as a white solid (1.33 g, 55% yield). mp = 192-193 °C. ^{1}H NMR (600 MHz, CH_3OD) δ 7.64 – 7.53 (m, *J* = 7.3, 2H), 7.37–7.24 (m, *J* = 7.2, 25.5, 3H), 4.63 (d, *J* = 9.8, 1H), 4.39 (d, *J* = 8.3, 1H), 4.27–4.17 (m, 1H), 4.11–4.03 (m, 1H), 3.95 (s, 1H), 3.93–3.88 (m, 1H), 3.87–3.74 (m, 3H), 3.58 (dt, *J* = 8.8, 17.5, 2H), 3.47 (t, *J* = 7.7, 2H), 3.32–3.27 (m, 1H), 1.49 (s, 3H, CH_3), 1.34 (s, 3H, CH_3). ^{13}C NMR (151 MHz, CH_3OD) δ 133.55, 131.61, 128.5, 127.1, 109.7, 102.7, 87.7, 79.5, 79.1, 79.0, 76.5, 74.0, 73.7, 73.1, 72.2, 61.0, 60.5, 27.0, 25.1. ESI-MS: 497.1 [$(M+Na)^+$].

Phenyl (2,6-di-*O*-acetyl-3,4-*O*-isopropylidene-β-D-galactopyranosyl)-(1→4)-2,3,6-tri-*O*-acetyl -1-thio-β-D-glucopyranoside (3.6): A solution of compound **3.5** (810 mg, 1.71 mmol) in pyridine (20.0 mL) was cooled in an ice-bath and treated with acetic anhydride (1.61 mL, 17.1 mmol). The reaction mixture was stirred at room temperature overnight, diluted with dichloromethane (50 mL) and poured into cold water (100 mL). After separation, the organic layer was washed successively with 10% sulfuric acid (2 × 50 mL), sat. aqueous sodium bicarbonate (2 × 50 mL) and brine (50 mL). Upon drying (sodium sulfate) and concentration, the crude residue was purified via flash chromatography (1:1 v/v ethyl acetate/Hexanes) to afford the desired product as a white solid (1.09 g, 93% yield). mp = 69-70 °C. ^{1}H NMR (600 MHz, $CDCl_3$) δ 7.54–7.42 (m, 2H), 7.36–7.29 (m, 3H), 5.21 (t, *J* = 9.1, 1H), 4.93 (t, *J* = 9.7, 1H), 4.88–4.82 (m, 1H), 4.68 (d, *J* = 10.1, 1H), 4.49 (d, *J* = 10.5, 1H), 4.30 (m, 3H), 4.21–4.09 (m, 3H), 3.93 (s,

1H), 3.72 (t, *J* = 9.5, 1H), 3.67 (m, 1H), 2.08 (m, 15H), 1.53 (s, 3H), 1.32 (s, 3H). ^{13}C NMR (151 MHz, $CDCl_3$) δ 170.7, 170.4, 169.9, 169.6, 169.2, 132.8, 132.1, 128.9, 128.2, 110.9, 100.4, 85.7, 76.8, 76.0, 73.4, 73.1, 72.7, 70.9, 70.3, 63.1, 62.4, 27.3, 26.1, 20.84, 20.83, 20.79, 20.7. ESI-MS: 381.1 [$(M+Na)^+$]

Phenyl (2,6-di-*O*-acetyl-β-D-galactopyranosyl)-(1→4)-2,3,6-tri-*O*-acetyl-1-thio-β-D-glucopyranoside (3.7): A solution of compound **3.6** (825 mg, 1.2 mmol) in water (5 mL) and glacial acetic acid (15 mL) was stirred at 70 °C and the reaction was monitored by TLC analysis, R_F = 0.43 (1:9 v/v methanol/dichloromethane). Upon completion, sat. aqueous sodium bicarbonate was added to neutralize the reaction mixture. After extraction with dichloromethane (3 × 50 mL), the combined organic layers were dried (sodium sulfate) and concentrated under reduced pressure. The crude residue was purified via flash chromatography (1:19 v/v methanol/dichloromethane) to afford the desired product as a colourless syrup (660.1 mg, 1.0 mmol, 85% yield). ^{1}H NMR (600 MHz, $CDCl_3$) δ 7.48 (m, 2H), 7.31 (m, 3H), 5.19 (t, *J* = 9.1, 1H), 4.97–4.89 (m, 1H), 4.81 (dd, *J* = 7.9, 9.6, 1H), 4.68 (d, *J* = 10.1, 1H), 4.54 (dd, *J* = 1.9, 11.8, 1H), 4.35 (m, 2H), 4.23 (dd, *J* = 6.4, 11.4, 1H), 4.17 (dd, *J* = 5.9, 11.8, 1H), 3.83 (d, *J* = 3.0, 1H), 3.76 – 3.69 (m, 1H), 3.69–3.64 (m, 1H), 3.64–3.57 (m, 2H), 2.12 (s, 3H), 2.10 (d, *J* = 3.6, 3H), 2.09 (s, 3H), 2.08 (s, 3H), 2.03 (s, 3H). ^{13}C NMR (151 MHz, $CDCl_3$) δ 171.8, 171.1, 170.4, 170.1, 169.6, 132.8, 128.9, 128.2, 100.7, 85.7, 76.9, 76.1, 74.0, 73.7, 72.9, 72.0, 70.2, 68.1, 62.4, 62.1, 20.90, 20.87, 20.83. ESI-MS: 662.2 [$(M+NH_4)^+$]

Phenyl (2,6-di-*O*-acetyl-4-*O*-(^{18}O)acetyl-β-D-galactopyranosyl)-(1→4)-2,3,6-tri-*O*-acetyl-1-thio-β-D-glucopyranoside (3.8): A flame-dried flask was charged with compound **3.7** (200 mg, 0.31 mmol), dry acetonitrile (10 mL), triethyl orthoacetate (0.3

mL, 1.6 mmol) and *p*-toluenesulfonic acid (10 mg, 0.05 mmol). The resultant solution was stirred at room temperature and was shown by TLC analysis to be complete after 30 min, R_F = 0.48 (1:4 v/v acetone/toluene). (^{18}O)-Water (25 μL, 1.24 mmol; Marshall Isotopes, 95.1% atom% O-18, batch no. 020414nw) was added to the mixture, which was stirred for an additional 1 hr. After addition of ethanol (5 mL), the volatiles were removed under reduced pressure. The crude residue was purified via flash chromatography (3:7 v/v acetone/toluene) to afford the desired product as a light yellow syrup (187.9 mg, 0.27 mmol, 88% yield). ^{1}H NMR (600 MHz, $CDCl_3$) δ 7.45–7.36 (m, 2H), 7.28–7.21 (m, 3H), 5.22 (s, 1H), 5.14 (t, *J* = 8.9, 1H), 4.85 (t, *J* = 9.5, 1H), 4.78 (s, 1H), 4.66–4.57 (m, 1H), 4.51–4.43 (m, 1H), 4.39–4.30 (m, 1H), 4.13–4.06 (m, 1H), 4.06–3.94 (m, 2H), 3.78–3.54 (m, 4H), 2.10 (d, *J* = 4.0, 6H), 2.07–2.00 (m, 6H), 1.97 (d, *J* = 19.7, 6H). ^{13}C NMR (151 MHz, $CDCl_3$) δ 171.1, 170.7, 170.5, 170.4, 169.9, 169.6, 132.9, 132.0, 128.9, 128.3, 100.8, 85.7, 76.8, 76.2, 73.7, 73.0, 71.6, 71.0, 70.2, 69.2, 62.4, 61.4, 31.0, 20.9, 20.8, 20.7.

Phenyl (2,6-di-*O*-acetyl-4-*O*-(^{18}O)acetyl-β-D-gulopyranosyl)-(1→4)-2,3,6-tri-*O*-acetyl-1-thio-β-D-glucopyranoside (3.9): A solution of compound **3.8** (152 mg, 0.2 mmol) in dichloromethane (10 mL) was cooled to –78 °C. Upon the addition of pyridine (69 μL, 0.85 mmol) and trifluoromethanesulfonic anhydride (74 μL, 0.35 mmol), the mixture was allowed to warm to room temperature. After 30 min, the mixture was successively washed with aq. hydrochloric acid (1N, 20 mL), sat. aqueous sodium bicarbonate (20 mL) and brine (20 mL). The organic layer was dried (sodium sulfate) and concentrated under reduced pressure. The resultant crude residue was dissolved in anhydrous DMF and treated with sodium nitrite (71 mg, 1.0 mmol). This reaction

mixture was stirred overnight at 50 °C. Upon removal of the solvent, the crude residue was purified via flash chromatography (3:7 v/v acetone/toluene) to afford the desired product as a white solid (113.4 mg, 75% yield two-steps). mp = 91-92 °C. ^{1}H NMR (600 MHz, $CDCl_3$) δ 7.55–7.48 (m, 2H), 7.38–7.31 (m, 3H), 5.24 (t, *J* = 9.1, 1H), 4.96 (s, 2H), 4.82 (s, 2H), 4.72 (d, *J* = 10.0, 1H), 4.50 (d, *J* = 13.5, 1H), 4.35–4.24 (m, 2H), 4.21 (s, 1H), 4.13 (d, *J* = 6.4, 2H), 3.79 (t, *J* = 9.5, 1H), 3.72–3.64 (m, 1H), 2.37–2.30 (m, 1H), 2.15 (s, 9H), 2.12 (s, 3H), 2.08 (d, *J* = 12.8, 6H). ^{13}C NMR (151 MHz, $CDCl_3$) δ 171.2, 170.5, 170.2, 170.1, 169.8, 169.7, 132.8, 129.0, 128.3, 98.6, 86.4, 85.9, 76.5, 73.9, 70.9, 70.2, 69.7, 69.4, 67.5, 62.5, 61.4, 20.9, 20.8, 20.7.

Phenyl (2,3,6-tri-*O*-acetyl-(3-^{18}O)-β-D-galactopyranosyl)-(1→4)-2,3,6-tri-*O*-acetyl-1-thio-β-D-glucopyranoside (3.10): A solution of compound **3.9** (95 mg, 0.14 mmol) in dichloromethane (15 mL) was treated with pyridine (150 μL, 1.85 mmol) and cooled to 0 °C. After the addition of trifluoromethanesulfonic anhydride (144 μL, 0.675 mmol), the resultant mixture was warmed to room temperature. After 4 hrs, the mixture was successively washed with aq. hydrochloric acid (1N, 20 mL), sat. aqueous sodium bicarbonate (20 mL) and brine (20 mL). The organic layer was dried (sodium sulfate) and concentrated under reduced pressure. The crude residue was dissolved in THF (10 mL), treated with water (100 μL, 5.5 mmol) and 2,6-lutidine (150 μL, 1.3 mmol) and stirred at 40 °C for 1 hr. The volatiles were removed under reduced pressure and the resultant crude residue was purified via flash chromatography (3:7 v/v acetone/toluene) to afford the desired product as a white solid (87 mg, 92% yield). mp = 90-92 °C. ^{1}H NMR (600 MHz, $CDCl_3$) δ 7.54–7.48 (m, 2H), 7.37–7.31 (m, 3H), 5.32 (s, 1H), 5.24 (t, *J* = 8.5, 1H), 4.95 (t, *J* = 9.7, 1H), 4.91–4.83 (m, 1H), 4.71 (d, *J* = 10.1, 1H), 4.57 (d, *J* = 11.9, 1H),

4.44 (d, *J* = 7.8, 1H), 4.19 (dd, *J* = 5.8, 11.9, 1H), 4.16–4.05 (m, 2H), 3.85–3.73 (m, 3H), 3.73–3.66 (m, 1H), 2.54 (d, *J* = 6.3, 1H), 2.20 (s, 3H), 2.15 (s, 3H), 2.14 (s, 3H), 2.12 (s, 3H), 2.09 (s, 3H), 2.06 (s, 3H). ^{13}C NMR (151 MHz, $CDCl_3$) δ 171.4, 170.5, 170.3, 170.2, 169.9, 169.6, 132.9, 132.0, 128.9, 128.3, 100.8, 85.6, 76.2, 73.7, 73.13, 73.08, 71.8, 71.0, 70.2, 69.1, 62.3, 61.4, 20.9, 20.8, 20.67.

Phenyl ((3-^{18}O)-β-D-galactopyranosyl)-(1→4)-1-thio-β-D-glucopyranoside (3.4): A solution of freshly prepared sodium methoxide solution in methanol (0.5 M, 20 mL) was added to compound **3.10** (80 mg, 0.12 mmol) and stirred at room temperature for 5 hrs. Amberlite IR-120+ resin (H^+ form) was added to neutralize the reaction. The suspension was further stirred for 15 min and then filtered. The filtrate was concentrated under reduced pressure afford the desired product as an off-white solid (46.1 mg, 0.11 mmol, 93% yield). The ^{1}H and ^{13}C NMR spectra were consistent with incorporation of ^{18}O at the 3' position. mp = 195-196 °C. ^{1}H NMR (600 MHz, D_2O) δ 7.57 – 7.47 (m, 2H, Ar-H), 7.34 (m, 3H, Ar-H), 4.76 (d, *J* = 10 Hz, 1H, 1'-H), 4.38 (d, *J* = 8 Hz, 1H, 1-H), 3.92 – 3.81 (m, 2H), 3.80 – 3.52 (m, 8H), 3.52 – 3.42 (m, 1H), 3.39 – 3.30 (m, 1H). ^{13}C NMR (151 MHz, D_2O) δ 132.3, 131.4, 131.2, 129.0, 128.8, 127.7, 102.4, 86.6, 78.2, 77.4, 75.3, 74.9, 72.0, 71.0, 70.5, 68.1, 60.5, 59.6. ESI-MS: 436.4 [$(M+H)^+$].

3.3 NMR Experiments

3.3.1 Acquisition of NMR Spectra

The NMR spectroscopic measurements of KIEs followed the published procedure[68] except for: i) deuterium oxide (5 μL, < 1.0% of final volume) was added directly into the NMR tube containing substrate (~ 1.5–2.0 mg) and buffer (645 μL) for signal locking; ii) automated gradient shimming of the magnetic field using the ^{2}H lock signal was initially performed and was followed by manual shimming by adjusting the various shim currents in order to optimize the ^{1}H NMR spectrum. Spectra were automatically "Fourier transformed" in real-time every three seconds during this procedure. The amount of VcNA was adjusted such that four half-lives were complete within approximately 8 hours. A simultaneous inverse-gated ^{1}H and ^{2}H decoupling sequence was used for all β-secondary ^{2}H-KIEs experiments. When measuring the β-secondary ^{2}H-KIEs for compound **3.2**, a filtered solution of *E. coli.* Neu5Ac aldolase was added to the reaction vessel to reduce the signal intensity of *β*-Neu5Ac. Experimental spectra were fit using the 'deconvolution' function from the Bruker Topspin 2.1 program. Peaks were fit to a Lorentzian shape, detection sensitivity = 0.5 and peak overlapping factor = 0.5 ppm.

3.3.2 Anomeric ^{13}C-KIE Measurements

A potential disadvantage of this technique is the possibility of signal overlap that may occur between the peak(s) of interest and those corresponding to other chemical species in the reaction mixture (i.e., products, starting material). In fact, this occurs

between the C-3 peak of Neu5Acα2,3LacβSPh (**3.2d**, w = ^{13}C) and the β-Neu5Ac product. This problem was resolved by including an additional enzyme, *E. coli* Neu5Ac aldolase, to the reaction mixture, which converted the product into an equilibrating mixture of Neu5Ac, pyruvate and ManNAc.[69] As such, the measured anomeric ^{13}C-KIE for the hydrolysis of Neu5Acα2,3LacβSPh were 1.0224(27), 1.0229(16) and 1.0211(19). The experimental spectra for the VcNA-catalyzed hydrolysis of singly (**3.2d**, w = ^{13}C) and doubly (**3.2g**, w = x = ^{13}C) labelled Neu5Acα2,3LacβSPh are shown below (Figure 3-4). Of note, the quantity of β-Neu5Ac product (black arrow: w = x = ^{13}C; violet arrow: w = ^{13}C) has been reduced by incorporation of aldolase in the NMR reaction tube. The fit for the spectrum at the F_1 value of 0.90 using the least-squares "NonlinearRegress" function in *Mathematica* is shown below (Figure 3-5). Experimental spectra (in black); calculated spectra (in red); difference spectra (in blue). The plots of the fits to eq. 2.1 for the experimental data from three separate runs are displayed below (Figure 3-6).

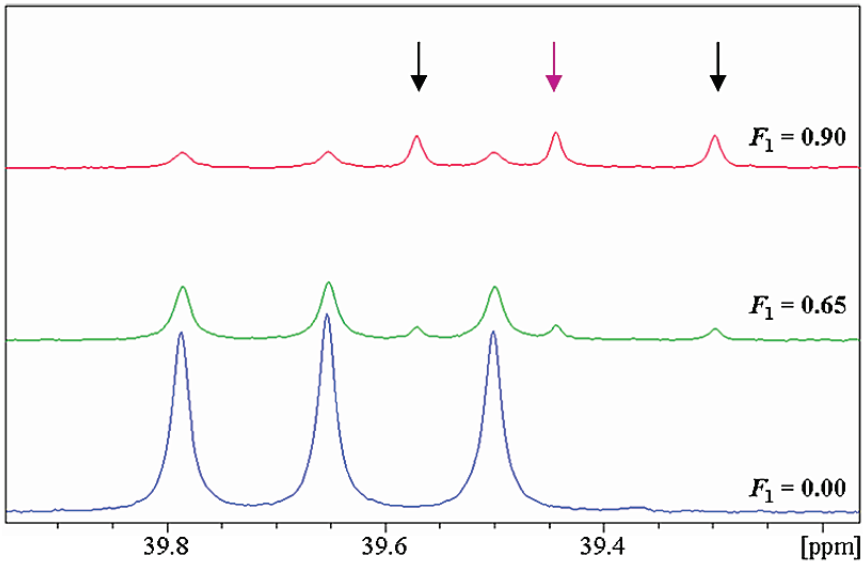

Figure 3-4 Experimental spectra at F_1 values of 0.00, 0.65 and 0.90 for the VcNA-catalyzed hydrolysis of **3.2d** and **3.2g**. Black arrow: w = x = ^{13}C; Violet arrow: w = ^{13}C.

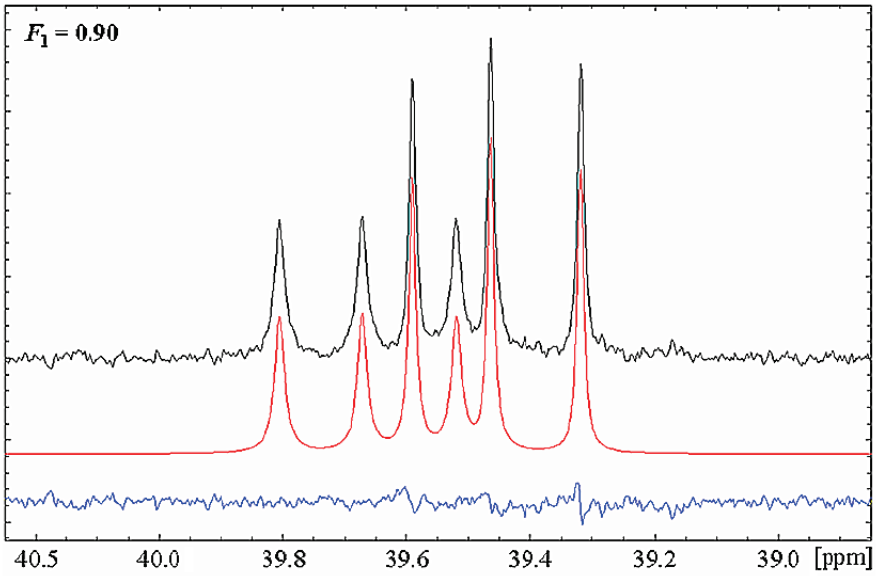

Figure 3-5 Fit of the experimental spectra for *V. cholerae* sialidase-catalyzed hydrolysis of **3.2d** and **3.2g** using the least-squares "NonlinearRegress" function in Mathematica. Experimental spectra in black; calculated spectra in red; and difference spectra in blue.

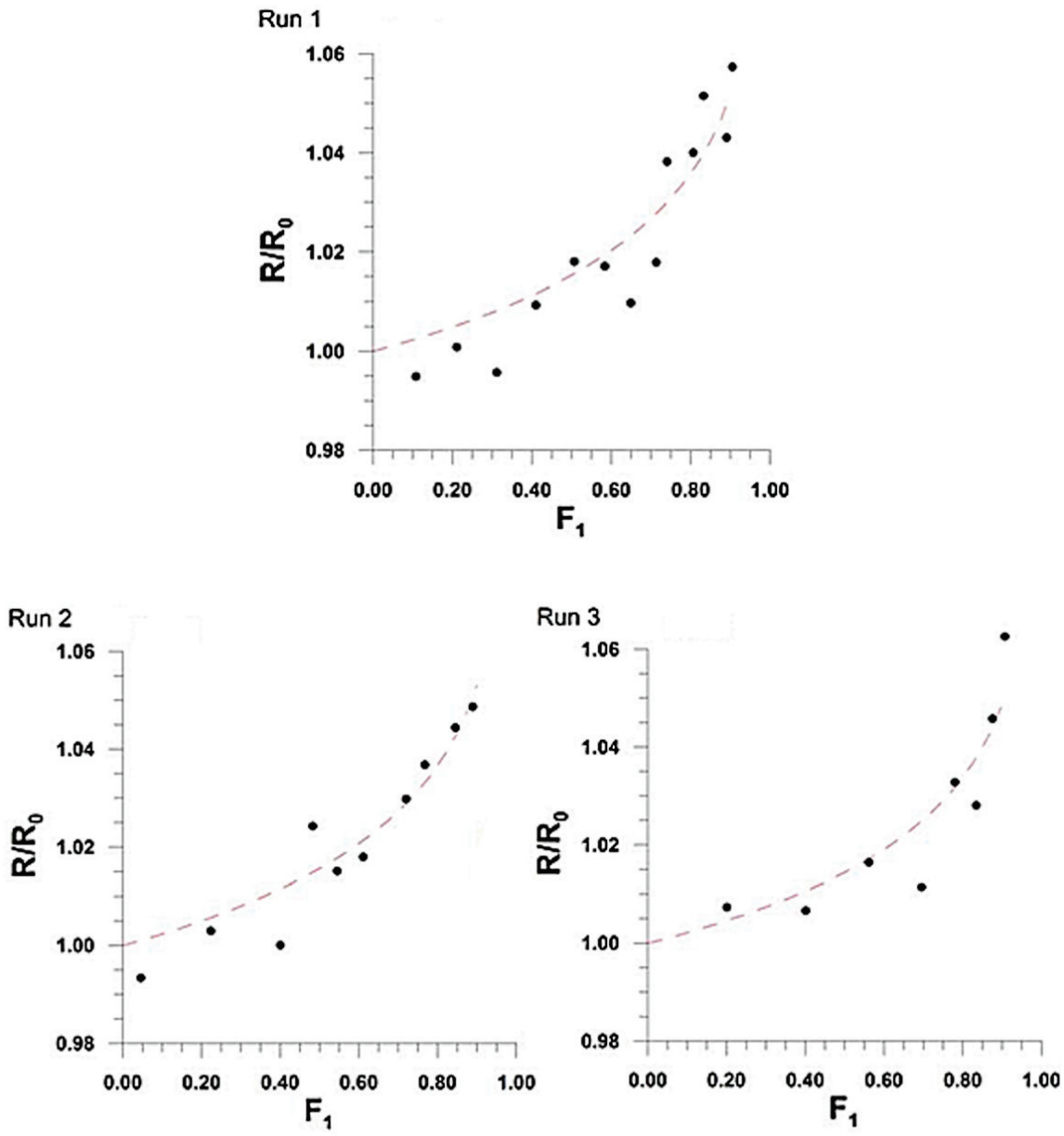

Figure 3-6 Plots of fits for the experimental data of the VcNA-catalyzed hydrolysis of singly (**3.2d**, w = ^{13}C) and doubly (**3.2g**, w = x = ^{13}C) labelled Neu5Acα2,3LacβSPh to Eq. 2.1. The best-fit line is shown in each plot.

3.3.3 ^{18}O-KIE Measurements

The leaving group ^{18}O-KIEs for competitive hydrolysis reactions between equimolar quantities of **3.2a** and **3.2c** were 1.0272 (27), 1.0312 (27) and 1.0281 (29). A

stacked plot of three ^{13}C NMR spectra collected at various 'fraction of reaction', F_1 is shown below (Figure 3.4a). The dotted lines are meant to serve as a visual aid to compare the relative peak intensities throughout the time course of the hydrolysis. Likewise, the derived ring oxygen ^{18}O-KIEs between compounds **3.2a** and **3.2b** were 0.9832 (16), 0.9840 (42) and 0.9832 (30). The corresponding stacked plot is shown below (Figure 3.4b).

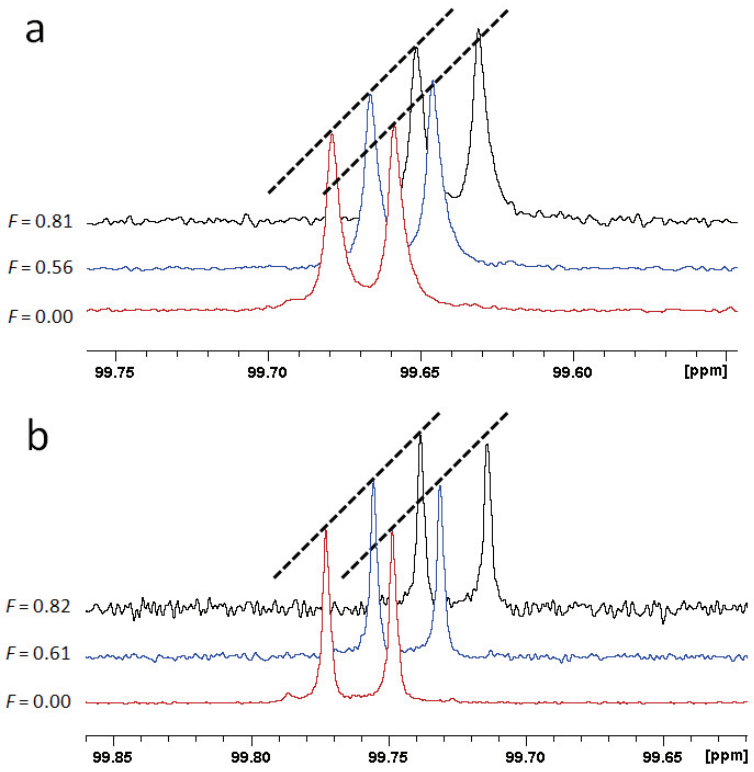

Figure 3-7 a) ^{13}C NMR spectra from an approximate 1:1 mixture of singly (**3.2a**) and doubly (**3.2c**) labelled Neu5Acα2,3βSPh. b) ^{13}C NMR spectra from an approximate 1:1 mixture of singly (**3.2a**) and doubly (**3.2b**) labelled Neu5Acα2,3βSPh.

3.3.4 ^{2}H-KIE Measurements

3.3.4.1 Neu5Acα2,3LacβSPh ^{2}H-KIEs

The equatorial (3*S*)-^{2}H KIEs for competitive hydrolysis reactions between **3.2d** and **3.2e** are 1.0323 (52), 1.0333 (36), 1.0365 (36) and 1.0312 (50). The axial (3*R*)-^{2}H KIEs for competitive hydrolysis reactions between **3.2d** and **3.2f** are 1.0459 (43), 1.0419 (36) and 1.0422 (29). Figure 3-8 displays the various ^{13}C-labelled chemical species that are present during the hydrolysis reaction.

Label	Compound	Structure	Chemical Shift (ppm)
A	Neu5Acα2,3LacβSPh	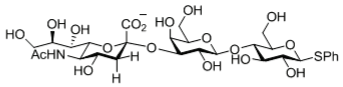	39.651
B	β-Neu5Ac	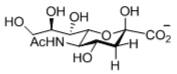	39.439
C	3S-(3-^{2}H) Neu5Acα2,3LacβSPh	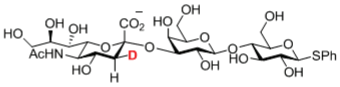	39.340
D	3R-(3-^{2}H) Neu5Acα2,3LacβSPh	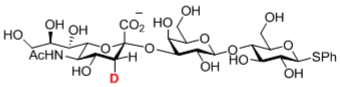	39.273
E	3S-(3-^{2}H) β-Neu5Ac	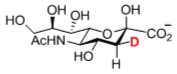	39.108
F	3R-(3-^{2}H) β-Neu5Ac	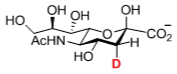	39.076

Figure 3-8 ^{13}C-labelled chemical species that are present during the hydrolysis reaction of **3.2**.

Representative stacked plots for the hydrolysis reactions involving compounds **3.2d** and **3.2f** are shown below. (Figure 3-9a and 3-9b, respectively). Fits of experimental spectra before the addition of enzyme and at a high fraction of reaction for competitive hydrolysis reactions between compounds **3.2d** and **3.2e** and between compounds **3.2d** and **3.2f** are shown below (Figure 3-10 and Figure 3-11, respectively).

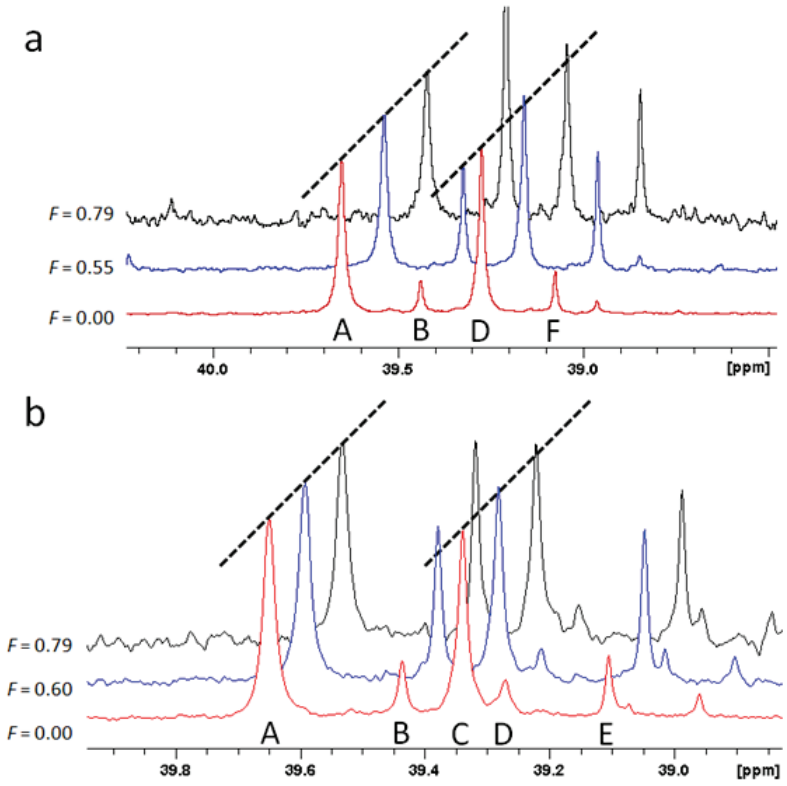

Figure 3-9 a) ^{13}C NMR spectra from an approximate 1:1 mixture of singly (**3.2d**) and doubly (**3.2e**) labelled Neu5Acα2,3βSPh. b) ^{13}C NMR spectra from an approximate 1:1 mixture of singly (**3.2d**) and doubly (**3.2f**) labelled Neu5Acα2,3βSPh.

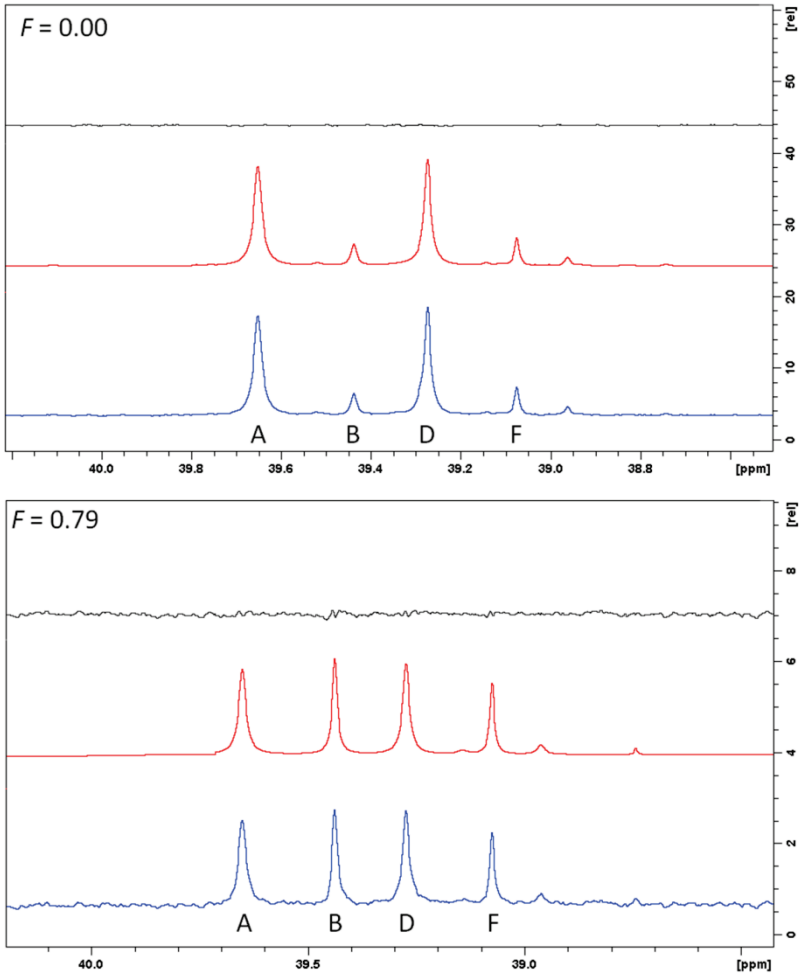

Figure 3-10 Fit of the experimental spectra for *V. cholerae* sialidase-catalyzed hydrolysis of **3.2d** (w = ^{13}C) and **3.2e** (w = ^{13}C, u = ^{2}H) using the deconvolution command in TopSpin. The experimental spectrum is in blue, the calculated spectrum is in red and a difference spectrum is in black.

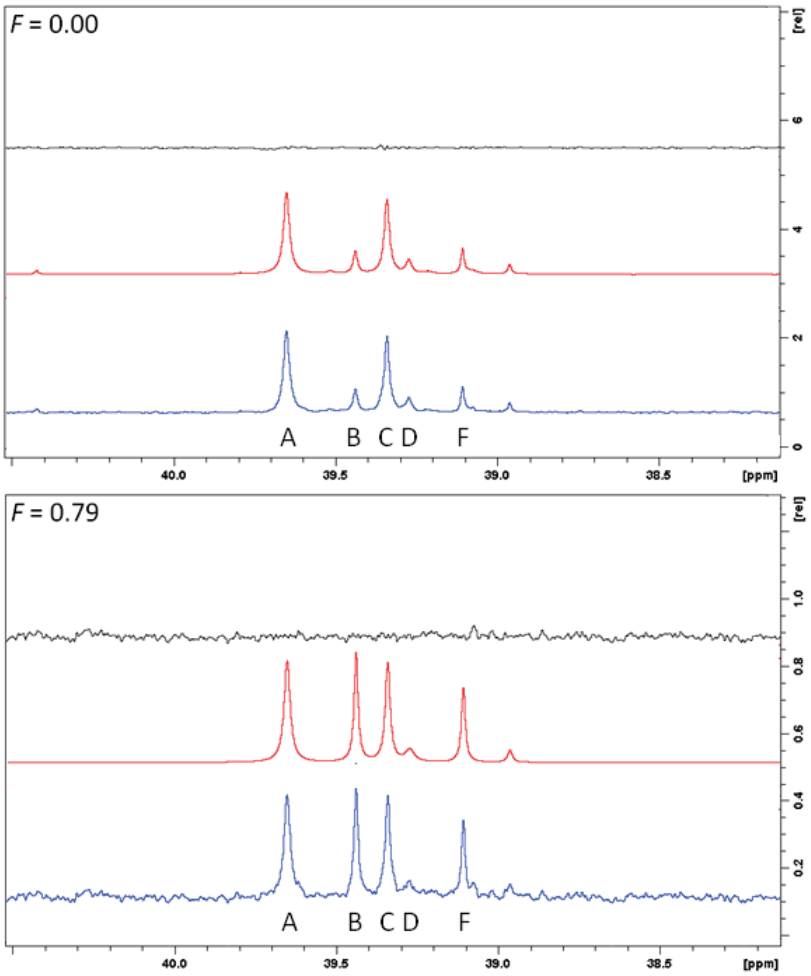

Figure 3-11 Fit of the experimental spectra for *V. cholerae* sialidase-catalyzed hydrolysis of **3.2d** (w = ^{13}C) and **3.2f** (w = ^{13}C, v = ^{2}H) using the deconvolution command in TopSpin. The experimental spectrum is in blue, the calculated spectrum is in red and a difference spectrum is in black.

3.3.4.2 Neu5Acα2,6LacβSPh ^{2}H-KIEs

The β-secondary ^{2}H KIEs for Neu5Acα2,6LacβSPh **3.3** could be determined simultaneously since there was no peak overlap. The equatorial (3*S*)-^{2}H KIEs are 1.0218 (21), 1.0212 (13) and 1.0219 (15). The axial (3*R*)-^{2}H KIEs are 1.0492 (18), 1.0483 (18) and 1.0482 (17). The ^{13}C-labelled chemical species are present during the hydrolysis reaction are shown below (Figure 3-12). The corresponding stacked plots are presented

below (Figure 3-13). Fits of experimental spectra before the addition of enzyme and at a high fraction of reaction for competitive hydrolysis reactions between compounds **3.3a**, **3.3b**, and **3.3c** are shown below (Figure 3-14).

Label	Compound	Structure	Chemical Shift (ppm)
3.3a A	Neu5Acα2,6LacβSPh	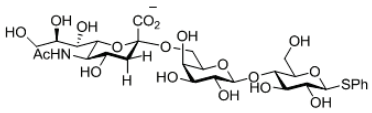	40.106
3.3b B	3S-(3-^{2}H) Neu5Acα2,6LacβSPh	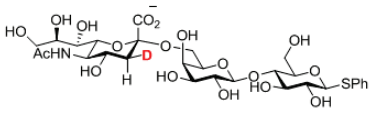	39.798
3.3c C	3R-(3-^{2}H) Neu5Acα2,6LacβSPh	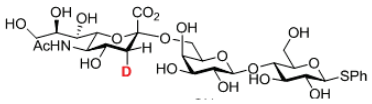	39.733

Figure 3-12 ^{13}C-labelled chemical species are present during the hydrolysis reaction of **3.3**.

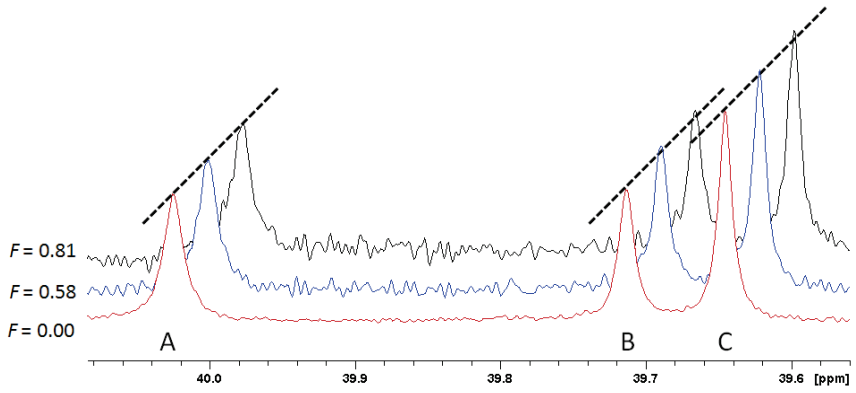

Figure 3-13 ^{13}C NMR spectra of an approximate 1:1:1 mixture of **3.3a**, **3.3b** and **3.3c**. The experimental spectrum is in blue, the calculated spectrum is in red and the difference spectrum is in black.

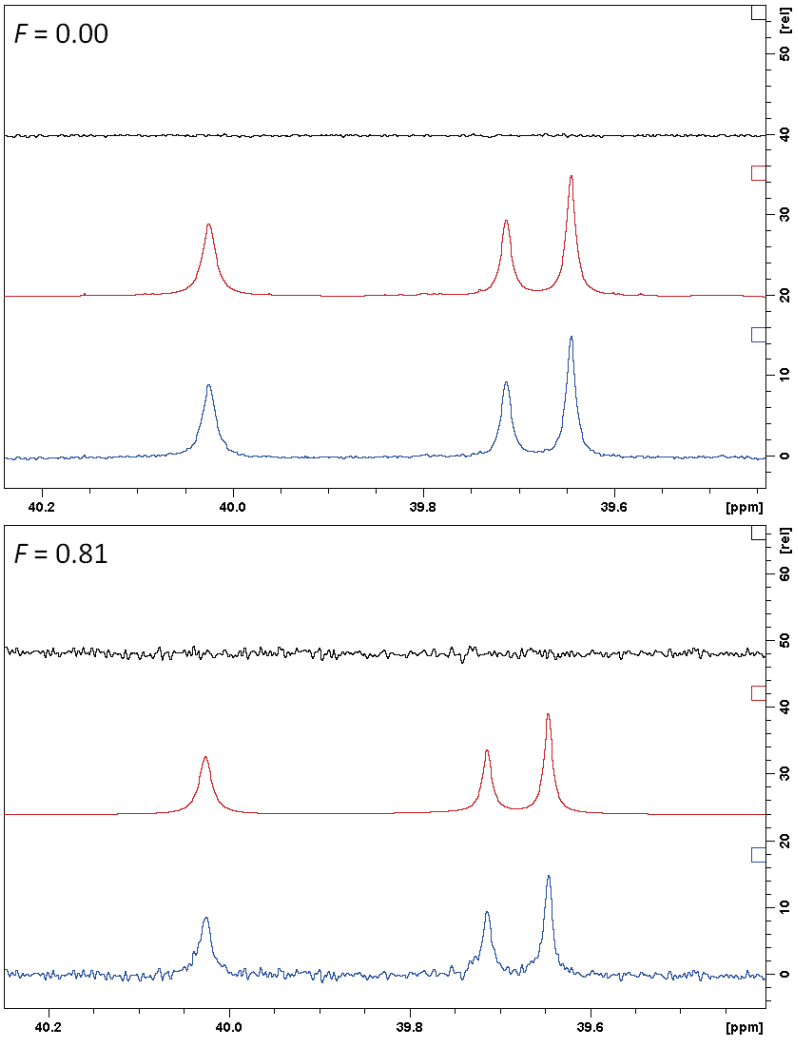

Figure 3-14 Fit of the experimental spectra for *V. cholerae* sialidase-catalyzed hydrolysis of compounds **3.3a** (w = ^{13}C), **3.3b** (w = ^{13}C, u = ^{2}H) and **3.3c** (w = ^{13}C, v = ^{2}H) using the deconvolution command in TopSpin. The experimental spectrum is in blue, the calculated spectrum is in red and a difference spectrum is in black.

3.4 Discussion

V. cholerae sialidase effectively catalyzes the hydrolysis of a range of naturally occurring sialic acids and glycosidic linkages.[70] For instance, substitution of Neu5Ac with Neu5Gc (*N*-glycolylneuraminic acid) diminishes the hydrolytic activity of VcNA to only a small extent. Furthermore, VcNA can process both α-(2→3)- and α-(2→6)-glycosidic linkages with a preference for the α-(2→3)-linkage when Neu5Ac is attached to a galactose residue.[70] Activated substrates such as Neu5AcαPNP are frequently used in kinetic assays because hydrolysis can be readily detected by using UV spectroscopy. However, given that *p*-nitrophenoxide is a far better leaving group than galactose or lactose, determination of the biologically relevant enzymatic TS structure should involve the use of natural substrates. In this present study, a series of isotopically labelled natural substrate analogues **3.2** and **3.3** were prepared chemoenzymatically to determine the KIEs at key reaction sites. The KIEs determined for the VcNA-catalyzed hydrolysis reactions are summarized below (Table 4).

Site of Substitution	Neu5Acα2,3LacβSPh	Neu5Acα2,6LacβSPh	Neu5AcαPNP[c]
Anomeric 2-^{13}C	1.022 ± 0.001[b]	1.017 ± 0.001[b]	N/A
Leaving group 2-^{18}O	1.029 ± 0.002	1.039 ± 0.001[b]	1.046 ± 0.015
Ring 6-^{18}O	0.983 ± 0.001	0.975 ± 0.001[b]	N/A
Equatorial (3*S*)-^{2}H	1.034 ± 0.002[d]	1.021 ± 0.001[e]	1.030 ± 0.017
Axial (3*R*)-^{2}H	1.043 ± 0.002	1.049 ± 0.001[e]	1.030 ± 0.017

[a] Reported values represent weighted averages (n = 3). [b] KIEs from reference (68). [c] KIEs from reference (45). [d] n = 4. [e] (*3S*) and (*3R*) KIEs determined simultaneously.

Table 4 KIEs on k_{cat}/K_m For the *V. Cholerae* Sialidase-Catalyzed Hydrolyses of Compounds **3.2** and **3.3** in 50 mM Sodium Acetate Buffer pH = 5.50 and Temperature = 25 °C.

The measured axial (3R) ^{2}H-KIEs for both compounds **3.2** and **3.3** were larger in magnitude than the equatorial (3S) ^{2}H-KIEs, (1.043 ± 0.002 cf. 1.034 ± 0.002) and (1.049 ± 0.001 cf. 1.021 ± 0.001), respectively. In general, β-secondary ^{2}H-KIEs result from hyperconjugation of the C–H/D bond with the developing p-orbital at the anomeric centre. Given that hyperconjugation is an angular dependent phenomenom,[71,72] these KIEs have been used as a mechanistic tool to determine the TS geometry for many sialidases as well as for the corresponding non-enzymatic hydrolysis reaction.[24,26,35,45,73,74] The general mechanism for sialidases is thought to involve the following sequential steps 1) formation of the Michaelis complex in which the substrate is bound as chair; 2) substrate conformational change from chair to boat; 3) hydrolysis of the glycosidic bond resulting in a tyrosinyl β-sialoside intermediate; 4) hydrolysis of the intermediate to yield

Neu5Ac bound in a boat conformation; 5) product conformational change from boat to chair; and 6) dissociation of Neu5Ac from the enzyme active site (Figure 3-15).[35]

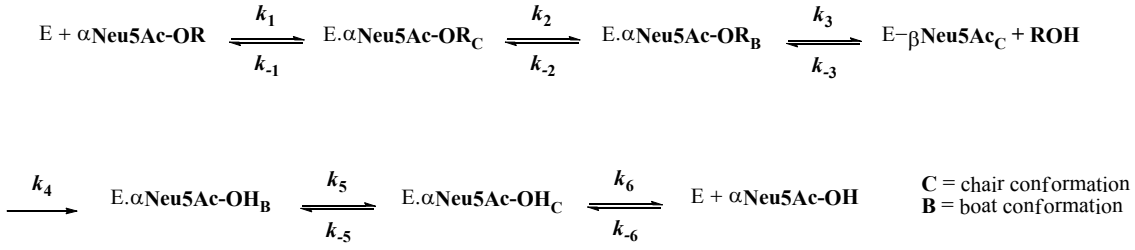

Figure 3-15 General mechanism for sialidase-catalyzed hydrolysis reactions.

This mechanism requires that substrate proceed through a $^{2}C_{5} \rightleftharpoons B_{2,5} \rightleftharpoons {}^{4}S_{2} \rightleftharpoons {}^{4}H_{5} \rightleftharpoons {}^{2}C_{5}$ conformational itinerary beginning from the Michaelis complex.[75] The β-secondary ^{2}H-KIEs from the present study are consistent with a flattened $^{4}H_{5}$ TS. This is in agreement with the conclusions drawn by Guo and Sinnott for the Neu5AcαPNP substrate as well as for the uncatalyzed reaction where the authors found the (3R) ^{2}H-KIE is larger than the (3S) ^{2}H-KIE.[24,45]

The ^{18}O-KIEs are typically complementary, that is, the leaving group ^{18}O-KIE is normal ($^{18}V/K > 1$) whereas the ring ^{18}O-KIE is inverse ($^{18}V/K < 1$). This general trend has been observed for a number of other glycosyl hydrolases and can be used to probe the 'timing' of the TS.[76,77] With regard to VcNA, the leaving group ^{18}O-KIEs are 1.029 ± 0.002 and 1.039 ± 0.001 for **3.2** and **3.3**, respectively. Similar results have been reported for the VcNA-catalyzed hydrolysis of Neu5AcαPNP ($^{18}V/K$ = 1.046 ± 0.015).[45] Since this effect is a consequence of a diminished oxygen bond order, the derived ^{18}O-KIEs suggest that there is extensive carbon-oxygen bond cleavage. There are several possible rationales for the smaller ^{18}O-KIE for compound **3.2**, i) less-advanced carbon-oxygen

bond fission; or 2) partial protonation by a general acid, which would likely be Asp250. As expected, both ring ^{18}O-KIEs are both inverse, 0.983 ± 0.001 and 0.975 ± 0.001 for compounds **3.2** and **3.3**, respectively. An inverse ring ^{18}O-KIE is consistent with an increased bond order and the occurrence of charge delocalization onto the pyranosyl oxygen at the TS. This effect is less pronounced for compound **3.2** suggesting either i) less stabilization of charge development in the developing oxacarbenium ion; and/or ii) a TS geometry which decreases the requisite orbital overlap ($\eta_p \rightarrow \sigma^*$).

The anomeric ^{13}C-KIEs for compound **3.3**, $^{13}V/K$ = 1.017 ± 0.001, was reported in Chapter 2 of this thesis while the corresponding KIE for compound **3.2** is $^{13}V/K$ = 1.022 ± 0.001. The magnitude of the anomeric ^{13}C-KIE has been used as a guideline to predict the mechanism of glycosidic bond cleavage for a number of reactions.[78,79] Typically, concerted S_N2-like reactions feature ^{13}C-KIEs in the range of 1.03–1.08.[80] In contrast, stepwise S_N1-like reactions exhibit smaller ^{13}C-KIE around 1.01.[43,76] The anomeric KIEs determined for VcNA-catalyzed hydrolysis fall within the range set by the S_N2 and S_N1 reactions and thus do not allow unambiguous distinction of the mechanism. Of note, whether sialidases operate via a step-wise or concerted mechanism is of considerable debate, most arguments are against a concerted reaction based on the reaction being at a crowded centre. However, Toney and co-workers have recently demonstrated that 1,4,7-trimethyloxatriquinane, a three-fold tertiary alkyl oxonium salt, undergoes a facile S_N2 displacement with azide ion.[81]

3.4.1 Conclusions

Based on the measured KIEs for both compounds **3.2** and **3.3**, it is likely that both natural substrate analogues have similar TSs. Specifically, TS structural features

includes i) extensive cleavage of the C-O glycosidic bond; ii) considerable charge delocalization on to the ring-oxygen atom; and iii) a flattened $^4H_5$ half-chair conformation (Figure 3-16).

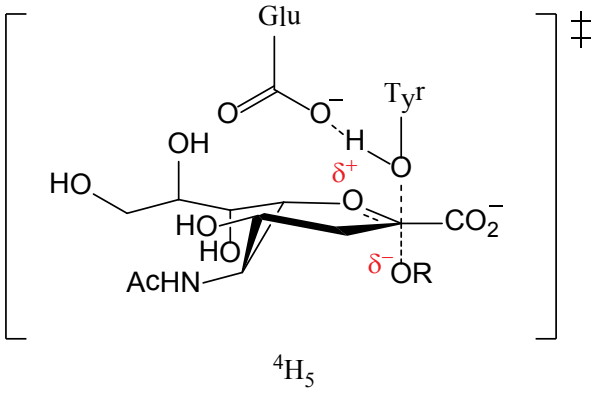

$^4H_5$

Figure 3-16 Possible TS for the VcNA-catalyzed hydrolysis of natural substrate analogues, **3.2** and **3.3**.

3.5 Supplementary Data

Run No.	Fraction of Reaction (F_1)	Anomeric - R/R_0
1	0.1078	0.9949
1	0.2106	1.0009
1	0.3109	0.9957
1	0.4099	1.0094
1	0.5065	1.0181
1	0.5834	1.0171
1	0.6492	1.0098
1	0.7133	1.0179
1	0.7402	1.0382
1	0.8061	1.0400
1	0.8318	1.0515
1	0.8904	1.0431
1	0.9044	1.0574
2	0.0454	0.9934
2	0.2233	1.0030
2	0.4005	1.0001
2	0.4823	1.0243
2	0.5445	1.0152
2	0.6105	1.0180
2	0.7198	1.0299
2	0.7672	1.0369
2	0.8450	1.0444
2	0.8892	1.0487
3	0.2007	1.0074
3	0.4009	1.0067
3	0.5616	1.0165
3	0.6951	1.0114
3	0.7798	1.0328
3	0.8343	1.0281
3	0.8754	1.0458
3	0.9067	1.0626

Table 5 Kinetic Data Taken From The *Vibrio Cholerae* Sialidase-Catalyzed Hydrolysis of a Mixture of Labelled Neu5Acα2,3LacβSPh (**3.2d** w = 13C, and **3.2g** w = x= ^{13}C) at 298 K in 50 mM Sodium Acetate Buffer (pH 5.5)

Run No.	Fraction of Reaction (F_1)	Leaving group - R/R_0
1	0.1315	1.0096
1	0.2617	1.0010
1	0.3421	0.9995
1	0.4332	1.0096
1	0.5600	1.0169
1	0.6221	1.0342
1	0.7362	1.0286
1	0.7827	1.0368
1	0.8092	1.0580
2	0.1846	0.9931
2	0.2539	1.0151
2	0.3123	1.0242
2	0.4281	1.0051
2	0.5131	1.0208
2	0.6247	1.0285
2	0.7650	1.0377
2	0.8095	1.0611
2	0.8540	1.0594
3	0.1332	1.0104
3	0.2330	0.9967
3	0.3335	1.0097
3	0.3957	1.0068
3	0.4481	1.0056
3	0.5514	1.0207
3	0.5965	1.0328
3	0.6626	1.0134
3	0.7045	1.0484
3	0.7381	1.0407
3	0.8233	1.0500

Table 6 Kinetic Data Taken From The *Vibrio Cholerae* Sialidase-Catalyzed Hydrolysis of a 1:1 Mixture of Labelled Neu5Acα2,3LacβSPh, (**3.2a** x = ^{13}C):(**3.2c** x = ^{13}C, z = ^{18}O) at 298 K in 50 mM Sodium Acetate Buffer (pH 5.5)

Run No.	Fraction of Reaction (F_1)	Ring oxygen - R/R_0
1	0.0829	1.0008
1	0.2094	0.9950
1	0.3768	0.9950
1	0.5090	0.9855
1	0.6169	0.9834
1	0.7005	0.9750
1	0.7684	0.9731
1	0.8214	0.9765
2	0.1289	0.9941
2	0.2394	1.0009
2	0.3268	1.0283
2	0.4061	0.9875
2	0.4781	0.9976
2	0.5419	1.0109
2	0.6472	0.9920
2	0.7553	0.9597
2	0.8781	0.9477
2	0.9051	0.9699
3	0.1630	0.9891
3	0.2642	1.0100
3	0.4290	0.9773
3	0.5978	0.9889
3	0.7263	0.9824
3	0.7656	0.9906
3	0.8083	0.9652
3	0.8607	0.9585

Table 7 Kinetic Data Taken From The *Vibrio Cholerae* Sialidase-Catalyzed Hydrolysis of a 1:1 Mixture of Labelled Neu5Acα2,3LacβSPh, (**3.2a** x = ^{13}C):(**3.2b** x = ^{13}C, y = ^{18}O) at 298 K in 50 mM Sodium Acetate Buffer (pH 5.5)

Run No.	Fraction of Reaction (F_1)	($3R$) - R/R_0
1	0.1650	1.0121
1	0.3330	1.0269
1	0.4320	1.0363
1	0.4970	1.0134
1	0.5510	1.0454
1	0.6010	1.0253
1	0.6850	1.0382
1	0.7460	1.0619
1	0.7920	1.0864
2	0.1140	1.0054
2	0.2380	1.0177
2	0.3250	1.0055
2	0.4050	1.0313
2	0.4670	1.0057
2	0.5100	1.0271
2	0.6050	1.0499
2	0.7090	1.0400
2	0.7340	1.0558
2	0.7890	1.0722
3	0.1510	1.0044
3	0.2770	1.0076
3	0.3790	1.0293
3	0.4710	1.0239
3	0.5540	1.0430
3	0.6210	1.0351
3	0.6780	1.0306
3	0.7340	1.0412
3	0.7690	1.0830
3	0.7990	1.0633
3	0.8260	1.0770

Table 8 Kinetic Data Taken From The *Vibrio Cholerae* Sialidase-Catalyzed Hydrolysis of a 1:1 Mixture of Labelled Neu5Acα2,3LacβSPh, (**3.2d** w = ^{13}C):(**3.2e** w = ^{13}C, u = ^{2}H) at 298 K in 50 mM Sodium Acetate Buffer (pH 5.5)

Run No.	Fraction of Reaction (F_1)	(3*S*) - R/R_0
1	0.1500	0.9892
1	0.3150	1.0238
1	0.4010	0.9828
1	0.5010	1.0254
1	0.5660	1.0249
1	0.6330	1.0342
1	0.6800	1.0278
1	0.7120	1.0350
1	0.8010	1.0685
2	0.1260	0.9972
2	0.2420	1.0046
2	0.2910	1.0093
2	0.3400	1.0105
2	0.3870	1.0051
2	0.4250	1.0151
2	0.4690	1.0359
2	0.5330	1.0292
2	0.5750	1.0396
2	0.6580	1.0473
2	0.7080	1.0209
2	0.7300	1.0600
2	0.7990	1.0389
3	0.1060	1.0120
3	0.2470	1.0097
3	0.3760	1.0345
3	0.4380	1.0127

3	0.5850	1.0226
3	0.6350	1.0489
3	0.7710	1.0459
3	0.8000	1.0591
4	0.1360	0.9817
4	0.1960	1.0090
4	0.2570	1.0159
4	0.3530	1.0139
4	0.4530	1.0235
4	0.5960	1.0339
4	0.6220	1.0159
4	0.7200	1.0630
4	0.7330	1.0173
4	0.7840	1.0514

Table 9 Kinetic Data Taken From The *Vibrio Cholerae* Sialidase-Catalyzed Hydrolysis of a 1:1 Mixture of Labelled Neu5Acα2,3LacβSPh, (**3.2d** w = ^{13}C):(**3.2f** w = ^{13}C, v = ^{2}H) at 298 K in 50 mM Sodium Acetate Buffer (pH 5.5)

Run No.	Fraction of Reaction (F_1)	(3*S*) - R/R_0	(3*R*) - R/R_0
1	0.1089	1.0037	1.0083
1	0.1885	1.0011	1.0180
1	0.2623	0.9943	1.0168
1	0.3311	1.0006	1.0140
1	0.4090	1.0130	1.0298
1	0.5321	1.0178	1.0342
1	0.6193	1.0190	1.0508
1	0.7114	1.0311	1.0571
1	0.8004	1.0361	1.0770
2	0.0864	0.9911	0.9968
2	0.1614	1.0084	1.0085
2	0.2421	1.0033	1.0207
2	0.3046	1.0167	1.0116
2	0.3817	1.0032	1.0220
2	0.4434	1.0191	1.0351
2	0.4837	1.0172	1.0401
2	0.5413	1.0175	1.0361
2	0.5844	1.0202	1.0470
2	0.6085	1.0219	1.0490
2	0.6709	1.0230	1.0540
2	0.7094	1.0298	1.0543
2	0.7386	1.0187	1.0430
2	0.7641	1.0238	1.0631
2	0.7988	1.0330	1.0752
2	0.8067	1.0353	1.0788
2	0.8380	1.0433	1.0998
3	0.1877	0.9947	1.0020
3	0.3298	1.0047	1.0144
3	0.4512	1.0084	1.0296
3	0.5519	1.0190	1.0339

3	0.6318	1.0152	1.0464
3	0.6561	1.0198	1.0610
3	0.6736	1.0254	1.0569
3	0.7170	1.0255	1.0520
3	0.7675	1.0349	1.0656
3	0.8202	1.0438	1.0850

Table 10 Kinetic Data Taken From the *Vibrio Cholerae* Sialidase-Catalyzed Hydrolysis of a 1:1:1 mixture of Labelled Neu5Acα2,6LacβSPh, (**3.3a** w = ^{13}C):(**3.3b** w = ^{13}C, u = ^{2}H):(**3.3c** w = ^{13}C, v = ^{2}H) at 298 K in 50 mM Sodium Acetate Buffer (pH 5.5)

4: TURNOVER IS RATE-LIMITED BY DEGLYCOSYLATION FOR *MICROMONOSPORA VIRIDIFACIENS* SIALIDASE-CATALYZED HYDROLYSES: CONFORMATIONAL IMPLICATIONS FOR THE MICHAELIS COMPLEX

4.1 Introduction

Micromonospora viridifaciens is a non-pathogenic gram-positive bacterium. Like other members from this genus, single spores are formed which function as a crucial component of the organism's life cycle.[82] While screening a pool of 460 microbes for *exo*-sialidase (neuraminidase) activity, *M. Viridifaciens* was found to secrete the most active enzyme (MvNA).[83] Production of MvNA is induced when the substrate colominic acid, an α(2→8)-linked polysialic acid, or the product *N*-acetylneuraminic acid (Neu5Ac) are present in the growth media as the sole carbon source.[83] This suggests that this enzyme may serve an important nutritional role.[16] Further studies have shown that MvNA displays a very high catalytic efficiency ($k_{cat}/K_m > 10^7$ $M^{-1}s^{-1}$, for activated substrates),[33,84] broad substrate specificity[84] and a remarkable tolerance to mutation of its active site residues.[33,34,85,86]

The mechanism for MvNA catalyzed hydrolysis has been probed by β_{lg} analyses.[33] The derived β_{lg} values on V/K and V are –0.30 + 0.04 and 0.02 + 0.03, respectively.[33] These findings suggest that glycosidic bond cleavage is at least partially rate-limiting for k_{cat}/K_m, but that k_{cat} is limited by an ensuing step. As such, the possible rate-determining steps for k_{cat} are: i) deglycosylation of the tyrosinyl β-sialoside intermediate; ii) a conformational change of the initial bound α-sialic acid-enzyme product complex; or iii)

product release. Of note, only one possibility, deglycosylation, involves covalent bond cleavage and formation. Therefore, it is conceivable that kinetic isotope effects (KIEs) on V_{max} will allow us to determine the limiting step for enzymatic turnover.

The current study expands upon a previously established coupled-enzyme assay using natural sialoside analogues to determine enzymatic rate constants.[87] Herein, we report a series of secondary deuterium and heavy-atom KIEs by employing a panel of seven isotopically labelled substrates (Figure 4-1).

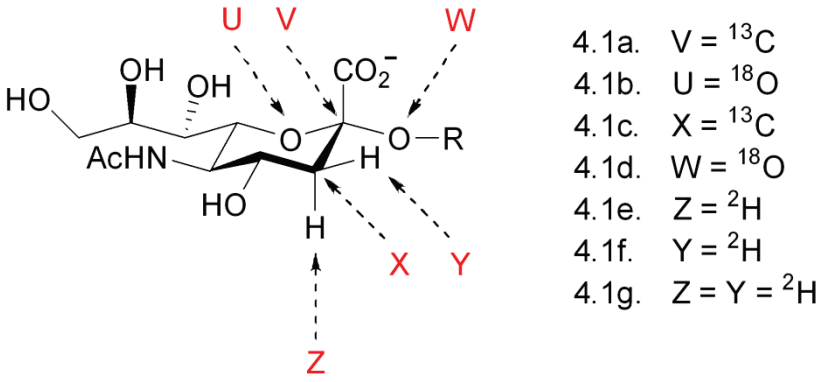

Figure 4-1 Panel of isotopically labelled Neu5Acα2,6GalβFMU used to measure KIEs on k_{cat} for *M. Viridifaciens* sialidase-catalyzed hydrolysis.

4.2 Substrate Synthesis

4.2.1 Synthesis of FMU

The series of transformations employed to prepare the requisite fluorophore, 8-fluoro-7-hydroxy-4-methylcoumarin (FMU), began with nucleophilic aromatic substitution of 2,3,4-trifluoronitrobenze to give compound **4.2** in 98% yield. Subsequent hydrogenation of the nitro functionality proceeds quantitatively to afford the corresponding aniline intermediate **4.3**. An acidified solution of **4.3** was treated with sodium nitrite to generate a diazonium salt *in situ*. Upon addition of hypophosphorus acid, nitrogen gas was liberated to afford compound **4.4** in 78% yield over two-steps. The penultimate step involved a Lewis-acid mediated cleavage of the methyl ether moieties to generate compound **4.5**. Finally, Pechmann conditions were employed to construct the desired coumarin **4.6** in 98% yield (Figure 4-2). Full experimental details are given below.

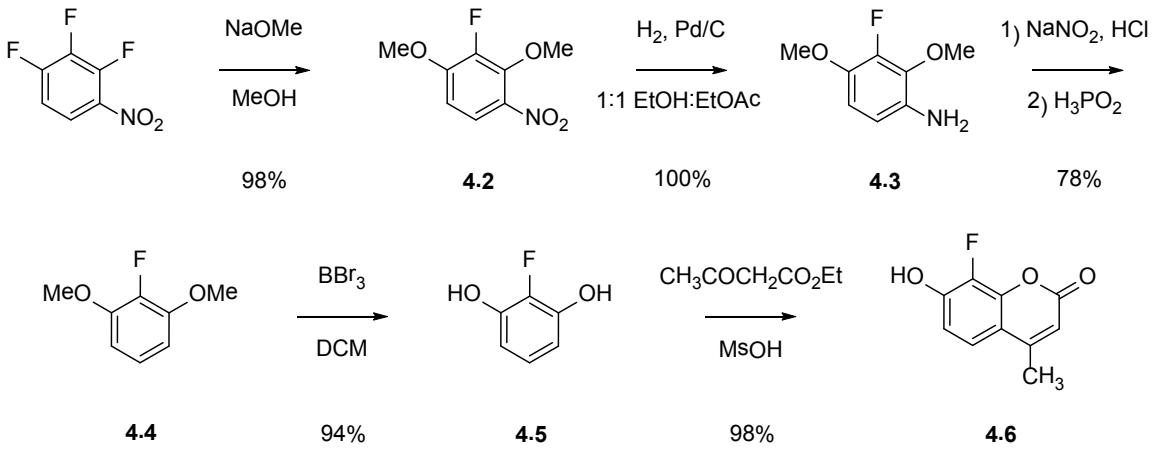

Figure 4-2 Synthetic route to 8-fluoro-7-hydroxy-4-methylcoumarin (FMU).

3-Fluoro-2,4-dimethoxy-nitrobenzene (4.2). A solution of 2,3,4-trifluoronitrobenze (25.0 g, 141 mmol) in methanol (350 mL) was cooled to 0 °C in an ice-bath and treated with freshly prepared sodium methoxide (2.5 M, 125 mL, 313 mmol). After stirring at room temperature overnight, the reaction was neutralized with an aqueous solution of citric acid (1.0 M, 30 mL) and concentrated under reduced pressure. The residue was dissolved in ether (400 mL) and washed successively with an aqueous solution of citric acid (2 × 150 mL) and brine (150 mL). After drying (sodium sulfate) volatiles were removed under vacuum to afford the desired compound which was re-crystallized from hexanes to yield yellow crystals (27.8 g, 98% yield). mp = 58.5–59.0 °C, ^{1}H NMR (600 MHz, $CDCl_3$) δ 7.77 (dd, J = 9.3, 2.2, 1H, Ar-H), 6.77 (dd, J = 9.3, 7.6, 1H, Ar-H), 4.10 (d, J = 1.6, 3H, CH_3), 3.99 (s, 3H, CH_3). ^{13}C NMR (151 MHz, $CDCl_3$) δ 152.6 (d, J_{CF} = 9.2 Hz, C-2), 145.6 (d, J_{CF} = 249.6 Hz, C-3), 143.6 (d, J_{CF} = 11.7 Hz, C-4), 136.6, 120.4 (d, J_{CF} = 4.1 Hz), 105.7 (d, J_{CF} = 1.2 Hz), 62.2 (OCH_3), 56.2 (OCH_3). ^{13}C NMR (151 MHz, DMSO-d6) δ 152.8 (d, J_{CF} = 9 Hz), 145.1 (d, J_{CF} = 248 Hz), 142.9 (d, J_{CF} = 12 Hz), 136.28, 121.3 (d, J_{CF} = 4 Hz), 107.7, 62.6 (d, J_{CF} = 5 Hz), 60.0. ESI-MS: 172.2 $[(M+H)^{+}]$.

3-Fluoro-2,4-dimethoxyaniline (4.3). To a solution of compound **4.2** (27.4 g, 136.2 mmol) in anhydrous ethanol (200 mL) and ethyl acetate (200 mL), palladium on activated carbon (10% w/w, 3.0 g) was added. A hydrogen atmosphere was applied and the reaction mixture was stirred at room temperature for 7 h. The catalyst was removed by filtration and washed with ethanol. The combined filtrates were concentrated and ethyl acetate was added to the residue which caused a solid to precipitate. The solid was separated and the supernatant was concentrated under reduced pressure to yield the

desired compound as a brown syrup (23.3 g, 100%). ^{1}H NMR (600 MHz, $CDCl_3$) δ 6.56 (t, J = 8.6, 1H, Ar-H), 6.43 (dd, J = 8.8, 2.2, 1H, Ar-H), 3.95 (s 3H, CH_3), 3.82 (s, 3H, CH_3). ^{13}C NMR (151 MHz, $CDCl_3$) δ 146.36 (d, J_{CF} = 246 Hz, C-3), 140.67 (d, J_{CF} = 9.8 Hz, C-4), 135.94 (d, J_{CF} = 11 Hz, C-2), 133.97 (d, J_{CF} = 3.5 Hz), 108.63 (d, J_{CF} = 3.8 Hz), 108.51 (d, J_{CF} = 1.9 Hz), 60.48 (OCH_3), 56.87 (OCH_3). ESI-MS: 202.1 [$(M+H)^+$].

2-Fluoro-1,3-dimethoxybenzene (4.4). A solution of compound **4.3** (20.0 g, 117 mmol) in water (300 mL) and hydrochloric acid (concentrated, 150 mL) was cooled to 0 °C. A cold solution of sodium nitrite (16.1 g, 233 mmol) in water (100 mL) was added drop-wise. The resultant solution was stirred for 15 min, treated with hypophosphorus acid (50% in water, 150 mL, 1.70 mol) and left to stand overnight at 4 °C. The reaction mixture was stirred at room temperature for 2 h prior to neutralization by addition of 10% aqueous sodium hydroxide. The reaction mixture was extracted with ether (3 × 250 mL) and the combined organic layers were dried (sodium sulfate) and concentrated to yield the crude product as a dark syrup. This material was purified via flash chromatography (3:17 v/v ethyl acetate/hexanes) to afford the desired product as a orange liquid (14.2 g, 78%). ^{1}H NMR (600 MHz, $CDCl_3$) δ 7.06–6.95 (m, 1H, Ar-H), 6.63 (dd, J = 8.4, 7.3, 2H, Ar-H), 3.92 (S, 6H, 2 x CH_3). ^{13}C NMR (151 MHz, $CDCl_3$) δ 148.1 (d, J_{CF} = 8 Hz, C-1/C-3), 142.2 (d, J_{CF} = 244 Hz, C-2), 122.7 (d, J_{CF} = 5.4 Hz, C-4/C-6), 105.4 (C-5), 56.0 (OCH_3). ESI-MS: 157.1 [$(M+H)^+$].

2-Fluorobenzene-1,3-diol (4.5). A cooled solution of compound **4.4** (10.7 g, 68.5 mmol) in anhydrous dichloromethane (200 mL) at 0 °C was kept under a nitrogen atmosphere. To this mixture a solution of boron tribromide in dichloromethane (1.0 M, 235 mL, 235 mmol) was added and the reaction was then stirred overnight at room temperature. Water

(200 mL) was slowly added to the reaction which was stirred for 2 h and then the mixture was extracted with ether (2 × 150 mL). The organic fractions were dried (sodium sulfate) and concentrated. The crude residue was purified via flash chromatography (3:10 v/v ethyl acetate/hexanes) to afford the desired product as a white solid (8.21 g, 94%). mp = 104-105 °C, ^{1}H NMR (600 MHz, $CDCl_3$) δ 6.91 (td, J = 8.3, 2.1, 2H, Ar-H), 6.58 (t, 4H, Ar-H). ^{13}C NMR (151 MHz, $CDCl_3$) δ 143.6 (d, J_{CF} = 11.8 Hz, C-1/C-3), 140.2 (d, J_{CF} = 229 Hz, C-2), 123.8 (d, J_{CF} = 4.9 Hz, C-4/C-6), 108.6 (C-5). ESI-MS: 129.0 [$(M+H)^+$].

8-Fluoro-4-methylumbelliferone (4.6). A solution of compound **4.5** (512 mg, 4 mmol) in methanesulfonic acid (25 mL) was treated with ethyl acetoacetate (510 μL, 4.0 mmol). The resultant solution was stirred at room temperature for 2 h and then poured into ice. The reaction mixture was extracted with ethyl acetate (5 × 20 mL). The combined organic fractions were concentrated to afford the desired product as a yellow solid (780 mg, 100%). An analytical sample was obtained by purification using flash chromatography (1:1 v/v ethyl acetate/hexanes). mp = 219-220 °C, ^{1}H NMR (600 MHz, DMSO-d6) δ 7.53–7.28 (m, 1H, Ar-H), 7.02–6.85 (m, 1H, Ar-H), 6.20 (s, 1H, Ar-H), 2.40 (s, J = 25.0, 3H, CH_3). ^{13}C NMR (151 MHz, DMSO-d6) δ 159.5, 154.2 (d, J_{CF} = 2.1 Hz), 151.1, 143.2 (d, J_{CF} = 8.5 Hz), 138.6 (d, J_{CF} = 242.2 Hz, C-8), 121.0 (d, J_{CF} = 3.5 Hz), 113.8, 112.9, 110.9, 18.7 (CH_3). ESI-MS: 217.0 [$(M+Na)^+$]. Anal. Calcd for $C_{10}H_7FO_3$: C, 61.86; H, 3.63 Found: C, 61.96; H, 3.63.

4.2.2 Synthesis of GalβFMU

Synthetic route to GalβFMU is shown below (Figure 4-3). The Koenigs–Knorr donor was prepared from peracetylated D-galactopyranose. Subsequent glycosylation under phase-transfer conditions afforded compound **4.7** in 44% yield over two-steps.

Zemplín deacetylation was employed to give the desired galactoside **4.8** in 65% yield.

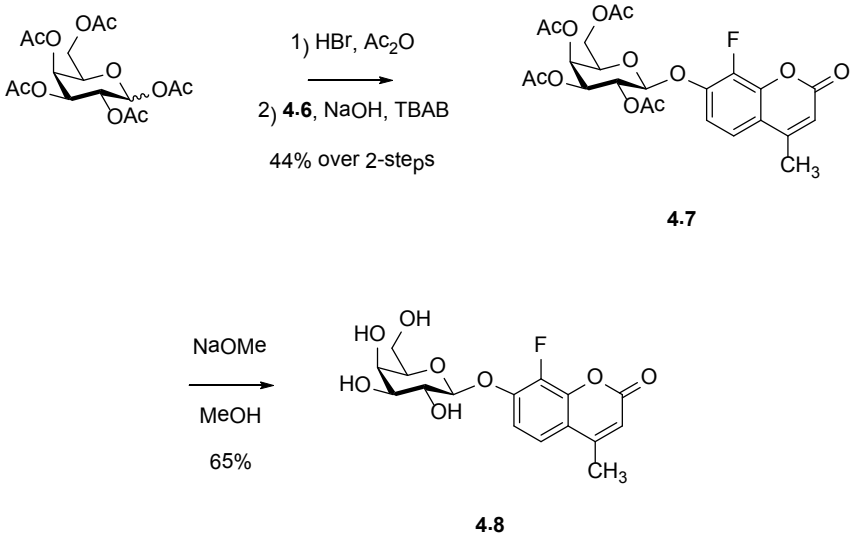

Figure 4-3 Synthetic route to GalβFMU.

8-Fluoro-4-methylumbelliferyl 2,3,4,6-tetra-*O*-acetyl-β-D-galactopyranoside (4.7). A solution of 33% hydrobromic acid in acetic acid (80 mL) and acetic anhydride (20 mL) was cooled to 0 °C in an ice-bath and treated with 1,2,3,4,6-penta-*O*-acetyl-β-D-galactopyranoside (10.0 g, 25.6 mmol). After warming and stirring at room temperature for 3.5 h, the reaction mixture was diluted with dichloromethane (150 mL) and poured into ice-water (~150 mL). After separation, the organic phase was washed with sat. aqueous sodium bicarbonate (150 mL), dried (sodium sulfate) and concentrated. The resultant residue was treated with **4.6** (2.49 g, 12.8 mmol), tetrabutylammonium bromide (3.90 g, 12.0 mmol), dichloromethane (300 mL) and aq. sodium hydroxide (1.0 M, 25 mL, 25 mmol). After stirring for 1 h, the reaction was quenched by the addition of sat. ammonium chloride and the resulting solution were extracted with ethyl acetate (3 × 100 mL). The organic fractions were dried (sodium sulfate) and concentrated. The residue was purified by flash chromatography to afford the desired product as a syrup [(2.95 g,

44% (over two-steps)]. ^{1}H NMR (600 MHz, $CDCl_3$) δ 7.32 (dd, *J* = 9.0 Hz, 2.0 Hz, 1H, Ar-H), 7.16 (dd, *J* = 9.0 Hz, 7.0 Hz, 1H, Ar-H), 6.29 (d, *J* = 1.0 Hz, 1H, Ar-H), 5.56 (dd, *J* = 10.4 Hz, 8.2 Hz, 1H), 5.49 (d = *J* = 2.9 Hz, 1H), 5.14 (dd, *J* = 10.4 Hz, 3.2 Hz, 1H), 5.07 (d, *J* = 7.8 Hz, 1H), 4.28-4.25 (m, 1H), 4.21-4.18 (m, 1H), 4.06 (t, *J* = 6.9 Hz, 1H), 2.45 (s, 3H, FMU-CH_3), 2.23 (s, 3H, CH_3), 2.14 (s, 3H, CH_3), 2.09 (s, 3H, CH_3), 2.05 (s, 3H, CH_3). ^{13}C NMR (151 MHz, $CDCl_3$) δ 169.9, 169.7, 169.7, 169.0, 158.7, 151.4, 146.4 (d, J_{CF} = 7.6 Hz, C-10), 141.5 (d, J_{CF} = 9.1 Hz, C-7), 137.7 (d, J_{CF} = 242.1 Hz, C-8), 118.6 (d, J_{CF} = 4.6 Hz, C-6), 117.1, 114.9, 113.8, 100.8, 70.95, 70.06, 67.87, 66.21, 60.88, 20.18 (× 2), 20.17, 20.10, 18.33. ESI-MS: 525.1 [$(M+H)^+$].

8-Fluoro-4-methylumbelliferyl β-D-galactopyranoside (4.8). A solution of compound **4.7** (1.4 g, 2.67 mmol) in sodium methoxide (0.5 M, 50 mL) was stirred at room temperature for 1.5 h. After 30 min, a white solid began to precipitate which was collected via filtration and rinsed with ether. Upon drying, the desired product was obtained as a white solid (620 mg, 1.74 mmol, 65%). mp = 181–182 °C, ^{1}H NMR (600 MHz, DMSO-d6) δ 7.55 (dd, *J* = 9.1, 1.5, 1H, Ar-H), 7.30 (dd, *J* = 9.0, 7.5, 1H, Ar-H), 6.35 (d, *J* = 1.2, 1H, Ar-H), 5.34 (bs, 1H, OH), 5.10 (d, *J* = 7.7, 1H, H-1), 4.94 (bs, *J* = 4.5, 1H, OH), 4.67 (bs, 1H, OH), 4.59 (bs, 1H, OH), 3.73 (s, 1H), 3.70–3.60 (m, 2H), 3.60–3.51 (m, 1H), 3.51–3.40 (m, 2H), 2.43 (s, *J* = 1.1, 3H, CH_3). ^{13}C NMR (151 MHz, DMSO-d6) δ 158.8, 153.4, 147.5 (d, J_{CF} = 7.4 Hz, C-10), 142.2 (d, J_{CF} = 8.9 Hz, C-7), 138.8 (d, J_{CF} = 247.4 Hz, C-8), 120.3 (d, J_{CF} = 4.1 Hz, C-6) 115.0, 112.4, 112.1, 100.9, 75.80, 73.26, 70.02, 68.02, 60.23, 18.19. ESI-MS: 357.1 [$(M+H)^+$]. Anal. Calcd for $C_{16}H_{17}FO_8$: C, 53.63; H, 4.78 Found: C, 53.37; H, 4.81.

4.2.3 Synthesis of Labelled ^{18}O-6-GalβFMU

The labelled starting materials, denoted by + symbol, for the seven isotopically substituted substrates are shown below (Figure 4-4). Labelled C3-deuterated Neu5Ac,[24] and 2-acetamido-2-deoxy-D-(3-^{18}O)mannose[47] were synthesized as reported in the literature. The ^{18}O-labelled compound **4.8** was accessed in six-steps beginning from D-galactose in 8% overall yield (Figure 4-5). Full experimental details are provided below.

Compound	Pyruvate	Neu5Ac	ManNAc	GalβFMU
4.1a	+			
4.1b			+	
4.1c	+			
4.1d				+
4.1e		+		
4.1f		+		
4.1g		+		

Figure 4-4 Labelled precursors for preparation of Neu5Acα2,6GalβFMU.

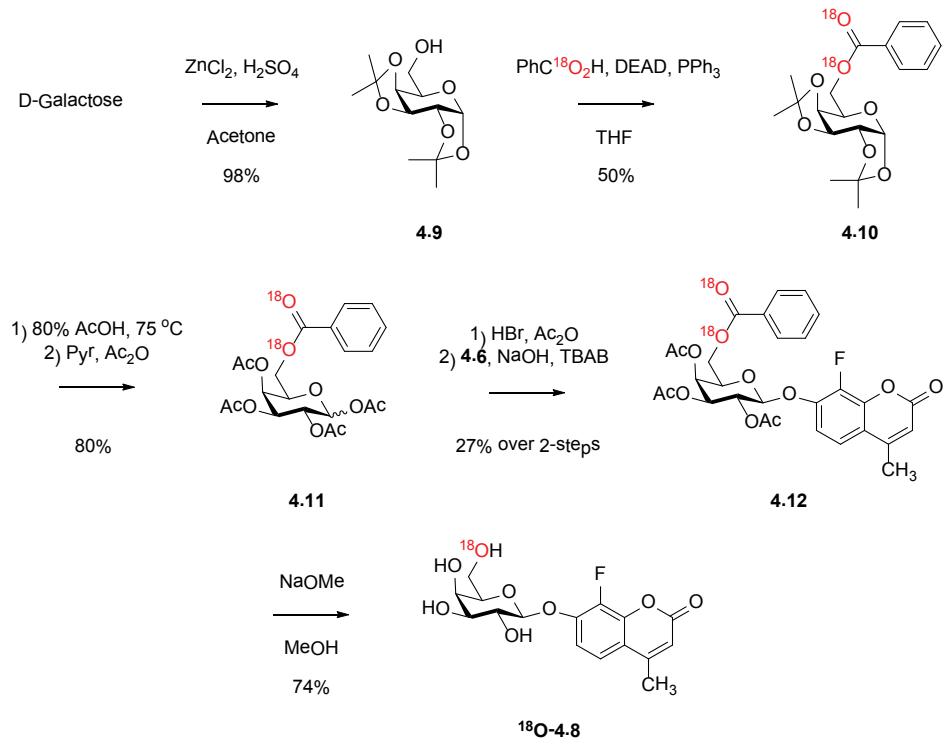

Figure 4-5 Preparation of (6-^{18}O)galactoside precursor **^{18}O-4.8**.

1,2:3,4-Di-*O*-isopropylidene-α-D-galactopyranose (4.9). A suspension of D-galactose (4.9 g, 27 mmol) in acetone (100 mL) was treated with zinc chloride (3.70 g, 27.2 mmol) and conc. sulfuric acid (0.1 mL). The resultant mixture was stirred at room temperature for 20 h. Potassium carbonate (1.0 g) was added and the resultant mixture was stirred for 10 min. The reaction mixture was filtered through a celite plug and washed with acetone. The filtrate and washings were concentrated under reduced pressure to afford the desired product as a colourless syrup (6.95 g, 98% yield). ^{1}H NMR (600 MHz, $CDCl_3$) δ 5.60 (d, *J* = 5.0, 1H, H-1), 4.64 (dd, *J* = 7.9, 2.4, 1H, H-3), 4.37 (dd, *J* = 5.0, 2.4, 1H, H-2), 4.30 (dd, *J* = 7.9, 1.6, 1H, H-4), 3.95–3.86 (m, 2H, H-5, H-6), 3.78 (dd, *J* = 15.7, 7.8, 1H, H-6'), 2.13 (bs, 1H, OH), 1.56 (s, 3H, CH_3), 1.49 (s, 3H, CH_3), 1.37 (s, 6H, 2 × CH_3): ^{13}C NMR (151 MHz, $CDCl_3$) δ 109.0, 108.2, 95.84, 71.18, 70.30, 70.11, 67.57, 61.94, 25.57,

25.46, 24.47, 23.83. ESI-MS: 283.1 [$(M+Na)^+$]. Anal. Calcd for $C_{12}H_{20}FO_6$: C, 55.37; H, 7.74 Found: C, 55.17; H, 7.81.

6-*O*-(^{18}O)-Benzoyl-1,2:3,4-di-*O*-isopropylidene-α-D-(6-^{18}O)galactopyranose (4.10). A flame dried flask was charged with compound **4.9** (500 mg, 1.92 mmol), ($^{18}O_2$)-benzoic acid (300 mg, 2.38 mmol),[68] triphenylphosphine (655 mg, 2.49 mmol) and anhydrous THF (25 mL). The reaction mixture was cooled in an ice-bath and treated with a 40% solution of diethyl azodicarboxylate in toluene (40% w/v, 1.1 mL, 2.3 mmol). After stirring at room temperature overnight, the solvent was removed under reduced pressure and the resultant residue was purified via flash chromatography (3:17 v/v ethyl acetate/hexanes) to afford the desired product as a syrup (371 mg, 50%).^{1}H NMR (600 MHz, $CDCl_3$) δ 8.13–8.04 (m, 2H, Ar-H), 7.63–7.54 (m, 1H, Ar-H), 7.51–7.42 (m, 2H, Ar-H), 5.60 (d, *J* = 5.0, 1H, H-1), 4.68 (dd, *J* = 7.9, 2.5, 1H, H-3), 4.56 (dd, *J* = 11.5, 4.9, 1H), 4.46 (dd, *J* = 11.5, 7.6, 1H), 4.40–4.34 (m, 2H, H-2), 4.26–4.17 (m, 1H, H-5), 1.55 (s, 3H, CH_3), 1.50 (s, 3H, CH_3), 1.39 (s, 3H, CH_3), 1.36 (s, 3H, CH_3). ^{13}C NMR (151 MHz, $CDCl_3$) δ 165.9, 132.5, 129.6, 129.2, 127.9, 109.2, 108.4, 95.87, 70.68, 70.27, 70.08, 65.68, 63.37, 25.55, 25.51, 24.51, 24.03. ESI-MS: 391.2 [$(M+Na)^+$].

1,2,3,4-Tetra-*O*-acetyl-6-*O*-(^{18}O)benzoyl-D-(6-^{18}O)galactopyranose (4.11). A solution of compound **4.10** (300 mg, 0.82 mmol) in aq. acetic acid (80% v/v, 10 mL) was stirred at 75 °C for 30 min. The solvent was evaporated under reduced pressure to yield a syrup was then treated with a mixture of pyridine:acetic anhydride (2:1, 20 mL) and stirred overnight at room temperature. The reaction mixture was diluted with dichloromethane (50 mL) and washed successively with water (50 mL), 10% sulfuric acid (50 mL), sat. aqueous sodium bicarbonate (mL) and brine (50 mL). The organic layer was dried

(sodium sulfate) and concentrated. The resultant residue was purified via flash chromatography (1:1 v/v ethyl acetate/hexanes) to afford the desired product as a colourless syrup (357 mg, 80%). ^{1}H NMR (600 MHz, $CDCl_3$) δ 8.05–7.98 (m, 2H, Ar-H), 7.63–7.57 (m, 1H, Ar-H), 7.50–7.44 (m, 2H, Ar-H), 6.44 (d, *J* = 3.1, 1H, H-1), 5.67–5.62 (m, 1H, H-3), 5.41 (dd, *J* = 5.2, 3.0, 2H, H-2, H-4/H-5), 4.53–4.44 (m, 2H, H-4/H-5, H-6), 4.30 (dd, *J* = 10.9, 6.9, 1H, H-6), 2.21 (s, 3H, CH_3), 2.19 (s, 3H, CH_3), 2.05 (d, *J* = 3.9, 3H, CH_3), 2.03 (d, *J* = 3.9, 3H, CH_3). ^{13}C NMR (151 MHz, $CDCl_3$) δ 169.6, 169.6, 169.4, 168.5, 165.4, 132.9, 129.3, 129.3, 128.8, 128.0, 89.29, 68.34, 67.06, 66.88, 66.04, 60.99, 20.42, 20.18, 20.16, 20.08.

8-Fluoro-4-methylumbelliferyl 2,3,4-tri-*O*-acetyl-6-*O*-(^{18}O)benzoyl-β-D-(6-^{18}O)galactopyranoside (4.12). A solution of 33% hydrobromic acid in acetic acid (60 mL) and acetic anhydride (11 mL) was cooled to 0 °C in an ice-bath and treated with compound **4.11** (3.09 g, 6.8 mmol). After warming and stirring at room temperature for 2 h, the reaction mixture was diluted with dichloromethane (150 mL) and poured into ice water (~100 mL). After separation of the organic phase, it was washed with sat. aqueous sodium bicarbonate (150 mL), dried (sodium sulfate) and concentrated. The resultant residue was treated with 8-fluoro-4-methylumbelliferone **4.6** (1.31 g, 6.8 mmol), tetrabutylammonium bromide (1.95 g, 6.0 mmol), dichloromethane (285 mL) and aq. sodium hydroxide (0.67 M, 38 mL, 25.4 mmol). After stirring for 1.5 h, the reaction was quenched by the addition of sat. ammonium chloride (20 mL) and the resulting solution was extracted with ethyl acetate (3 × 100 mL). The organic fractions were dried (sodium sulfate) and concentrated. The residue was purified by flash chromatography (1:39 v/v methanol/dichloromethane) to afford the desired product as a white solid (1.10 g, 28%

over two-steps). mp = 88–89 °C, ^{1}H NMR (600 MHz, $CDCl_3$) δ 8.08–8.00 (m, 2H, Ar-H), 7.66–7.59 (m, 1H, Ar-H), 7.54–7.43 (m, 2H, Ar-H), 7.16–7.03 (m, 2H, Ar-H), 6.26 (d, *J* = 1.2, 1H, Ar-H), 5.63–5.55 (m, 2H), 5.23–5.15 (m, 1H), 5.09 (d, *J* = 7.9, 1H), 4.61 (dd, *J* = 11.4, 7.5, 1H), 4.38 (dd, *J* = 11.4, 5.8, 1H), 4.25–4.18 (m, 1H), 2.38 (s, 3H, CH_3), 2.25 (s, 3H, CH_3), 2.14 (s, 3H, CH_3), 2.06 (s, 3H, CH_3). ^{13}C NMR (151 MHz, $CDCl_3$) δ 169.7, 169.6, 169.0, 165.3, 158.7, 151.3, 146.3, 146.3, 142.6, 141.3, 139.7, 133.0, 129.3, 128.8, 128.1, 118.5, 118.5, 116.9, 114.7, 113.8, 100.7, 71.14, 70.08, 67.93, 66.41, 61.22, 20.21, 20.16, 20.10, 18.25. ESI-MS: 591.2 [(M+H)+].

8-Fluoro-4-methylumbelliferyl β-D-(6-^{18}O)galactopyranoside (^{18}O-4.8). A solution of compound **4.12** (100 mg, 0.169 mmol) in a solution of sodium methoxide in methanol (0.5 M, 20 mL) was stirred at room temperature for 1.5 h. After 30 min of stirring a white solid began to precipitate but the reaction was stirred for an additional 1 h. The precipitate was collected via filtration and rinsed with ether. Upon drying in vacuo, the desired product was obtained as a white solid (45 mg, 74%). mp = 181–182 °C, ^{1}H NMR (600 MHz, DMSO-d6) δ 7.55 (dd, *J* = 9.1, 1.5, 1H, Ar-H), 7.30 (dd, *J* = 9.0, 7.5, 1H, Ar-H), 6.35 (d, *J* = 1.2, 1H, Ar-H), 5.34 (bs, 1H, OH), 5.10 (d, *J* = 7.7, 1H, H-1), 4.94 (bd, *J* = 4.5, 1H, OH), 4.67 (bs, 1H, OH), 4.59 (bs, 1H, OH), 3.73 (s, 1H), 3.70–3.60 (m, 2H), 3.60–3.51 (m, 1H), 3.51–3.40 (m, 2H), 2.43 (s, *J* = 1.1, 3H, CH_3). ^{13}C NMR (151 MHz, DMSO-d6) δ 158.8, 153.4, 147.5, 147.4, 142.2, 142.2, 139.6, 138.0, 120.4, 115.0, 112.4, 112.1, 100.9, 75.80, 73.26, 70.02, 68.02, 60.22, 18.19. Anal. Calcd for $C_{16}H_{17}FO_7{}^{18}O$: C, 53.63; H, 4.78 Found: C, 53.37; H, 4.81.

4.2.4 Preparation and Purification of Neu5Acα2,6GalβFMU

Neu5Acα2,6GalβFMU **4.1** and the requisite seven labelled isotopologues **4.1a-g**

were prepared chemoenzymatically from GalβFMU, ManNAc and pyruvate (Figure 4-6). Of note, in contrast to many chemical syntheses,[88-90] enzymatic coupling does not generate 5-acetamido-2,6-anhydro-3,5-dideoxy-D-glycero-D-galacto-non-2-enonic acid (DANA), a potent inhibitor of sialidases, as an unwanted side product.

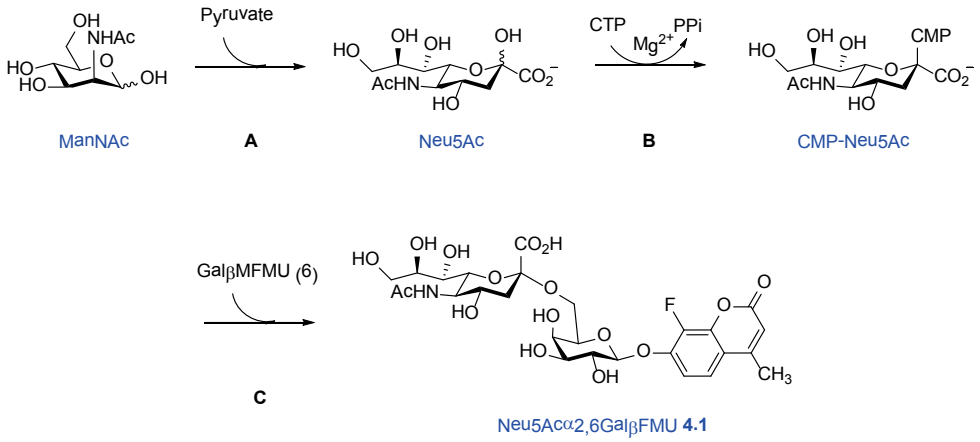

Figure 4-6 Enzyme mediated synthesis of Neu5Acα2,6GalβFMU.

The procedure for a typical reaction is described: A 50 mL autoclaved Falcon tube was charged with *N*-acetyl-D-mannosamine (50.0 mg, 226 μmol), sodium pyruvate (37.3 mg, 339 μmol), water (2.5 mL) and E. coli Neu5Ac aldolase (2 mg). The reaction vessel was incubated and shaken at 37 °C for 3 h. Subsequently, cytidine 5'-triphosphate disodium salt (178.7 mg, 339 μmol), aq. tris (1.0 M, 2.5 mL), aq. magnesium chloride (1.0 M, 1.0 mL), aq. dithiothreitol (1.0 M, 1.5 μL) and CMP Neu5Ac synthase (0.6 mL, 50 U/mL) were added to the reaction mixture. After a further incubation at 37 °C for approximately 1.5 h, the reaction mixture was centrifuged (10 min @ 2500 rpm). The supernatant was separated from the pellet and transferred to a new 50 mL autoclaved falcon tube, after which GalβMFMU (50.1 mg, 103 μmol) and α2,6-sialyltransferase (0.5 mL, 2.1 U/mL) were added to the solution, and the resultant mixture was incubated at 37 °C overnight.

The reaction mixture was loaded onto a reversed-phased C18 sep-pak cartridge (20 cc, 5 gram), and the cartridge was eluted successively with water (~50 mL) and 1:19 v/v acetonitrile/water (~150 mL). The fractions containing product were pooled and lyophilized to afford the product as a white solid. Typical yields ranged from 35-40%. Samples of Neu5Acα2,6GalβFMU in water were then loaded onto a HP/Agilent 1100 equipped with a C6 reverse phase HPLC column equilibrated in 95% solvent A (0.1% TFA in water) and 5% solvent B (100% acetonitrile-0.1% TFA). The desired analytically pure substrate was eluted from the column by increasing the gradient of solvent B over 30 min from 5% to 30%. The column flow rate was maintained at 2 mL/min and 300 μL fractions were collected. The absorbance of the effluent was monitored at 340 nm. Unlabelled Neu5Acα2,6GalβMFMU: mp = 149-149.5 °C. ^{1}H NMR (600 MHz, D_2O) δ 7.53 (d, J = 9.1, 1H, Ar-H), 7.25 (dd, J = 8.9, 7.5, 1H, Ar-H), 6.26 (d, J = 0.9, 1H, Ar-H), 5.10 (s, 1H, 1-H), 3.93-3.85 (m, 3H, 4-H, 5'-H), 3.80 (m, 1H, 2-H), 3.74-3.70 (m, 3H, 3-H), 3.65-3.54 (m, 4H, 4'-H), 3.51 (m, 1H), 3.44 (m, 1H), 2.70–2.61 (m, 1H, 3'-H_{eq}), 2.40 (s, 3H, Ar-CH_3), 1.91 (s, 3H, CH_3), 1.55 (t, J = 12.1, 1H, 3'-H_{ax}). ^{13}C NMR (151 MHz, D_2O) 174.96 (C=O, amide), 173.51 (C-1''), 162.46 (Ar), 155.52 (Ar), 146.37 (d, J_{CF} = 8.1 Hz, C-10), 141.48 (d, J_{CF} = 8.8 Hz, C-7), 140.31 (Ar), 139.00 (d, J_{CF} = 248.2 Hz, C-8), 119.19 (d, J_{CF} = 4.1 Hz, C-6), 116.00, 112.41, 111.57, 100.78 (C-1'), 99.04 (C-2''), 74.09 (C-4'), 72.31 (C-2'), 71.68, 70.27, 68.35, 68.13, 67.76, 62.98, 62.55 (C-5''), 51.79 (C-4''), 40.19 (C-3''), 21.93 (CH_3, FMU), 18.05 (CH_3). HR-MS m/z (M + H+), $C_{27}H_{34}FNO_{16}$ requires 648.1934, found 648.1929. All labelled Neu5Acα2,6GalβMFMU exhibited the predicted ^{1}H and ^{13}C NMR spectra consistent with incorporation of isotopes (^{2}H, ^{13}C and ^{18}O) at the expected positions.

4.3 Kinetic Measurements

Ms. April Lu aided this work by performing some kinetic measurements reported in this chapter.

4.3.1 Enzyme Kinetics

Michaelis-Menten kinetic parameters for *M. viridifaciens* sialidase and *A. oryzae* β-galactosidase, the auxiliary enzyme, were determined from a minimum of seven initial rate measurements within a substrate concentration range of at least $K_m/4$ to $4 \times K_m$ at 25 °C. The progress of each reaction was continuously monitored for 5 min using a Cary Eclipse Fluorescence Spectrometer equipped with a temperature controller. Each 500 μL reaction mixture was prepared by addition of the appropriate volume of buffer, substrate and enzyme. The rate versus substrate data were fitted to the Michaelis-Menten equation using a standard nonlinear least-squares program Prism 4.0.

In order to measure KIEs on V_{max} it was necessary to confirm whether the current coupled-enzyme assay reported only on the sialidase reaction (Figure 4-7). Therefore, the concentration of the β-galactosidase was doubled to ensure the observed rate did not change. Furthermore, at constant β-galactosidase concentrations, halving or doubling the concentration of *M. viridifaciens* sialidase resulted in a corresponding change of the observed rate. The fluorescence intensity of the galactoside aglycone (FMU) was found to be linear up to concentrations of at least 25 μM. This concentration corresponds to ~5% hydrolysis. Also, no photobleaching of FMU was observed under the experimental conditions over a time-course of 60 minutes.

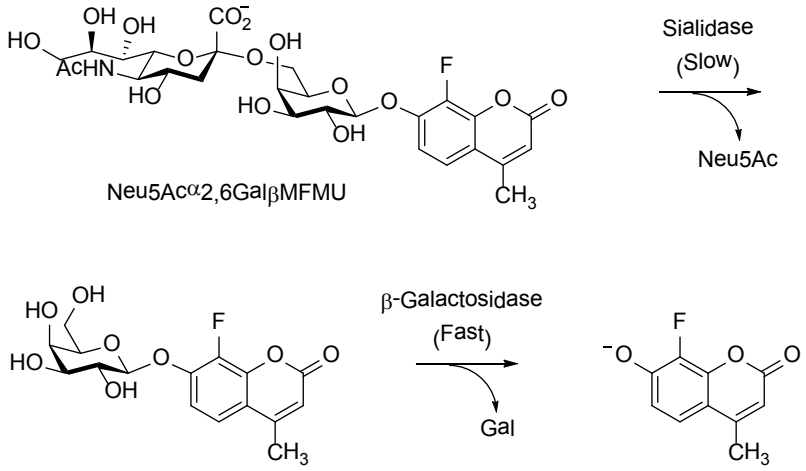

Figure 4-7 Coupled-enzyme assay for measurement of sialidase activity.

4.3.2 KIE Measurements

The stability of the enzyme solution (containing 0.1 mg/mL BSA), incubated at 25 °C, was evaluated by testing sialidase activity with the substrate Neu5AcαMU at periodic intervals. The measured enzyme activity remained invariant, within experimental error for over 48 h. Measurements of KIEs were performed at 25 °C in 100 mM MES ([BSA] = 0.1 mg/mL), adjusted to pH = 5.85. Concentrations of least seven times the K_m value of compound **4.1** were used. The fraction of substrate hydrolyzed during the course of the KIE measurements did not exceed 5%. The analysis order of the isotopically-labelled compounds was alternated (i.e., ^1H ^2H ^2H ^1H ^1H ^2H ^2H ^1H ^1H ^2H etc.). Consecutive pairs of kinetic runs were compared, the mean and standard deviation of at least seven such dyads were taken. To avoid biasing the results, a double-blind procedure was used whereby the identity of the 'labelled' and 'unlabelled' samples used in the experiments were unknown to both experimenters. Specifically, samples marked as 'A' and 'B' were prepared by experimenter 1, and the relative concentrations

were adjusted to < 1% difference based on UV/Vis absorbance by experimenter 2, who then relabelled the samples 'C' and 'D'.

The averaged KIE values from at least seven consecutive dyad measurements that are corrected to account for incomplete isotopic substitution according to either a literature procedure[91] or equation 4.1 in the case of β-secondary deuterium effects where unlabelled, mono-deuterated and di-deuterated isotopomers are present is summarized below (Table 11). The fractions of each isotopomer in the sample are represented by f_{HH}, f_{HD}, f_{DH}, and f_{DD}. For the dideuterio isotopomer **4.1g** the deuteration at C3 was assumed to be complete (i.e., $f_{DD} = 1$, and $f_{HH} = f_{HD} = f_{DH} = 0$).

Eq 4.1.

$$\mathrm{KIE}_{obs} = \frac{k_{\mathrm{HH}}}{(f_{\mathrm{HH}} \times k_{\mathrm{HH}}) + (f_{\mathrm{HD}} \times k_{\mathrm{HD}}) + (f_{\mathrm{DH}} \times k_{\mathrm{DH}}) + (f_{\mathrm{DD}} \times k_{\mathrm{DD}})}$$

Compound	Site of Substitution	KIE[a]	Weighted Average[b]
4.1a	Anomeric 2-^{13}C	1.022 ± 0.008	1.021 ± 0.006
		1.020 ± 0.008	
4.1b	Ring Oxygen 6-^{18}O	0.986 ± 0.004	0.986 ± 0.003
		0.984 ± 0.006	
		0.989 ± 0.010	
4.1c	C3-^{13}C	1.002 ± 0.010	1.001 ± 0.008
		1.001 ± 0.012	
4.1d	Leaving group 2-^{18}O	1.003 ± 0.006	1.003 ± 0.005
		1.002 ± 0.010	
		1.003 ± 0.011	
4.1e	Axial (3*R*)-^{2}H	1.035 ± 0.012	1.029 ± 0.007
		1.027 ± 0.011	
		1.025 ± 0.018	
4.1f	Equatorial (3*S*)-^{2}H	0.890 ± 0.012	0.891 ± 0.008
		0.893 ± 0.014	
		0.890 ± 0.014	
4.1g	Dideutero 3-$^{2}H_2$	0.885 ± 0.014	0.890 ± 0.006
		0.897 ± 0.009	
		0.885 ± 0.011	
		0.881 ± 0.009[c]	
Control	n/a	1.002 ± 0.008[d]	n/a

[a] Average and standard error from at least seven dyad measurements. [b] Calculated according to reference 92 [c] concentration of **4.1** was doubled (~14 × K_m), n = 3, [d] control experiment represents a ratio of observed rates between two separately prepared batches of unlabelled **4.1**, n = 5.

Table 11 Kinetic Isotope Effects on k_{cat} for the *M. viridifaciens* Sialidase-Catalyzed Hydrolysis of **4.1** in 100 mM MES Buffer pH = 5.85, [BSA] = 0.1 mg/mL and Temperature = 25 °C.

4.3.3 Solvent Kinetic Isotope Effect

Buffers were prepared by adding equivalent amounts of sodium hydroxide or

sodium deuteroxide, to MES in water or deuterium oxide, respectively. Reaction rates were determined at varying deuterium fractions by mixing the water and deuterium oxide buffers accordingly. Substrate concentrations ($7 \times K_m$) in water and deuterium oxide buffers were adjusted to < 1% difference based on the UV-Vis spectra of each stock solution. To ensure that the enzyme concentrations do not influence the observed rates, the same enzyme stock solution in water was added into each reaction. After dilution, the total water content from the enzyme solution was less than 2% of the total volume.

The solvent deuterium KIE (^{D_2O}V) for the sialidase-catalyzed hydrolysis of compound **4.1** was measured to be 1.585 ± 0.004. A proton inventory for this reaction displayed a linear correlation between the rate of hydrolysis (Figure 4-8).

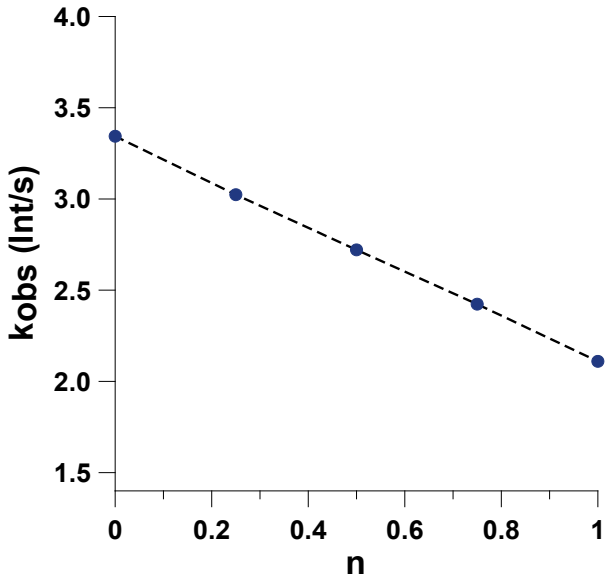

Figure 4-8 Proton inventory graph for MvNA-catalyzed hydrolysis of **4.1**. *n* = the fraction of deuterium in the solvent.

4.4 Discussion

4.4.1 Mechanism of Sialidase-Catalyzed Reactions

The current established mechanism for sialidases[35] under the initial rate conditions which is thought to involve the following sequential steps 1) formation of the Michaelis complex in which the substrate is bound as chair (k_1); 2) substrate conformational change from chair to boat (k_3); 3) hydrolysis of the glycosidic bond resulting in a tyrosinyl β-sialoside intermediate (k_5); 4) hydrolysis of the intermediate to yield Neu5Ac bound in a boat conformation (k_7); 5) product conformational change from boat to chair (k_9); and 6) dissociation of α-Neu5Ac from the enzyme active site (k_{11}) (Figure 4-9).

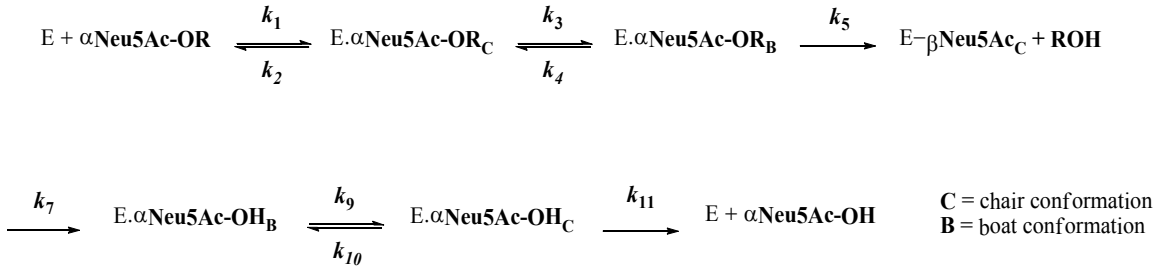

Figure 4-9 Proposed mechanism for sialidase-catalyzed hydrolysis reactions.

The first irreversible chemical step is the cleavage of the glycosidic bond (k_5). For a number of sialidases probed by Brønsted analysis, this step is at least partially rate-limiting for both V/K and V.[35,45,93] However, the derived β_{lg} values on V/K and V for MvNA are –0.30 ± 0.04 and 0.02 ± 0.03,[33] respectively, thus suggesting that a step after glycosylation, either k_7, k_9 and/or k_{11}, is limiting for V_{max}. Product inhibition studies (data not shown) demonstrates that Neu5Ac has little or no effect on the observed rate up to at

least 680 μM. This observation rules out product dissociation (k_{11}) as a possible candidate since this step would require that product inhibition be observed during catalysis. Of the remaining steps, only hydrolysis of the tyrosinyl β-sialoside intermediate (k_9) involves cleavage and formation of covalent bonds. As such, detection of KIEs on MvNA-catalyzed hydrolysis will differentiate the remaining steps.

Contrary to competitive techniques that report on V/K, measurement of KIEs on V can only be made by a direct comparison of individually measured rates of unlabelled and labelled substrates at saturating levels.[39,91] Thus, it is inevitable that these measurements are prone to greater systematic errors such as differences in substrate and enzyme concentrations, temperature fluctuations and inhibition by impurities. Although more difficult to determine, a number of reports have been published that exhibit a high-level of precision.[45,94] Furthermore, sophisticated computer-controlled continuous-flow methods have emerged for the measurement of carbon-13 KIEs (^{13}V) for formate dehydrogenase[95] and dialkylglycine decarboxylase.[96]

With regard to sialidases, it is common to measure KIEs using activated substrates such as Neu5AcαPNP[35,45,93] or Neu5AcαMU.[26] However, it is crucial to interpret such results cautiously since *p*-nitrophenoxide and the 4-methylumbelliferone anion are far better leaving groups than galactose by at least six orders of magnitude (pK_a values 7.08 and 7.80, respectively cf. ~13.6). As such, it is ideal to use substrates containing only natural sialyl-linkages;[68,87] however, this requires the use of auxiliary enzymes, which converts the aglycone into a species that is readily detectable.[87,97,98] For instance, Indurugalla *et al.* showed that accurate sialidase kinetic parameters could be obtained from α-2,3- and 2,6-sialyl-galactoside linkages, where a chromophore is

released in the presence of an *exo*-β-galactosidase.[87]

In order to ensure that the data obtained from a coupled-enzyme assay is accurate and reliable, several conditions must be met: i) the primary enzyme is irreversible and zero-order with respect to the substrate; and ii) the auxiliary enzyme is irreversible and first-order with respect to the intermediate generated by the primary enzyme.[99] The first condition is met by employing high substrate concentrations of at least 7 × K_m. Saturating levels are maintained throughout the assay by acquiring data only during the initial 5% of substrate hydrolysis. With regard to the second condition, using an excess of the auxiliary enzyme guarantees that the concentration of the intermediate formed is maintained well below its K_m value. The coupled-enzyme assay used in the present study involves the MvNA-catalyzed hydrolysis of Neu5Acα2,6GalβFMU **4.1** which releases the transient intermediate, GalβFMU. In the presence of excess β-galactosidase, GalβFMU is rapidly hydrolyzed to liberate the fluorescent aglycone, FMU for detection (Figure 4-7). Of note, FMU was chosen for this study, rather than the previously used 4-methylumbelliferone leaving group (4-MU),[87] because at the assay pH of 5.85 a larger fraction of the leaving group is present in a highly fluorescent anion form (pK_a value of 6.4 vs. 7.8).

4.4.2 Interpretation of KIEs

4.4.2.1 Oxygen-18 KIEs

The derived β_{lg} value on V is 0.02 ± 0.03[33] which requires that a step after cleavage of the glycosidic bond (k_5) be rate-limiting. As such, the leaving group ^{18}O-KIE for the hydrolysis of compound **4.1d** (^{18}V = 1.003 ± 0.005) is consistent with this conclusion since the ^{18}O-containing bond is broken prior to the rate-limiting step. In

contrast, the complementary endocyclic oxygen atom is associated with a prominent inverse KIE (compound **4.1b**; ^{18}V = 0.986 ± 0.003). This result suggests there is significant charge delocalization occurring onto the pyranosyl oxygen at the deglycosylation transition state (k_7, Figure 4-9).[68,76,77]

4.4.2.2 β-Secondary Deuterium KIEs

The magnitude of the two diastereomeric β-secondary deuterium KIEs (β-SDKIEs) are strikingly dissimilar with the *3S*-isotopomer displaying a large inverse KIE (**4.1f**; $^{D}V_S$ = 0.891 ± 0.008) and the *3R*-diastereomer a small normal effect (**4.1e**; $^{D}V_R$ = 1.029 ± 0.007) (Table 11). Of note, the C3-dideutero β-SDKIE ($^{D}V_{R,S}$ = 0.890 ± 0.006) is, within experimental error, the product of the individual 3S and 3R β-SDKIEs. Also, when the substrate concentrations for both unlabelled and dideutero isotopomers were doubled to approximately 14 × K_m, the measured 3-$^2H_2$ KIE remained invariant ($^{D}V_{R,S}$ = 0.881 ± 0.009; n = 3). With regard to solvolysis reactions of various glycosides, β-SDKIEs are typically normal and result from a hyperconjugative weakening of the C–H/D bond by overlap with the anomeric centre's developing p-orbital at the solvolysis reaction TS.[76,100,101] Given that hyperconjugation is an angular dependent phenomenon, the magnitude of β-SDKIEs has been used to probe the TS geometry for a number of sialidase-catalyzed reactions.[26,35,45]

In general, inverse β-SDKIEs are associated with either steric or inductive effects.[102,103] However, the magnitude of β-SDKIE for the enzyme catalyzed hydrolysis of compound **4.1f** falls well outside the range associated with a KIE originating from either of these two causes. As such, this KIE requires that the rate-limiting step involve a substantial strengthening of this C–H/D bond at the TS relative to the ground state. This

necessitates that the accumulating Michaelis-complex adopts a conformation where only one of the C–H/D bonds becomes weakened by a hyperconjugative interaction and that this effect either disappears or is considerably diminished at the TS (Figure 4-10).

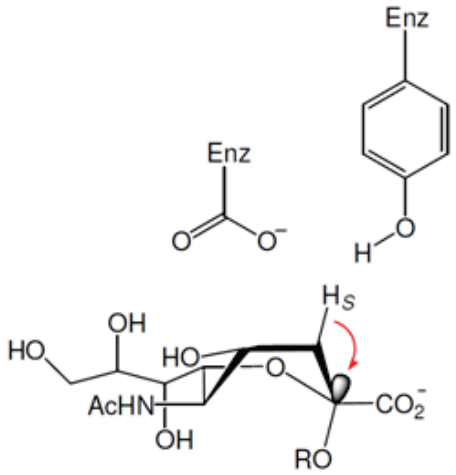

Figure 4-10 Proposed conformation adopted by the substrate in the accumulating Michaelis-complex where 3S σ(C-H) → σ*(C-O) hyperconjugation is maximized.

The most likely cause for the reduction in the ground-state force constant of 3*S* C–H/D bond is hyperconjugation to the σ(C–H/D) bond into the σ*(C–O) orbital of the aglycone moiety at the ground state. Specifically, it is expected that the inverse KIE will be fully manifested where the hyperconjugative weakening, which varies as a function of $\cos^2\theta$, is maximal (180° dihedral angle) in the ground state and absent in the TS (90° dihedral angle to the nascent p-orbital at the anomeric centre).

With regard to the measured inverse β-SDKIE ($^{D}V_S$ = 0.891), the magnitude of this value is consistent with an accumulating Michaelis-complex in which the substrate is positioned in a $^{6}S_2$ skew-boat conformation (Figure 4-11). This geometry allows for maximal hyperconjugative weakening because the dihedral angle between the *3S* σ(C–H)

bond and the σ*(C–O) orbital is 180° ($\cos^2\theta = 1$). A subsequent conformational change into a $^4S_2$ conformation, via the $B_{2,5}$, reduces the dihedral angle to approximately 150° and the corresponding interaction by 25% ($\cos^2\theta = 0.75$). Formation of the tyrosinyl β-sialoside intermediate (k_5) moves the *3S* σ(C–H) bond to a dihedral angle of about 60° to the σ*(C–O) orbital of the anomeric carbon to tyrosine oxygen bond ($^2C_5$ chair conformation; $\cos^2\theta = 0.25$). Breakdown of the enzyme-bound intermediate (k_7, Figure 4-9) requires that the anomeric carbon undergoes an oxygen-to-oxygen electrophilic migration from the enzymatic tyrosine residue to an acceptor water molecule. During this migration the dihedral angle between the 3S σ(C–H) bond and the developing p-orbital at the anomeric centre increases from 60° and based on the inverse secondary deuterium KIE, it is likely between 75-105° at the deglycosylation TS ($\cos^2\theta < 0.07$).

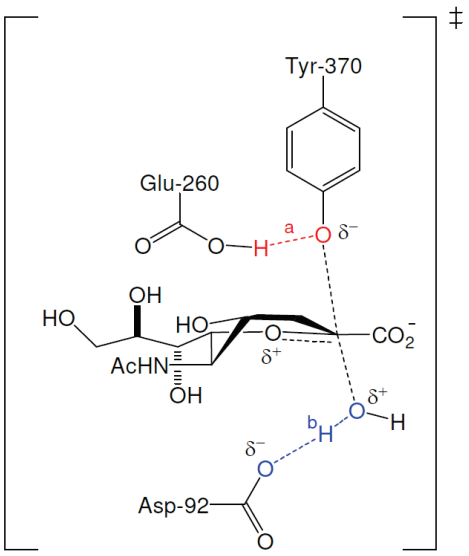

Figure 4-11 Putative TS structure for deglycosylation of the β-sialosyl-enzyme intermediate formed during the MvNA-catalyzed reactions.

In contrast, the 3R β-SDKIE is small and normal (**4.1e**; $^DV_R = 1.029 \pm 0.007$, Table 11) suggesting that there is a small hyperconjugative interaction at the

deglycosylation TS. This value is consistent with the β-SDKIEs reported for the *Vibrio cholerae*[45] sialidase-catalyzed hydrolysis of Neu5AcαPNP and the corresponding non-enzymatic hydrolysis.[24] In both studies the 3R β-SDKIE is the same or larger than the 3S β-SDKIE.

4.4.2.3 Carbon-13 KIEs

The anomeric ^{13}C KIE for the MvNA-catalyzed hydrolysis of compound **4.1a** is $^{13}V = 1.021 \pm 0.006$. Taken together with the β_{lg} on V and the ^{18}V KIEs (Table 11), the anomeric ^{13}C KIE is consistent with a deglycosylation (k_7, Figure 4-9) rate-determining step. Furthermore, the measured secondary ^{13}C KIE on carbon 3 (**4.1c**; $^{13}V = 1.001 \pm 0.008$) serves as an internal control given that it is unlikely that ^{13}C-labelling at this position would give rise to a significant KIE.

The magnitude of the anomeric ^{13}C KIE is commonly used as a guideline to distinguish between concerted or step-wise mechanisms. Typically, S_N2 reactions of glycosides in solution exhibit ^{13}C KIE values in the range of 1.03–1.08[80] In contrast, S_N1 reactions that proceed via non-equilibrated short-lived glycopyranosylium ions exhibit ^{13}k values around 1.00–1.01.[76,101] Unfortunately, the magnitude of the anomeric ^{13}C KIE from this study falls between the two ranges and does not allow an unambiguous distinction to be made between these separate mechanistic possibilities. Specifically, it is not known whether the water nucleophile has begun its attack on the anomeric centre. Regardless, it is certain that the deglycosylation TS is late and "exploded" with significant cleavage of the tyrosinyl-sialoside C–O bond and delocalization of positive charge from the anomeric centre occurring via a *n*p(O)→p(C) interaction (**4.1b**, $^{18}V = 0.986$).[75,103]

4.4.2.4 Solvent KIE and Proton Inventory

Based on the magnitude of the solvent deuterium KIE ($^{D2O}V = 1.585 \pm 0.004$) and the associated linear proton inventory (Figure 4-8), only one of the two possible proton transfer events is occurring at the deglycosylation TS. Specifically, the two possibilities are: i) general acid-catalyzed protonation of the tyrosine leaving group by Glu260; and ii) general base assisted nucleophilic attack of water by Asp92. Since the deglycosylation TS is S_N1-like and involves little or no participation of the water nucleophile, deprotonation via general base catalysis can be ruled out. In contrast, if general acid catalysis were absent, the enzymatic tyrosine residue would be required to depart as an anion resulting in a high energy intimate ion-pair.

4.4.2.5 Mechanistic Summary

All *exo*-sialidases characterized to date are retaining enzymes where the first released product has the same stereochemistry as that of the substrate. With regard to MvNA, the corresponding double inversion mechanism involves an accumulating Michaelis complex that positions the substrate in a $^6S_2$ skew boat conformation. Of note, at the present time it is not certain whether the initial binding event occurs simultaneously with, or prior to, the requisite enzyme-mediated conformational change. However, seeing as MvNA is a highly proficient enzyme ($k_{cat}/K_m > 10^7$ M^{-1} s^{-1} with activated substrates)[84] this conformational change is likely to be very rapid. The subsequent two steps involve: i) cleavage of the glycosidic bond which generates an enzyme bound intermediate; and ii) hydrolysis of the intermediate to produce α-Neu5Ac. It is likely that both glycosylation and deglycosylation feature similar "exploded" TSs. Finally, the product sialic acid dissociates from the enzyme active site to complete the catalytic cycle.

4.5 Conclusions

The work presented in this chapter reports a series of kinetic isotope effects measured on k_{cat}. This is the only characterized sialidase in which k_{cat} is solely rate-limited by deglycosylation. In addition, we observed an unusually large inverse β-secondary deuterium KIE, an effect that has allowed us to characterize the conformation of the accumulating Michaelis-complex and at the deglycosylation TS. Thus, we are well on our way to characterizing the transition state structures for each chemical step in the catalytic cycle for this important family of enzymes.

4.6 Supplementary ^{1}H NMR Spectra

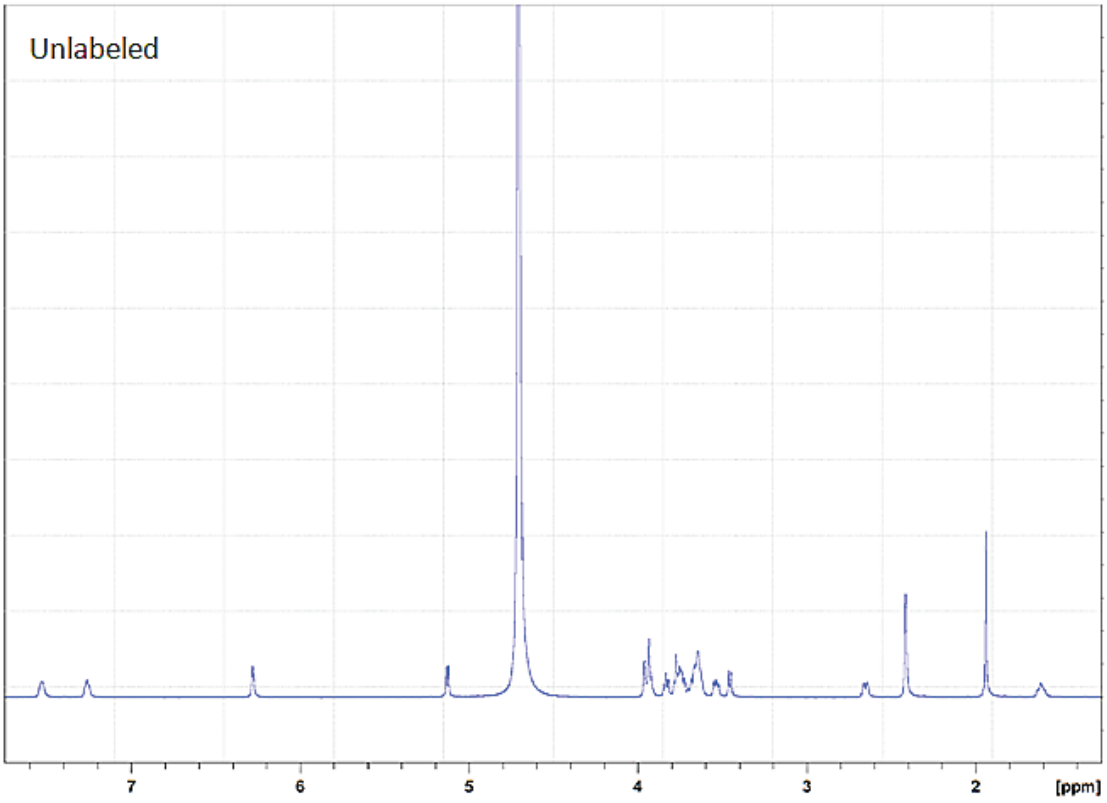

4.1a HR/MS *m/z* ($M^{+}H^{+}$), $C_{26}{}^{13}CH_{35}FNO_{16}$ requires 649.1973, found 649.1961.

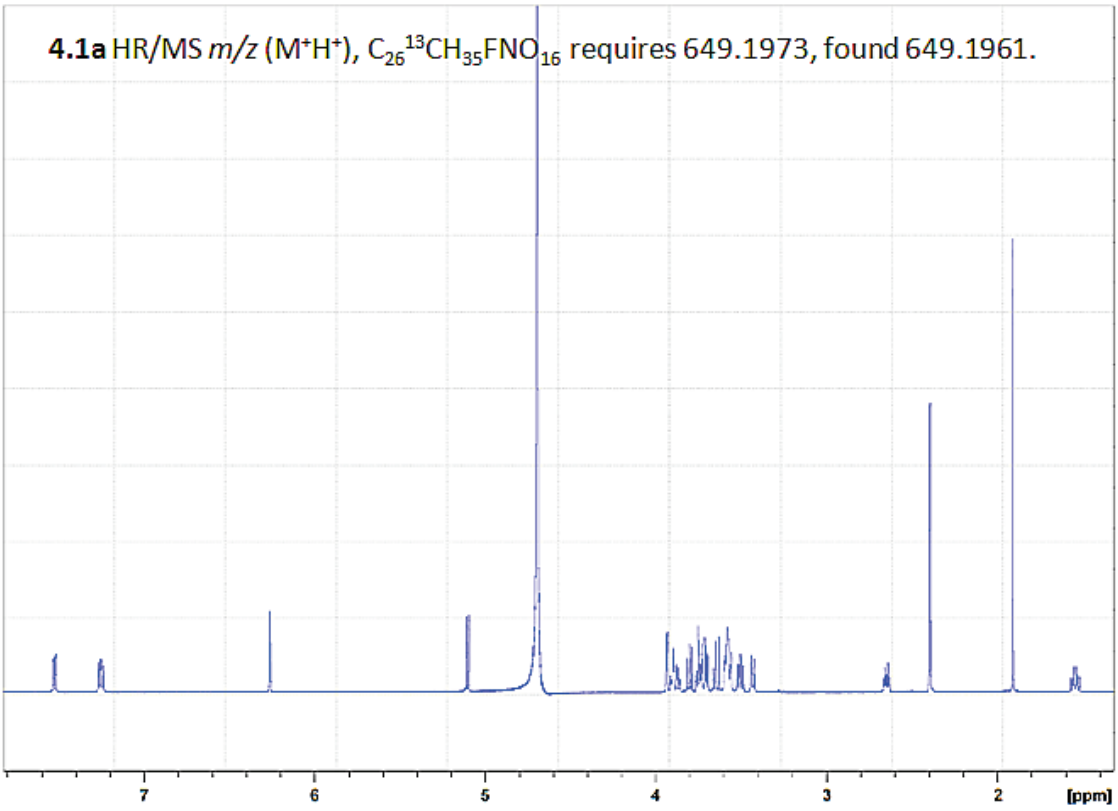

4.1b HR/MS *m/z* (M^+H^+), $C_{27}H_{35}FNO_{15}{}^{18}O$ requires 650.1982, found 650.1970.

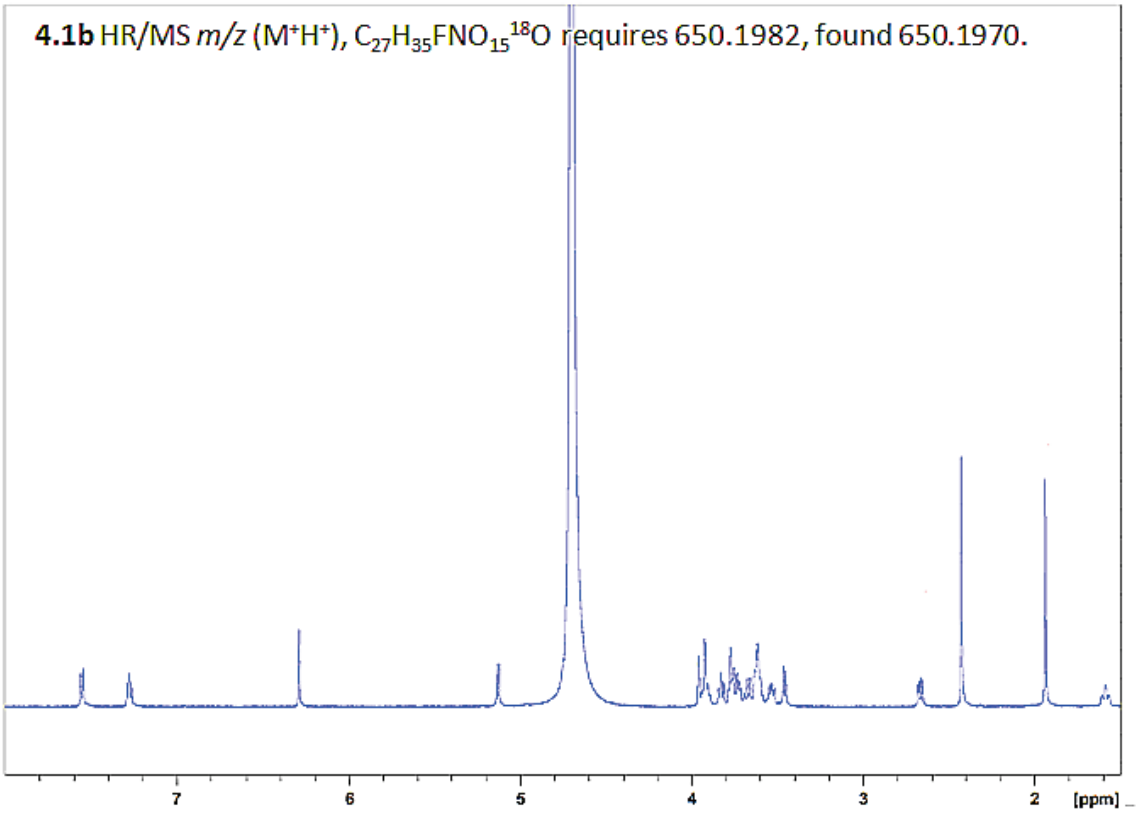

4.1c HR/MS *m/z* (M^+H^+), $C_{26}{}^{13}CH_{35}FNO_{16}$ requires 649.1973, found 649.1951.

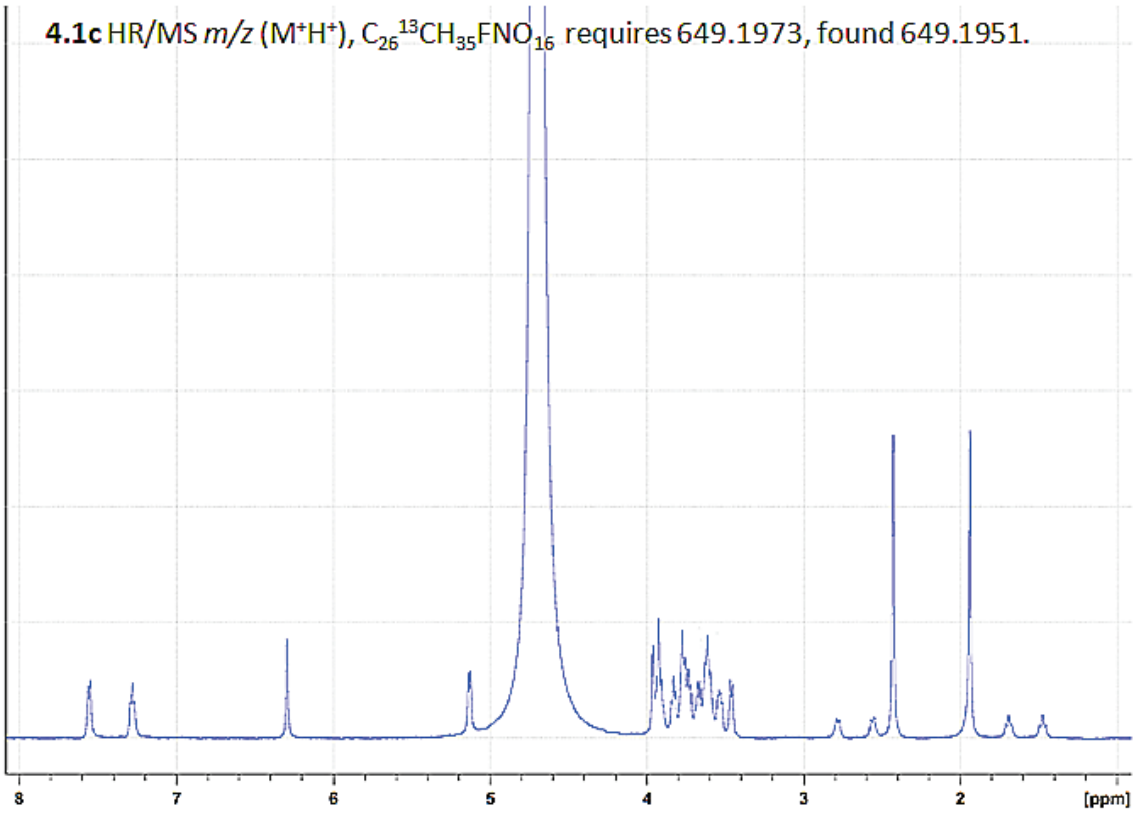

4.1d HR/MS *m/z* (M^+H^+), $C_{27}H_{35}FNO_{15}{}^{18}O$ requires 650.1982, found 650.1976.

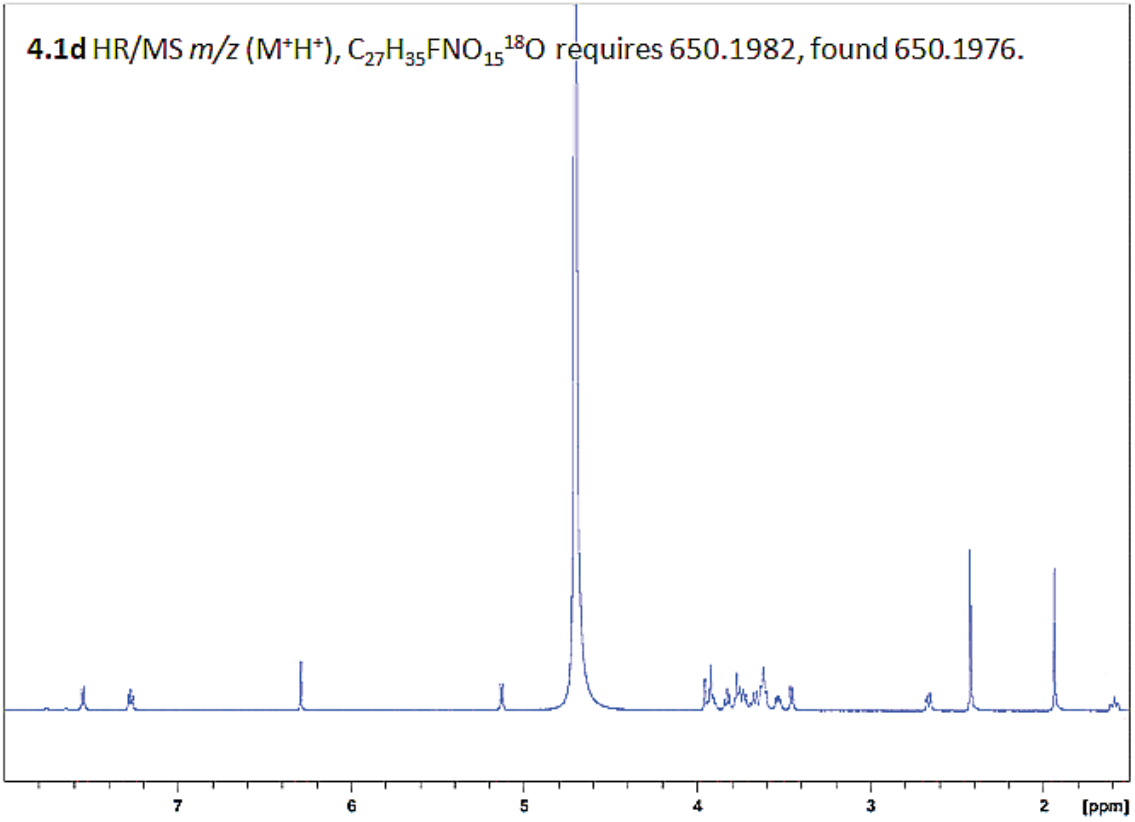

4.1e HR/MS *m/z* (M^+H^+), $C_{27}H_{34}DFNO_{16}$ requires 649.2003, found 649.2094.

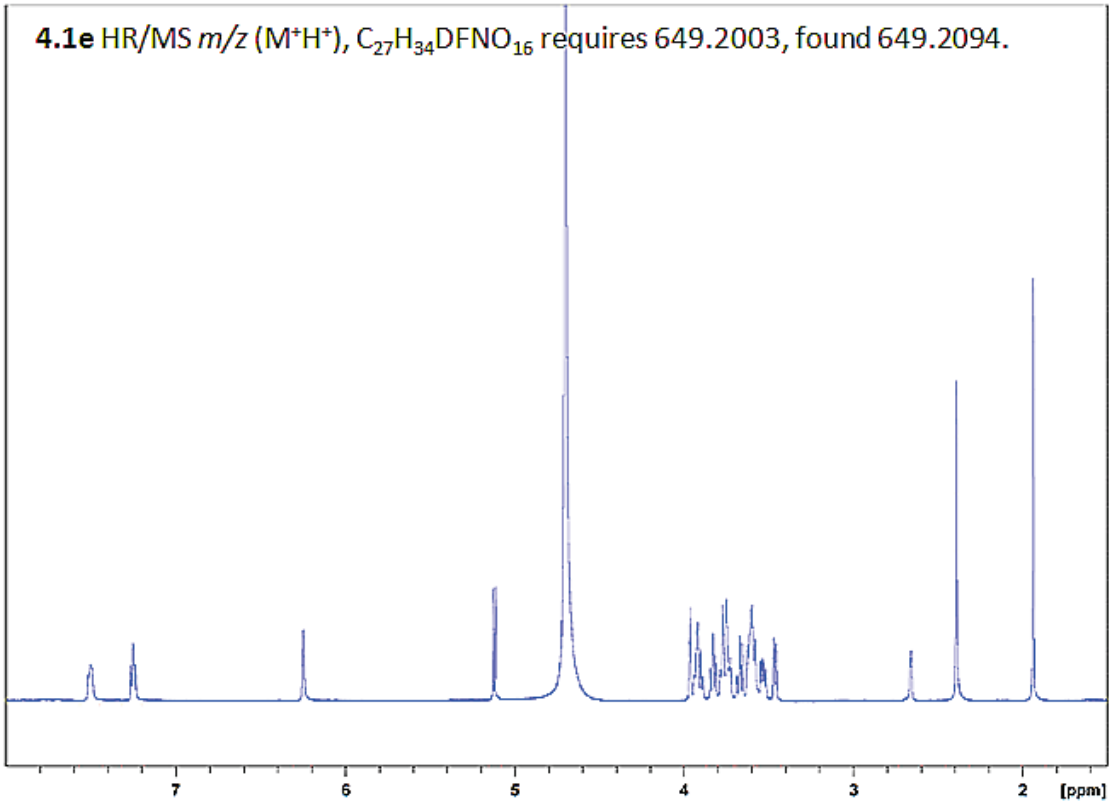

4.1f HR/MS *m/z* (M^+H^+), $C_{27}H_{34}DFNO_{16}$ requires 649.2003, found 649.1996.

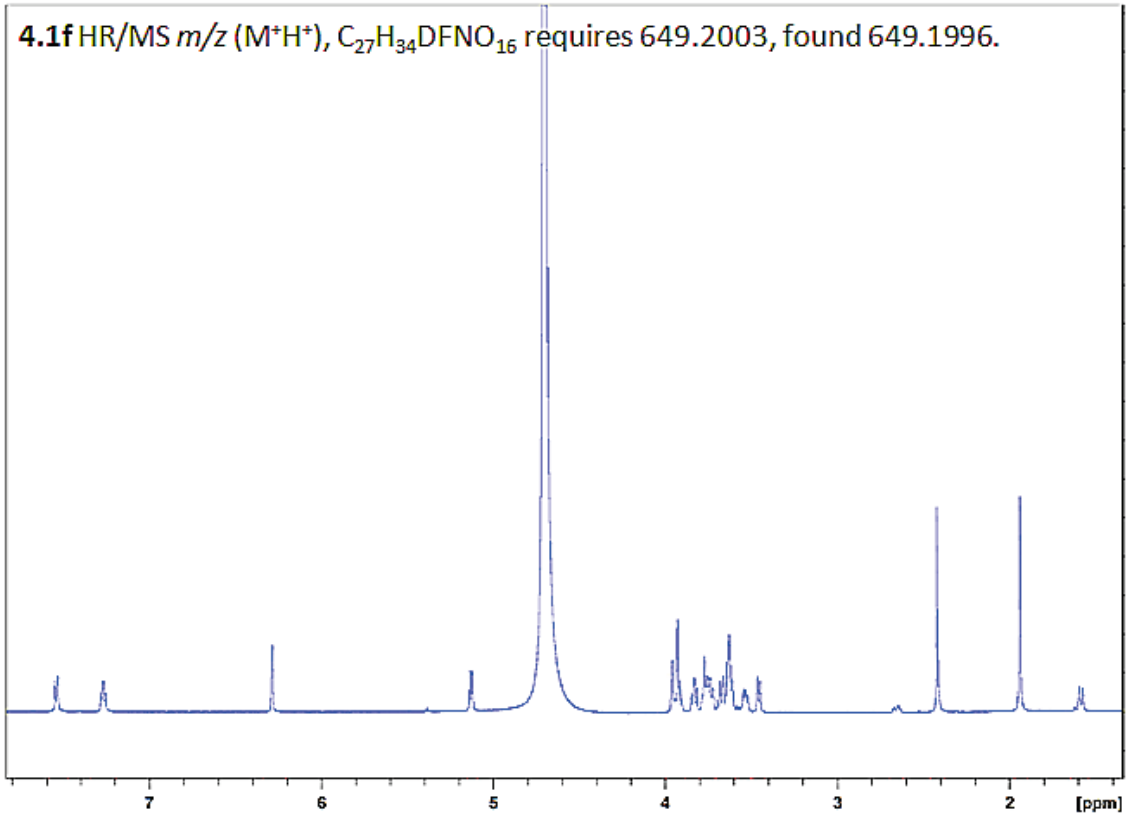

4.1g HR/MS *m/z* (M^+H^+), $C_{27}H_{33}D_2FNO_{16}$ requires 650.2065, found 650.2058 94.

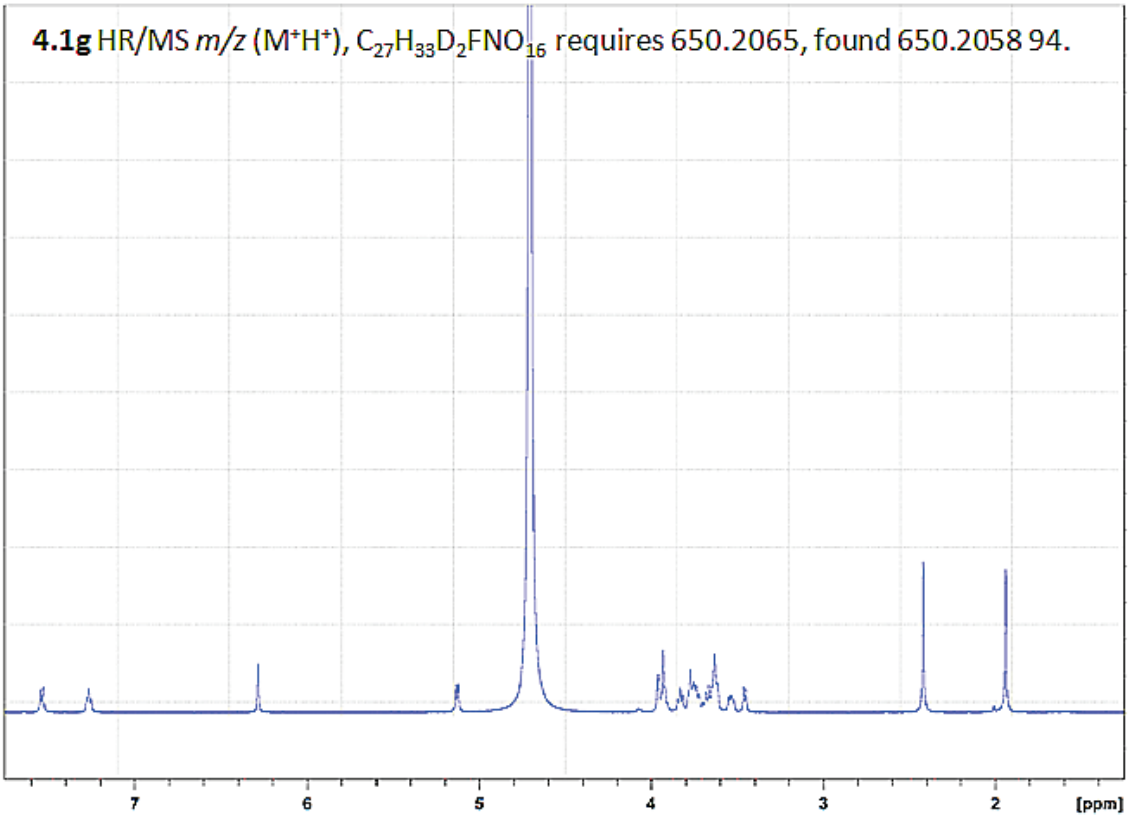

5: BACTERIAL AND VIRAL SIALIDASES: CONTRIBUTION OF THE CONSERVED ACTIVE SITE GLUTAMATE TO CATALYSIS

5.1 Introduction

The sialidase family is widely distributed throughout nature and has been linked to an array of different biological functions. The most-thoroughly studied viral and bacterial sialidases are those from influenza and *Micromonospora viridifaciens*, respectively. With regard to the influenza sialidase, this enzyme is critical for the release for viral progeny from infected host cells.[104] As such, a number of inhibitors have emerged as prominent anti-influenza therapeutics.[105,106] Sialidases feature a highly conserved active site[20] which includes three key catalytic residues, an aspartic acid, a glutamic acid and a tyrosine.[107-109]

Presented in Figure 5-1 is the current mechanism for glycosylation[33,34,85,110] which is a refinement of several previous proposals (active site residues in blue).[25,111,112] The subsequent reaction, deglycosylation, involves hydrolysis of the enzyme bound intermediate to complete the catalytic cycle. During glycosylation, the tyrosine[31,33,113] and aspartic acid[85,114] residues have been determined to operate as the nucleophile and general-acid, respectively. The active site glutamic acid, which is the third catalytic residue, has been proposed to function as a general-base during glycosylation and as a general-acid during the microscopic reverse deglycosylation reaction.[114] However, its specific role and extent of contribution during catalysis has been inadequately examined.

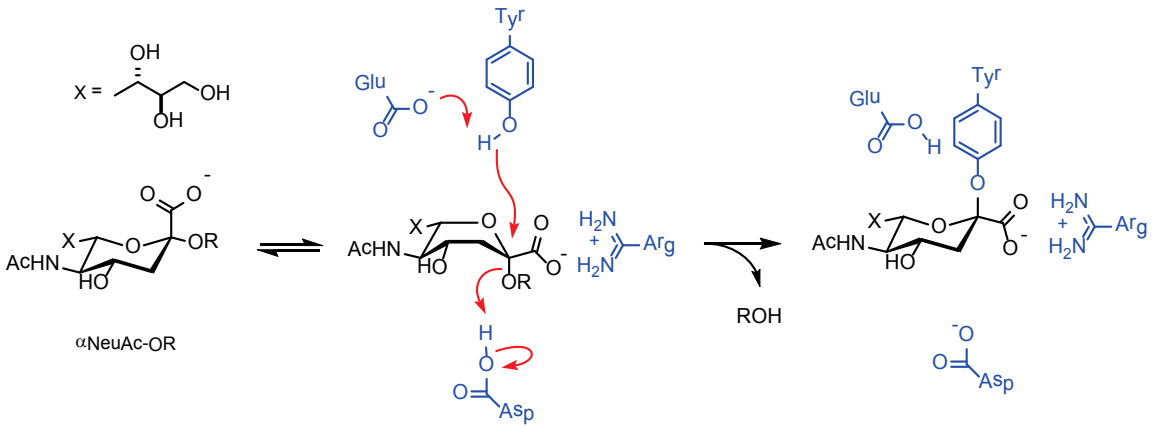

Figure 5-1 The mechanism of glycosylation for sialidases.

The present study details the results from kinetic studies on mutant sialidases, from *M. viridifaciens* and Influenza type A in which the active site glutamic acid residue has been replaced, using the technique of site-directed mutagenesis, by several different residues. The mechanistic implications of this residue are discussed.

5.2 Experimental

Dr. Jacqueline N. Watson performed the: 1) polyclonal antibodies; 2) mutagenesis experiments; 3) cloning, expression and purification of bacterial and viral sialidases; and 4) kinetic measurements for influenza sialidases.

Ms. April Lu aided in constructing some of the Brønsted plots for the *M. viridifaciens* mutants.

5.2.1 Influenza Sialidase Mutagenesis

Plasmid pJW1[115] was used as the template for the A/Tokyo/3/67 sialidase gene. Substitution of the codon for residues E277 and D151 involved making mutations in both strands in two PCR experiments. All five mutants were created in a similar fashion (data not shown). The front (3'-end) of the gene was amplified using the universal forward primer M13F' with the reverse mutagenic primer. The back portion (5'-end) of the gene was amplified using the forward mutagenic primers with the universal reverse primer M13R'. The front and back fragments had an overlapping sequence at the site of mutation, and were subsequently used to prime each other in an extension reaction of one cycle, followed by addition of universal primers to amplify the full gene. Following digestion with *Eco*RI and *Bam*HI, the purified 1.5 kb product was ligated into the pVL1392 expression vector (Pharmingen) and propagated in *E. coli*. Each mutant-containing plasmid was sequenced using primers NA400' (5'-CAA GTG TTA TCA ATT TGC-3') and NA782' (5'-CTA TTC ATT GAA GAG GGG-3'). The recombinant baculovirus DNA was isolated from high-titer virus stocks following established procedures [116] and sequenced using primers NA400'; NA782'; BV1' (5'-TTT ACT GTT

TTC GTA ACA GTT TTG-3'); and BV2' (5'-CAA CAA CGC ACA GAA TCT AGC-3'). Sequence analysis confirmed that the recombinant baculovirus stocks did indeed contain the correct substitutions for the five different mutations.

5.2.2 Polyclonal antibodies

A polyclonal antibody was raised against a peptide from a known antigenic loop region that is not close to the catalytic site.[23] Peptide NA324 (DTPRNDDRSSNSNC) conjugated to the carrier protein keyhole limpet hemocyanin was used to immunize two rabbits (Genemed Synthesis, Inc). Immunoblotting[117] and ELISA procedures were performed using a primary antibody dilution of 1/1000. The antiserum raised against peptide NA324 was tested by ELISA and western blotting for response to the peptide itself as well as crude and pure wild-type A/Tokyo/3/67 sialidase under denaturing conditions (data not shown). Antiserums from both rabbits solicited a specific response from the whole recombinant A/Tokyo/3/67 sialidase with minimal background.

5.2.3 Cloning Influenza Sialidase and Viruses

High-titer virus stocks were produced from single isolates in three passages. The final titers of the stocks used for expression were as follows: E277D, 8×10^7 pfu/ml and E277Q, 1×10^8 pfu/ml. Isolation of viral DNA from virus stocks yielded 100–940 ng. Full sequence analysis of the mutated genes confirmed that the recombinant baculovirus stocks did indeed contain the correct sialidase gene sequences for the two different mutations.

5.2.4 Influenza Viral Sialidase Mutant Expression

The mutant plasmids were co-transfected, isolated, and amplified as described for the wild-type.[115] Two separate small-scale expressions of the five mutants were performed in *Trichopluisa ni* insect cells using 60-mm plates as well as 100-mL spin-cultures. After 65 h at 37ºC and 100 rpm, crude supernatants were analyzed. Crude culture supernatant samples from the small-scale trial expressions of the two mutants were analyzed by western blotting and activity assays (Figure 5-2). Based on the western blot data, mutants D151N and E277D were expressed and purified on a large-scale (1.0–2.4 L) for characterization. Although the small-scale production of the D151A mutant gave no detectable protein by western blot analysis, it was also expressed on a 2 L scale in order to determine whether any mutant sialidase was present, even at extremely low levels. Comparison of concentrated D151A expression samples with the wild-type, D151N and E277D revealed that no D151A mutant was present. A total of six different virus isolates were analyzed by western blotting to check for a positive sign of expression, though nothing was observed for D151A, D151G or E277Q.

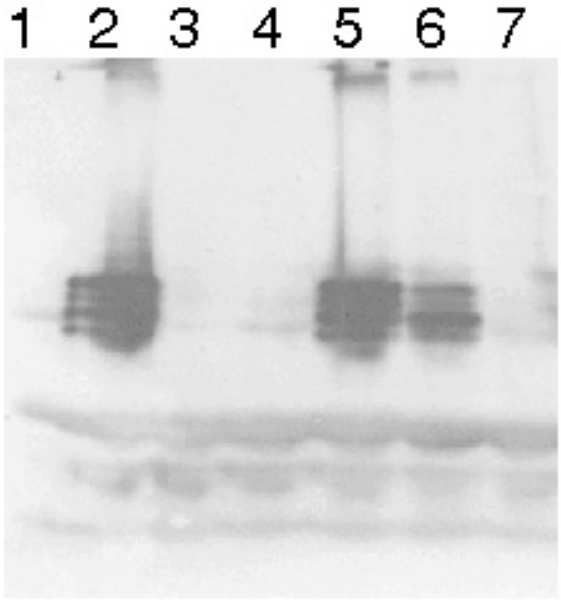

Figure 5-2 Western blot analysis of crude expression supernatant samples (both virus-associated and free forms). Each lane contains 100 μl of culture supernatant harvested 65 h post-infection. Lanes: 1) negative control from cells infected with baculovirus but no neuraminidase gene; 2) expression of the recombinant wild-type influenza neuraminidase; 3) mutant D151A; 4) D151G; 5) D151N; 6) E277D; 7) E277Q.

5.2.5 Purification of D151N and E277D

The purification of E277D and D151N followed the same protocol as that used for the wild-type enzyme.[115] Purification was monitored using both the sialidase assay as well as immunological techniques. Total protein concentration of the pure stocks determined by the Micro BCA assay were within 3% agreement of Bradford assay results, using ultra-pure BSA as the standard. Overall yields were 105 and 57 μg/L culture of E277D and D151N, respectively.

5.2.6 Enzyme Kinetics – *M. viridifaciens*

The progress of the reactions were continuously monitored for 10 min using either a Cary 3E spectrophotometer (UV/vis) or a Cary Eclipse fluorimeter equipped with a Peltier temperature controller. Michaelis-Menten parameters were determined from a minimum of seven initial rate measurements within a substrate concentration range of at least $K_m/4$ to $4K_m$. The rate versus substrate concentration data were fit to a standard Michaelis-Menten equation using the computer program Prism 4.0. The effect of leaving group ability was monitored at 25 °C in 100 mM acetate buffer (pH 5.25) using a series of aryl *N*-acetylneuraminides and 3'MUG-αNeuAc. The reactions of aryl substrates were monitored using UV/vis spectroscopy at various wavelengths (data not shown) and the reactions of MU-αNeuAc and 3'MUG-αNeuAc were monitored as reported.[87] For the case of the ED mutant, ^{1}H NMR spectroscopy was used to construct a relative Brønsted plot for k_{cat}/K_m. Specifically, MU-αNeu5Ac and an aryl *N*-acetylneuraminide (approximately 0.5 mg of each substrate) were combined in sodium formate buffer in deuterium oxide (600 μL; 100 mM; pD 5.25). Following the addition of enzyme the relative amounts of each substrate remaining were monitored as a function of time. The ratio of substrates remaining (R) versus the fraction of reaction of MU-αNeu5Ac (F) were fit to equation 5.1, where the aldehyde signal from the sodium formate buffer was used as the internal standard. The Brønsted plot on k_{cat} for the ED mutant was generated by monitoring the hydrolysis reactions at high substrate concentrations.

Eq. 5.1

$$\frac{\mathrm{R}}{\mathrm{R_o}} = (1 - F_1)^{\left(\left(\frac{1}{k_{\mathrm{rel}}}\right) - 1\right)}$$

5.2.7 pH-Rate Profile

To determine the effect of pH on catalysis, kinetic measurements were carried out using MU-αNeu5Ac as the substrate over a pH range of 3.78–7.90. The buffers (50 mM, I = 0.1, potassium chloride) used were sodium acetate-acetic acid (pH range 3.78–5.00), 2-(*N*-morpholino)ethanesulfonic acid (MES-sodium hydroxide) (pH range 5.62–6.50), and 3-(*N*-morpholino)propanesulfonic acid (MOPS-sodium hydroxide) (pH range 7.20–7.90). Fluorescence intensity calibration plots were generated for each of the eleven buffers used in these experiments.

5.2.8 Solvent Kinetic Isotope Effect

Buffers were prepared by adding 12 mM of hydrochloric acid or deuterochloric acid (12 mM), to sodium acetate (50 mM) in water or deuterium oxide, respectively. Reaction rates were determined at varying deuterium fractions by mixing the appropriate ratios of the water and deuterium oxide buffers. Substrate concentrations ($10.75 \times K_m$) in water and deuterium oxide buffers were adjusted to < 1% difference using UV-Vis spectroscopy. To ensure that the enzyme concentrations did not influence the observed rates, the same enzyme stock solution in water was added into each reaction. After dilution, the total water content from the enzyme solution was less than 2% of the total volume.

5.2.9 Enzyme Kinetics – Influenza Virus

The pure mutant sialidases were characterized in comparison to the wild-type enzyme with PNP-αNeuAc as substrate.[115] In order to achieve E277D mutant-catalyzed hydrolysis rates that were significant compared to the background reaction, it was necessary to measure kinetic parameters in a pH 8.0 buffer (50 mM HEPES, 0.1 mM calcium chloride, 0.32 mM magnesium chloride, 60 mM sodium chloride, T = 25 °C). Kinetic parameters with an abridged natural substrate, α-(2→3)sialyl-lactose (3'Lac-αNeuAc, V-labs) were determined by assaying for the liberated sialic acid product (Sialic-Q Quantitation Kit, Sigma-Aldrich). The binding constant of 3'Lac-αNeuAc with E277D was measured using a competitive binding assay. Specifically, the IC_{50} of 3'Lac-αNeuAc with E277D was measured using MU-αNeuAc under conditions where the value for IC_{50} is within 10% of that for K_i.[118]

5.3 Results and Discussion

5.3.1 *M. Viridifaciens* Sialidase Mutants

In this current study, five *M. viridifaciens* sialidase mutants were cloned, expressed and purified to probe the role played by the conserved glutamic acid during catalysis. The relative activities of these five E260 mutant enzymes were determined based on their ability to catalyze the hydrolysis of Neu5AcαMU. The preliminary kinetic data showed that the two most active mutants were the cysteine and aspartic acid mutants. As such, subsequent detailed kinetic experiments were performed using E260C and E260D. The ^{1}H NMR spectra accumulated during the hydrolysis of Neu5AcαPNP are shown below (Figure 5-3). These experiments unambiguously demonstrate that both mutants are retaining sialidases and thus suggest that the gross mechanism of action has not changed, in contrast to some active site tyrosine mutants.[110,119]

The derived Michaelis-Menten parameters for the E260C mutant sialidase-catalyzed hydrolysis of a series of α-sialosides are shown in Table 12. The E260D mutant was associated with small apparent K_m values. As such, it was impossible to measure accurate k_{cat}/K_m values for substrates in which the leaving group was not fluorescent. Therefore, k_{cat} values were measured at high substrate concentrations (Table 13) and k_{cat}/K_m values were measured relative to that for NeuAcαMU by comparing the proportionate rates of reaction in an NMR spectrometer (data not shown, see experimental section for full details).

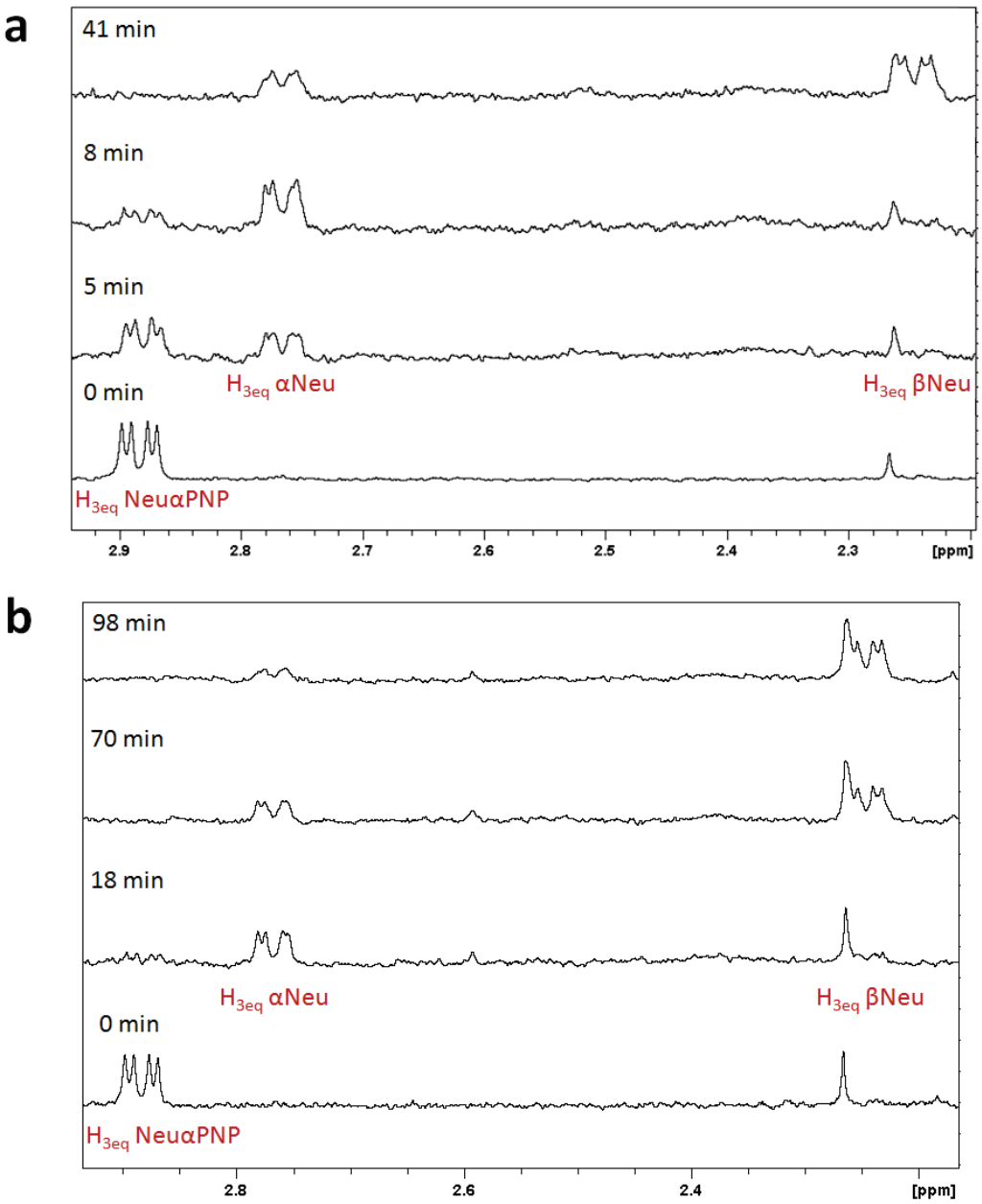

Figure 5-3 ^{1}H NMR spectroscopy: Hydrolysis of Neu5AcαPNP by a) E260C and b) E260D.

Leaving Group	pK_a	k_{cat} (s^{-1})	K_m app (M)	k_{cat}/K_m (M^{-1} s^{-1})
4-MU	7.80	0.183 ± 0.006	$(2.27 \pm 0.44) \times 10^{-6}$	$(8.05 \pm 1.86) \times 10^{4}$
4-Cyanophenol	7.96	0.081 ± 0.003	$(2.91 \pm 0.48) \times 10^{-6}$	$(2.80 \pm 0.54) \times 10^{4}$
3-Nitrophenol	8.27	0.218 ± 0.006	$(5.11 \pm 0.67) \times 10^{-6}$	$(4.26 \pm 0.68) \times 10^{4}$
3-Chlorophenol	9.09	0.094 ± 0.003	$(6.68 \pm 0.82) \times 10^{-6}$	$(1.40 \pm 0.21) \times 10^{4}$
Phenol	9.92	0.113 ± 0.015	$(7.62 \pm 2.33) \times 10^{-6}$	$(1.48 \pm 0.64) \times 10^{4}$
α(2,3)SMUG	13.6	0.069 ± 0.074	$(20.88 \pm 3.03) \times 10^{-6}$	$(0.33 \pm 0.40) \times 10^{4}$

Table 12 Michaelis-Menten Parameters for Hydrolysis of α-D-Sialosides by the *M. viridifaciens* E260C Mutant Sialidase, at pH 5.25 and 37 ºC.

Leaving Group	pK_a	k_{cat} (s^{-1})
4-MU	7.80	0.016 ± 0.022
4-Cyanophenol	7.96	0.030 ± 0.006
3-Nitrophenol	8.27	0.097 ± 0.030
3-Chlorophenol	9.09	0.030 ± 0.006
Phenol	9.92	0.030 ± 0.005
α(2,3)SMUG	13.6	0.025 ± 0.003

Table 13 Determination of the k_{cat} Parameter For Hydrolysis of α-D-Sialosides by the *M. viridifaciens* E260D Mutant Sialidase at High Substrate Concentrations, pH 5.25 and 37 ºC.

The derived Brønsted β_{lg} values on k_{cat} for the E260C and E260D mutant sialidases are –0.06 ± 0.04 and –0.02 ± 0.06, respectively (Figure 5-4), while the corresponding β_{lg} values on k_{cat}/K_m are –0.20 ± 0.04 and –0.54 ± 0.07, respectively (Figure 5-5). Also, shown in Figures 5-4 and 5-5 are the kinetic data for the wild type *Micromonospora viridifaciens* sialidase [119,120] where the reported β_{lg} values for k_{cat} and k_{cat}/K_m are 0.02 ± 0.03 and –0.30 ± 0.04, respectively.[119]

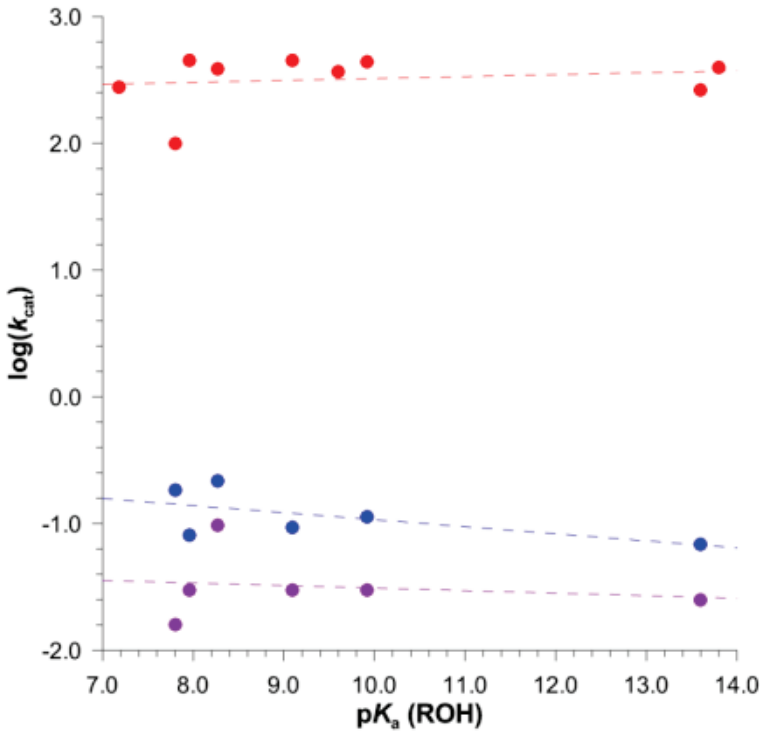

Figure 5-4 Effect of leaving-group ability on k_{cat} for wild-type (red circles), E260C (blue circles) and E260D (purple circles) at 25 °C, pH 5.25. Data for wild-type enzyme taken from references 119,120.

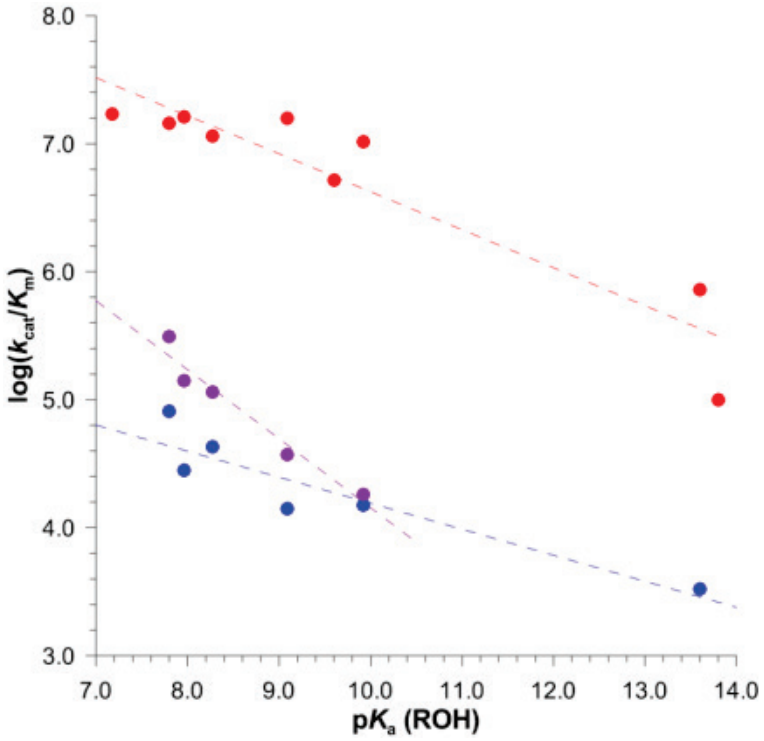

Figure 5-5 Effect of leaving-group ability on k_{cat}/K_m for wild-type (red circles), E260C (blue circles) and E260D (purple circles) at 25 °C, pH 5.25. Data for wild-type enzyme taken from references 119,120.

With regard to the cysteine mutant, the β_{lg} values for both kinetic parameters, k_{cat} and k_{cat}/K_m, are essentially unchanged from those of the wild-type *M. viridifaciens* sialidase. This result suggests that the corresponding rate-limiting steps for both enzymes are very similar. As such, the rate constant differences between the wild-type and the E260C mutant sialidase is likely due to a difference in TS stabilization caused by mutation. When the glutamate side-chain is truncated by a methylene unit to an aspartic acid residue, the β_{lg} value on k_{cat} is not changed. This is consistent with deglycosylation being rate-limiting for E260D mutant as was the case for the wild-type[73] and E260C enzymes. In contrast, for k_{cat}/K_m a significant increase in β_{lg} values occurs to –0.54 from

–0.30 (wild-type).[119] These two observations indicate that catalysis for the glycosylation reaction is more severely compromised in the E260D mutant than is the subsequent deglycosylation step. With regard to deglycosylation, the picture that emerges from the current data is that only weak general acid-catalysis from the glutamic acid residue is occurring at the TS.[73,121] Accordingly, mutation of this group, to either an aspartic acid or a cysteine, only retards breakdown of the sialosyl intermediate by factors of around 10^4, even for unactivated, natural leaving groups.

pH-Rate profiles were constructed for both mutants to probe the enzymatic activity at various ionization states. The kinetic data for the hydrolysis of NeuAcαMU catalyzed by the E260C mutant enzyme are shown below (Figure 5-6). It is apparent that for both kinetic parameters, k_{cat} (in red) and k_{cat}/K_m (in blue), the E260C mutant enzyme is more active at low pH values. Furthermore, both profiles feature an inflection point occurring at the same pH value, k_{cat} 6.73 ± 0.13; and k_{cat}/K_m 6.68 ± 0.20. The higher activity under more acidic conditions is likely caused by either: 1) the protonated cysteine being more active than its thiolate form; or 2) the cysteine residue providing little catalysis and removing the general acid/base glutamate amplifies the catalytic role being provided by the active site aspartic acid residue, and it is this ionization that is reported in these kinetic experiments.

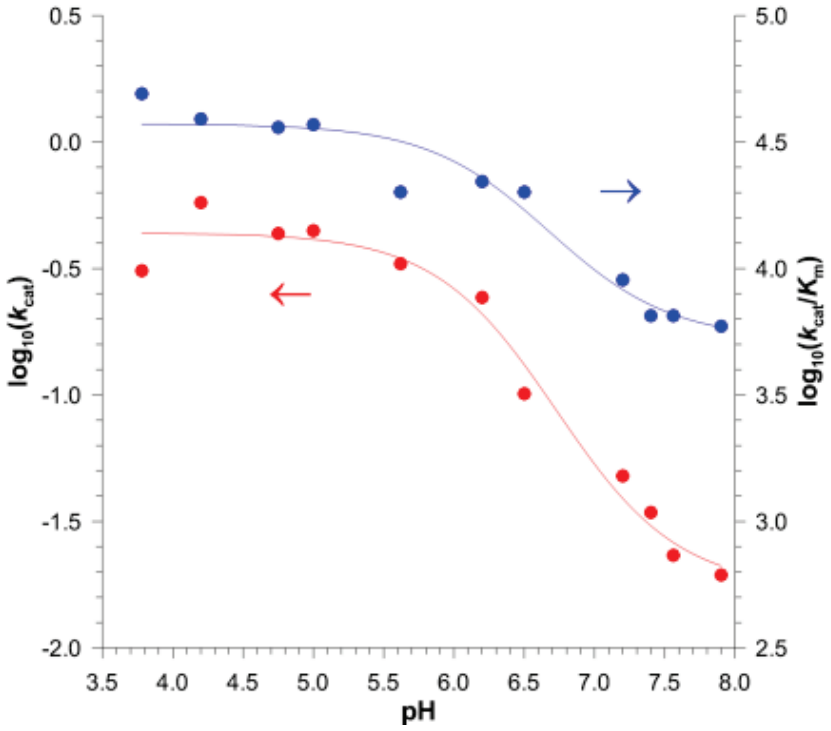

Figure 5-6 Effect of pH on k_{cat} (red circles) and k_{cat}/K_m (blue circles) for the E260C mutant sialidase catalyzed hydrolysis of NeuAcαMU at 25 °C.

On the other hand, the pH-rate profiles for both k_{cat} and $k_{cat}/K_m$with the E260D mutant enzyme show classic bell-shaped profiles, which suggest the involvement of two important ionizations (Figure 5-7). Based on the single critical ionization involved in catalysis by the E260C mutant the drop in activity at low pH values evidently arises from protonation of the aspartate-260 residue, and the drop in activity at higher pH values likely arises from deprotonation of the general-acid Asp-92.

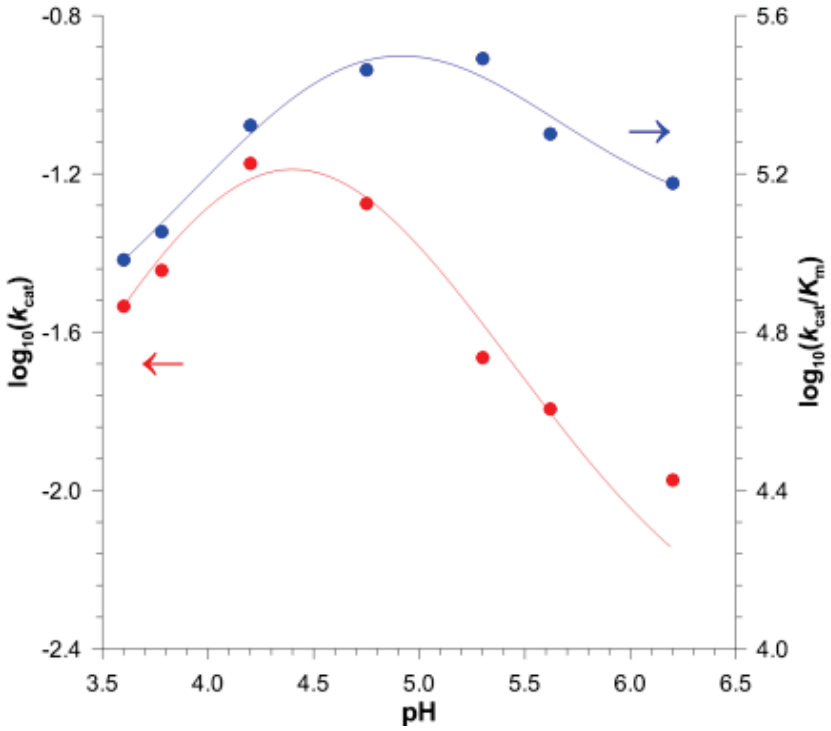

Figure 5-7 Effect of pH on k_{cat} (red circles) and k_{cat}/K_m (blue circles) for the E260D mutant sialidase catalyzed hydrolysis of NeuAcαMU at 25 °C.

The solvent deuterium KIE (k_{H2O}/k_{D2O}) = 2.31 ± 0.07 and the proton inventory (Figure 5-8)[122] on k_{cat} for the E260C mutant-catalyzed hydrolysis of NeuAcαMU is consistent with a single proton "in flight" at the TS for deglycosylation. This KIE is unlikely to have arisen from general acid-catalyzed protonation of the tyrosine leaving group since the Brønsted analysis has demonstrated that there is only weak general acid catalysis for this process. As such, the solvent deuterium KIE is likely associated with general-base catalyzed deprotonation of the water nucleophile. Of note, accurate measurements of the solvent deuterium KIE and the proton inventory for the E260D was impossible due to low activity.

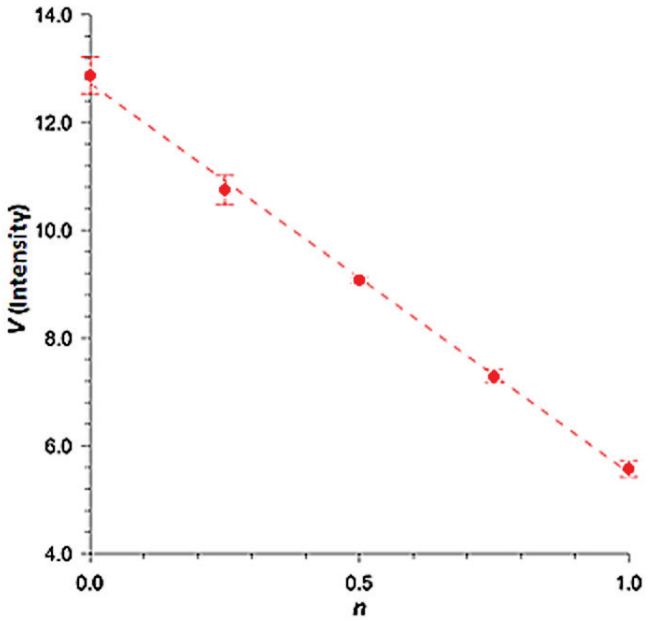

Figure 5-8 Measurement of V_{max} for the E260C mutant-catalyzed hydrolysis of MU-αNeuAc at as a function of *n* (mole fraction of deuterium in solvent) at 25 °C. The dotted line is the best linear fit to the data.

5.3.2 Influenza Viral Sialidase Mutants

The influenza viral mutant proteins were expressed in *Trichopluisa ni* insect cells and by assay, the E277D but not the E277Q mutant hydrolyzed the substrate NeuAcαMU. A western blot for crude expression samples of all five (two glutamate-277 and three asparate-92) mutants in comparison with the wild-type expression and negative control cultures is shown (Figure 5-2).

The samples shown on the western blot contain all protein, both virus-bound and free in the supernatant after prolonged expression (see experimental section). As a result, there are multiple forms of the sialidase present, presumably resulting from different glycoforms and proteolytic cleavage sites. For large-scale expressions, the cultures were

harvested much earlier and a single species of sialidase was isolated by protease cleavage from the surface of the baculovirus particles.

5.3.2.1 Influenza Sialdase E277 Mutants

Substitution E277D yielded an active protein, while E277Q did not. Due to the low activity of E277D, kinetic experiments were performed at 25 °C and pH 8.0 to increase the sensitivity of the assay. The measured catalytic constants for the wild-type and E277D sialidases are shown below (Table 14). Although no turnover was detected for the abridged natural substrate (3'Lac-αNeuAc), in the presence of E277D it binds to both the mutant's and wild-type's active sites with comparable affinities (K_d = 2.2 and 0.5 mM, respectively).

	NeuAcαPNP		3'Lac-αNeuAc	
Enzyme	k_{cat} (s^{-1})	k_{cat}/K_m (M^{-1} s^{-1})	k_{cat} (s^{-1})	k_{cat}/K_m (M^{-1} s^{-1})
WT[a]	26.2 ± 1.3	$(2.8 \pm 0.5) \times 10^5$	10.7 ± 0.6	$(9.8 \pm 2.2) \times 10^3$
WT[b]	1.82 ± 0.05	$(1.8 \pm 0.2) \times 10^4$	4.52 ± 0.24	$(9.6 \pm 2.1) \times 10^3$
E277D[b]	0.012 ± 0.002	13 ± 4.5	$< 5.7 \times 10^{-4}$[c]	< 0.26 [c]

[a] pH = 6.0 at 37 °C. [b] pH = 8.0 at 25 °C. [c] These values represent upper limits as no activity was detected.

Table 14 Michaelis–Menten Kinetic Parameters for the Recombinant Influenza A/Tokyo/3/67 Wild-type and E277D Mutant Sialidases with Various Substrates

5.4 Conclusions

Mutagenesis is a common tool used to probe the contribution of a specific amino acid residue to catalysis. Our group has previously used this technique to generate a series of tyrosine (nucleophile) and aspartate (general acid) mutants of MvNA. The work presented in this chapter probes the contribution of the glutamate residue (general base) to catalysis. Our findings suggest that overall mechanism does not change, despite large decreases in catalytic efficiency when the glutamate is substituted with either a cysteine or aspartate. For instance, both E260C and E260D mutants are retaining enzymes as determined by ^{1}H NMR spectroscopy and the global rate-limiting step is deglycosylation of the enzyme-bound intermediate.

6: A MECHANISTIC STUDY OF SIALIC ACID MUTAROTATION: IMPLICATIONS FOR MUTAROTASE ENZYMES

6.1 Introduction

N-acetylneuraminic acid (Neu5Ac), the most prevalent and frequently studied member of the sialic acid family, has been implicated in a number of human pathologies including cancer.[123] Many metastatic cancer cells exhibit hypersialylation of their surface glycoproteins, a modification which is believed to facilitate migration of these cells into the blood stream.[124] Enzymatic degradation of these glycoproteins is frequently used to delineate the role and effect of hypersialylation. Upon application of an *exo*-sialidase, the initial product formed, α-Neu5Ac, undergoes spontaneous mutarotation to produce an equilibrium mixture, which consists of the β-anomer (91.2%), the α-anomer (5.8%) and three open-chain species (a ketone, an enol and a *gem*-diol).[6]

In 1846, Dubrunfaut observed that the specific rotation of aqueous sugar solutions changed as a function of time until a value of +52.7° was established.[125] This process, coined as mutarotation,[126] was later attributed to the interconversion between the two anomers of glucopyranose. This reaction involves a key ring-opening event that generates an open-chain carbonyl species followed by subsequent σ-bond rotation of the carbonyl group and ring-closing. Since the initial discovery, the mutarotation of numerous sugars[127,128] has been studied extensively. Polarimetry is the analytical method of choice for many sugars to monitor this reaction because one or both anomers are readily isolable as crystalline solids. In contrast, investigation of Neu5Ac mutarotation

has proven to be far more challenging as neither of the anomers have been isolated in pure form from the equilibrium mixture. Friebolin *et al.* were the first to address this problem by treating 2-azido-*α*-Neu5Ac with an *exo*-sialidase to generate *α*-Neu5Ac *in situ*.[55,129] Hydrolysis of the substrate and the subsequent mutarotation were monitored by ^{1}H NMR spectroscopy at five pD values (1.3, 3.9, 5.4, 6.7 and 11.7). The authors were unable to determine rate constants at pD 1.3 and 11.7 but reported a half-life of 80 minutes at a pD value of 5.4.[129] Many mechanistic details of this fundamental process of Neu5Ac mutarotation remain unclear, for instance, what are the respective efficiencies of acid- and base-catalysis? Is there a water-catalyzed process? Also, is this equilibration reaction catalyzed by buffers?

Recently, a β-propeller protein, YjhT, from *E. coli* was found to possess Neu5Ac mutarotase activity.[130] As such, a mechanistic study on the corresponding non-enzymatic reaction will provide valuable insight as to how nature evolved an enzyme to accelerate this spontaneous and facile process. In this chapter we use ^{13}C and ^{1}H NMR spectroscopy to provide pH- and pD-rate profiles for the mutarotation of Neu5Ac, respectively. In addition, the proton inventory technique[131] was used to probe the timing and number of protons "in-flight" at the transition state for the water-catalyzed reaction.

6.2 Experimental

6.2.1 Protocol for Generating α-Neu5Ac

Neu5Acα2,6LacβSPh **6.1a** and its ^{13}C-labelled isotopomer **6.1b** were prepared chemoenzymatically as described previously.[68] These substrates were treated with a concentrated solution of *M. viridifaciens* neuraminidase (MvNA), dialyzed into non-buffered deuterium oxide prior to use, under conditions in which α-Neu5Ac is rapidly generated *in situ* (Figure 6-1).[33] The subsequent interconversion to β-Neu5Ac, the thermodynamically favored species in solution, was monitored by ^{1}H or ^{13}C NMR spectroscopy. MvNA was chosen for the current study, rather than other *exo*-sialidases, because this enzyme displays a very high catalytic efficiency[33,84] and it remains active over a large pH range.[33] Essentially, all substrate is completely hydrolyzed to yield α-Neu5Ac by the time the first NMR spectra can be acquired.

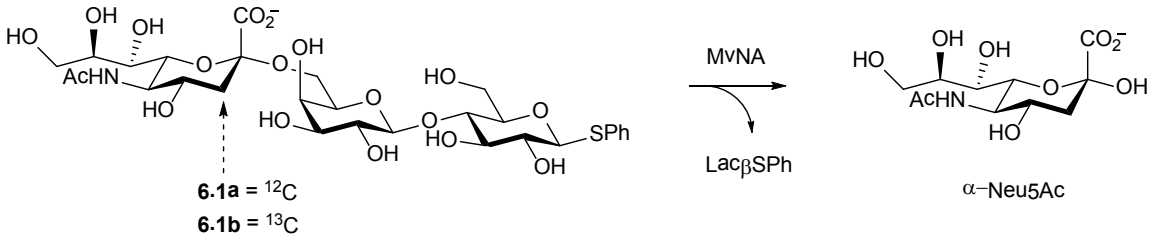

Figure 6-1 Application of MvNA to generate α-Neu5Ac *in situ*.

6.2.2 ^{1}H and ^{13}C NMR Spectroscopy for Kinetic Measurements

^{1}H NMR spectra for experiments performed in deuterium oxide were acquired on a Bruker AVANCE II 600 MHz spectrometer equipped with a 5 mm TCI cryoprobe. ^{13}C NMR spectra for experiments performed in water were acquired on a Bruker AVANCE II 600 MHz spectrometer equipped with a 5 mm QNP cryoprobe. Quantitative, proton-decoupled ^{13}C NMR spectra were acquired using an inverse-gated pulse sequence to eliminate NOE enhancements.[50] The spectral width was 240 ppm, transmitter frequency was set to 100 ppm. Proton decoupling was performed using the WALTZ-16 decoupling sequence[51] ^{1}H pulses of 100 μs, ^{1}H transmitter set to 4.00 ppm. ^{13}C T_1 values for C3 of α-Neu5Ac (135 ms) and β-Neu5Ac (142 ms) were in good agreement with reported literature values.[51] ^{13}C T_1 values were measured using a standard inversion recovery pulse sequence. A typical ^{1}H NMR experiment involves rapidly hydrolyzing compound **6.1a** (~1.0 mg in 600 μL of deuterated buffer) with a concentrated solution of MvNA. The H-3 axial signals corresponding to *α*-Neu5Ac (~1.66 ppm) and β-Neu5Ac (~1.85 ppm) were integrated and normalized throughout the time-course of the experiment. Similarly, ^{13}C NMR spectroscopy was used for experiments performed in water. Upon hydrolysis of compound **6.1b**, the C-3 signals of *α*-Neu5Ac (~40.8 ppm) and β-Neu5Ac (~39.5 ppm) were processed as described above. Typical NMR spectra are shown below for reactions run in deuterium oxide and water, repectively (Figure 6-2 and 6-3).

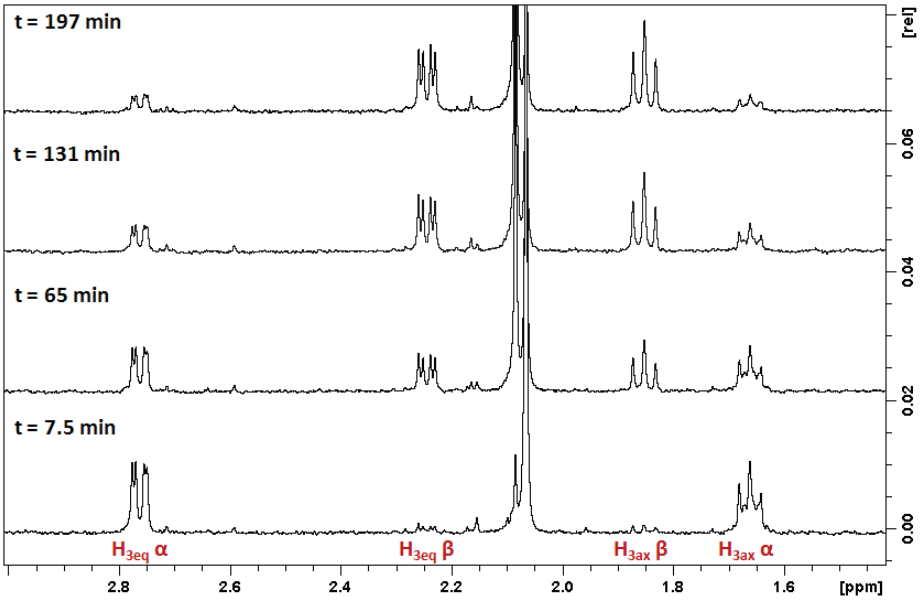

Figure 6-2 Representative ^{1}H NMR spectra acquired during Neu5Ac mutarotation, pD 4.45 (25 mM sodium formate, I = 0.5).

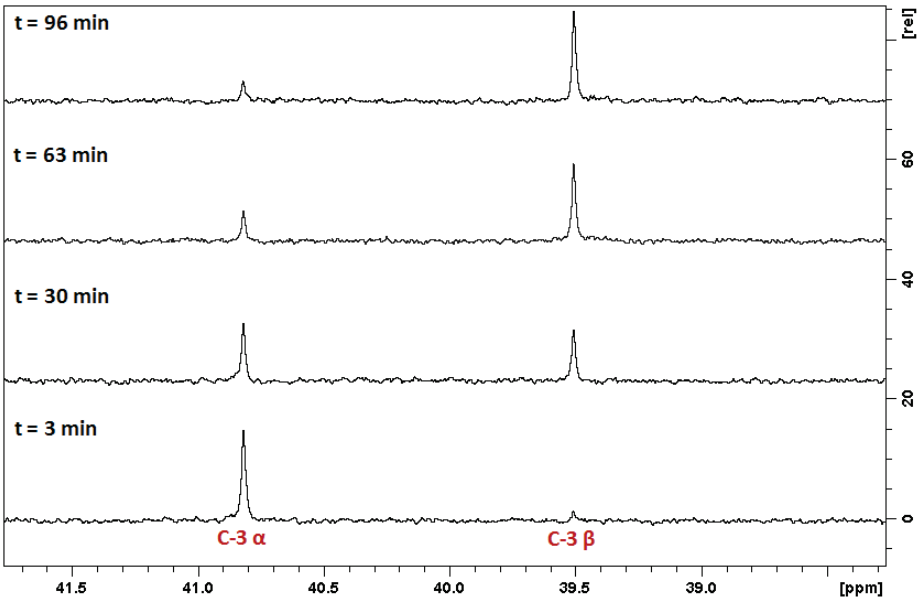

Figure 6-3 Typical ^{13}C NMR spectra acquired during Neu5Ac mutarotation, pH 4.45 (25 mM sodium formate, I = 0.5).

6.2.3 Buffers for pH- and pD-Rate Profiles

The effect of pH and pD on mutarotation, were determined by performing kinetic measurements over a range of 2.75–6.70 and 0.55–7.45, respectively. The water buffers (I = 0.5, potassium chloride) used were sodium dihydrogen phosphate-phosphoric acid (pH range 2.75–2.99), sodium formate-formic acid (pH range 3.30–4.50), sodium acetate-acetic acid (pH range 3.60–5.20) and 2-(*N*-morpholino)ethanesulfonic acid (MES-sodium hydroxide) (pH range 5.50–6.70). The deuterium oxide buffers (I = 0.5, potassium chloride) used were NaD_2PO_4-D_3PO_4 (pD range 2.10–3.00), HCO_2Na-HCO_2D (pD range 3.40–4.90), MES-sodium deuteroxide (pD range 5.85–6.75) and 3-(*N*-morpholino)propanesulfonic acid (MOPS- sodium deuteroxide) (pD range 7.10–7.45). For pD 0.55–1.85, kinetic measurements were performed using solutions of deuterochloric acid (I = 0.5, potassium chloride). The pD was measured using a standard pH electrode and applying the following conversion, pD = pH reading + 0.4.[132] The extent of buffer catalysis was probed by measuring the rate of mutarotation at various concentrations and extrapolating to zero buffer concentration.

6.2.4 Proton Inventory Experiment

A proton inventory plot was constructed by determining the rate of mutarotation at various mixtures of water and deuterium oxide. Buffers were prepared by adding equivalent amounts of hydrochloric acid or deuterochloric acid to 50 mM sodium acetate in water or deuterium oxide, respectively. The corresponding measured pH of the water buffer was 4.98 and the pD of the deuterium oxide buffer was 5.52. All runs were monitored using ^{13}C NMR spectroscopy.

6.3 Results and Discussion

The key intermediate for the interconversion of anomers is the open-chain ketone form (Figure 6-4). Previously, Serianni and co-workers tried using a ^{13}C saturation transfer technique[133] to determine the energy barriers associated with ring-closing of the ketone to either α-Neu5Ac (k_{-1}) or β-Neu5Ac (k_2). This method involves selective irradiation of the C2 signal of the ketone intermediate; the corresponding rate by which the C2 signals of α-Neu5Ac and β-Neu5Ac lose intensity can be correlated with the activation energy barriers for ring-closing.[6]

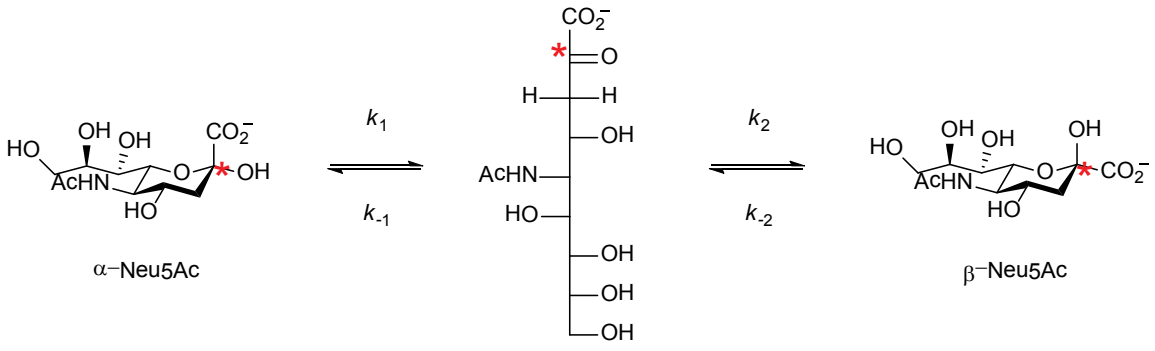

Figure 6-4 Mutarotation of Neu5Ac involves an open-chain ketone intermediate, the C2 position is indicated by a red asterix.

These authors noted that at pH 2.0 and 30 °C, selective irradiation did not affect the C2 signal intensities for either anomer, thus suggesting that the unidirectional rate constants were very small (<0.05 s^{-1}). In the current study, these same experiments were performed with [C2-^{13}C]-Neu5Ac[68] in order to conduct ^{13}C saturation transfer experiments at pH values of 4.5 and 6.0. Unfortunately, despite the greater sensitivity

afforded by a QNP-cyroprobe, no ketone C2 signal was observed under these conditions. As such, the observed rate constants for equilibration presented in this chapter can be summarized by eq. 6.1, where $k_\alpha = (k_1k_2)/(k_{-1}+k_2)$ and $k_\beta = (k_{-1}k_{-2})/(k_{-1}+k_2)$.

Eq. 6.1

$$k_{\text{obs}} = k_\alpha + k_\beta$$

Hydrolysis of sialosides has been shown to be governed by four kinetic processes,[24] and therefore it is expected that mutarotation will involve the following: i) an acid-catalyzed reaction of the neutral Neu5Ac species, $k_{L_3O^+}$ (L denotes either deuterium or protium); ii) the spontaneous reaction of neutral Neu5Ac or the kinetically equivalent acid-catalyzed reaction of the carboxylate anion, k_o; iii) the spontaneous, water-catalyzed, reaction of the anion, k_{L_2O} and; iv) a base-catalyzed reaction of the carboxylate, k_{OL^-}. An added complication is that mutarotation involves two separate ionization events that are associated with the pK_a values of the two anomers. Unfortunately, our experimental data was insufficiently robust to allow the individual pK_a values of α-Neu5Ac and β-Neu5Ac to be resolved. However, the pK_a values of α-Neu5Ac and β-Neu5Ac in water are identical within experimental error,[6] and thus only a single pK_a value was used in the kinetic expression (eq 6.2).

Eq. 6.2

$$\log(k_{\text{obs}}) = \log\left\{\frac{k_{L^+}[L^+]}{1+\frac{K_a}{[L^+]}} + \frac{k_o}{1+\frac{K_a}{[L^+]}} + \frac{k_{L_2O}}{1+\frac{[L^+]}{K_a}} + \frac{k_{OL^-}K_w}{[L^+]\left(1+\frac{[L^+]}{K_a}\right)}\right\}$$

pD [a]	k_{obs} (s^{-1})	$t_{1/2}$ (min)
0.55	$(1.36 \pm 0.11) \times 10^{-3}$	8.5
0.95	$(8.24 \pm 0.91) \times 10^{-4}$	14.0
1.25	$(7.89 \pm 0.98) \times 10^{-4}$	14.5
1.55	$(9.39 \pm 0.68) \times 10^{-4}$	12.3
1.85	$(6.74 \pm 0.27) \times 10^{-4}$	17.1
2.10	$(8.87 \pm 0.17) \times 10^{-4}$	13.0
2.35	$(7.73 \pm 0.60) \times 10^{-4}$	15.0
2.60	$(5.37 \pm 0.30) \times 10^{-4}$	21.5
3.00	$(6.31 \pm 0.05) \times 10^{-4}$	18.3
3.40	$(2.82 \pm 0.60) \times 10^{-4}$	41.0
3.90	$(1.17 \pm 0.79) \times 10^{-4}$	98.8
4.45	$(1.05 \pm 0.57) \times 10^{-4}$	109.9
4.90	$(9.91 \pm 1.44) \times 10^{-5}$	116.5
5.85	$(1.08 \pm 0.16) \times 10^{-4}$	98.7
6.30	$(1.45 \pm 0.01) \times 10^{-4}$	69.9
6.75	$(2.40 \pm 0.17) \times 10^{-4}$	45.5
7.10	$(4.45 \pm 0.13) \times 10^{-4}$	24.5
7.45	$(1.38 \pm 0.14) \times 10^{-3}$	11.3

[a] For pD 0.55–1.85, reported k_{obs} represents an average of 3 runs.

Table 15 Observed Rate Constants for Neu5Ac Mutarotation in Deuterium Oxide at 25 °C. Rate constants were obtained by extrapolating to zero buffer concentration.

pH	k_{obs} (s^{-1})	$t_{1/2}$ (min)
2.75	$(1.34 \pm 0.87) \times 10^{-3}$	8.6
2.99	$(1.25 \pm 0.19) \times 10^{-3}$	9.3
3.30	$(6.86 \pm 0.16) \times 10^{-4}$	16.9
3.60	$(5.40 \pm 0.34) \times 10^{-4}$	21.4
3.80	$(5.41 \pm 0.09) \times 10^{-4}$	21.4
4.00	$(4.35 \pm 0.18) \times 10^{-4}$	26.6
4.15	$(3.94 \pm 0.11) \times 10^{-4}$	29.3
4.40	$(3.85 \pm 0.73) \times 10^{-4}$	30.0
4.50	$(4.27 \pm 0.15) \times 10^{-4}$	27.1
4.80	$(4.04 \pm 0.03) \times 10^{-4}$	28.6
5.20	$(3.58 \pm 0.22) \times 10^{-4}$	32.3
5.50	$(3.62 \pm 0.31) \times 10^{-4}$	32.0
5.90	$(6.17 \pm 0.44) \times 10^{-4}$	18.7
6.30	$(6.69 \pm 0.46) \times 10^{-4}$	17.3
6.70	$(1.67 \pm 0.34) \times 10^{-3}$	6.9

Table 16 Observed Rate Constants for Neu5Ac Mutarotation in Water at 25 °C. Rate constants were obtained by extrapolating to zero buffer concentration.

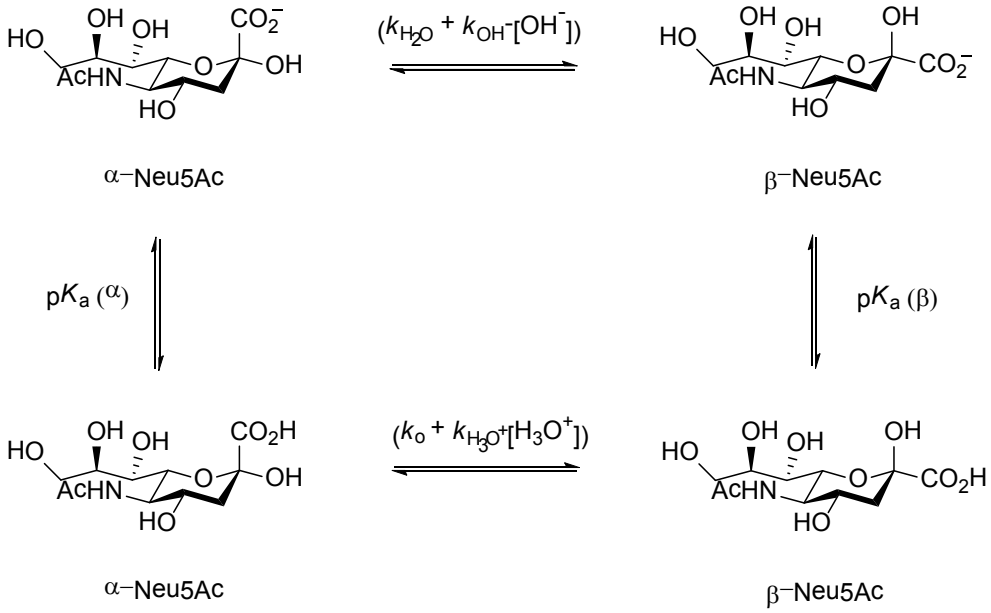

Figure 6-5 Reaction pathways used to fit kinetic data.

Presented in Figure 6-6 are the logarithms of the pseudo-first-order rate constants for Neu5Ac mutarotation as a function of pH and pD at 25 °C. The dotted lines represent the least-squares best fit to Eq. 2 where L denotes either deuterium or protium. The deuterium oxide autoprotolysis constant, $K_{w(D2O)}$, at 25 °C is 1.352×10^{-15}.[134] However, in order to fit the kinetic data in water, it was necessary to constrain the pK_a value to 2.55[6] since reliable data could not be obtained for solutions more acidic than those at a pH value of 2.75. Consequently, the rate constant for the acid-catalyzed reaction of the neutral molecule, k_{H3O+}, could not be determined.

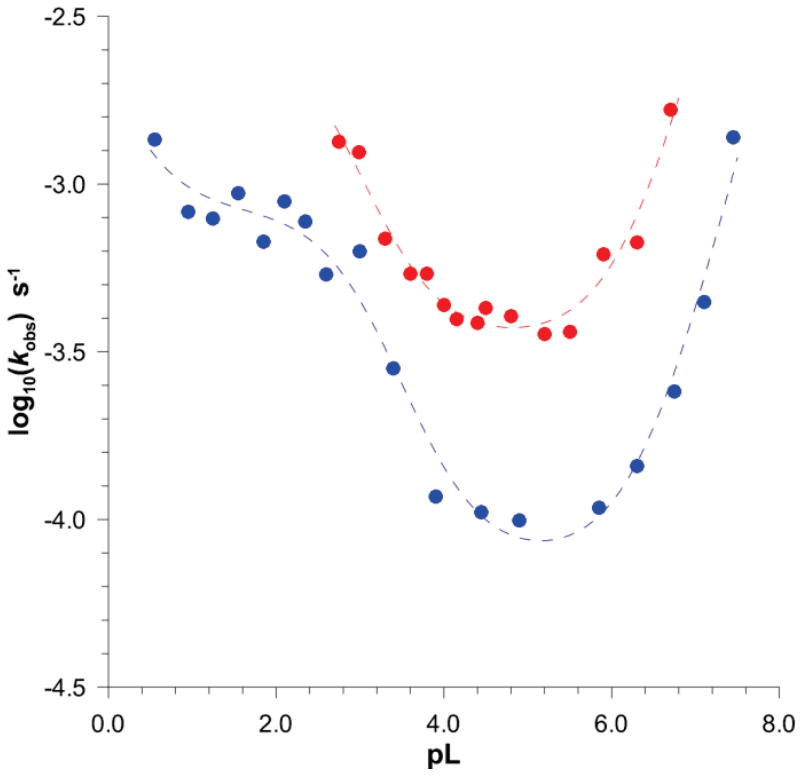

Figure 6-6 Plot of log(k_{obs}) values versus pH (red circles) and pD (blue symbols) for Neu5Ac mutarotation at 25 °C. The lines shown are the best non-linear least-squares fits to eq 6.2.

6.3.1 Derived Kinetic Parameters

The pK_a value for Neu5Ac in deuterium oxide derived from Eq.6.2 is 2.98 ± 0.15. The larger pK_a in deuterium oxide is consistent with the expected decrease in acidity of a carboxylic acid in deuterium oxide.[135] Moreover, it is evident from Figure 6-6 that Neu5Ac mutarotation is, as expected,[24] governed by four kinetic processes. All of the derived rate constants are listed in Table 17.

Kinetic parameter	*H_2O*	*D_2O*	*KIE*
pK_a	2.55	2.98 ± 0.15	-
k_{L3O+}	N.D.	$(1.36 \pm 0.92) \times 10^{-3}$ $M^{-1}s^{-1}$	N.D.
k_o	$(3.13 \pm 0.53) \times 10^{-3}$ s^{-1}	$(8.37 \pm 0.53) \times 10^{-4}$ s^{-1}	3.74 ± 0.68
k_{L2O}	$(3.42 \pm 0.21) \times 10^{-4}$ s^{-1}	$(7.63 \pm 1.17) \times 10^{-5}$ s^{-1}	4.48 ± 0.74
k_{OL}-	$(2.32 \pm 0.30) \times 10^{4}$ $M^{-1}s^{-1}$	$(2.63 \pm 0.36) \times 10^{4}$ $M^{-1}s^{-1}$	0.88 ±0.17
N.D. = not determinable			

Table 17 Summary of Derived Kinetic Parameters for Neu5Ac Mutarotation

When comparing the second-order rate constants for acid- and base-catalyzed Neu5Ac mutarotation in deuterium oxide, it is apparent that the base process is more efficient by a factor of almost 2×10^7. The corresponding rate constants for acid and base-catalyzed glucose mutarotation are 9.90×10^{-3} M^{-1} s^{-1} and 374 M^{-1} s^{-1}, respectively.[136] This suggests that acid-catalysis is moderately more efficient for glucose, whereas base is a more efficient catalyst for Neu5Ac mutarotation. With regard to buffer catalysis, in all cases, the base form is more efficient than the acid form. In addition, the extent of catalysis was unexpectedly small. For instance, at pH 4.15, increasing the buffer concentration from 25 mM to 100 mM sodium formate only increases the rate by

3.5%. Given that it is not known whether TS 1 α-Neu5Ac to ketone (k_1, Figure 6-4), TS 2 ketone to β-Neu5Ac (k_2, Figure 6-4) or both govern the rate of mutarotation, the current kinetic data allows only a general structural analysis of the TS.

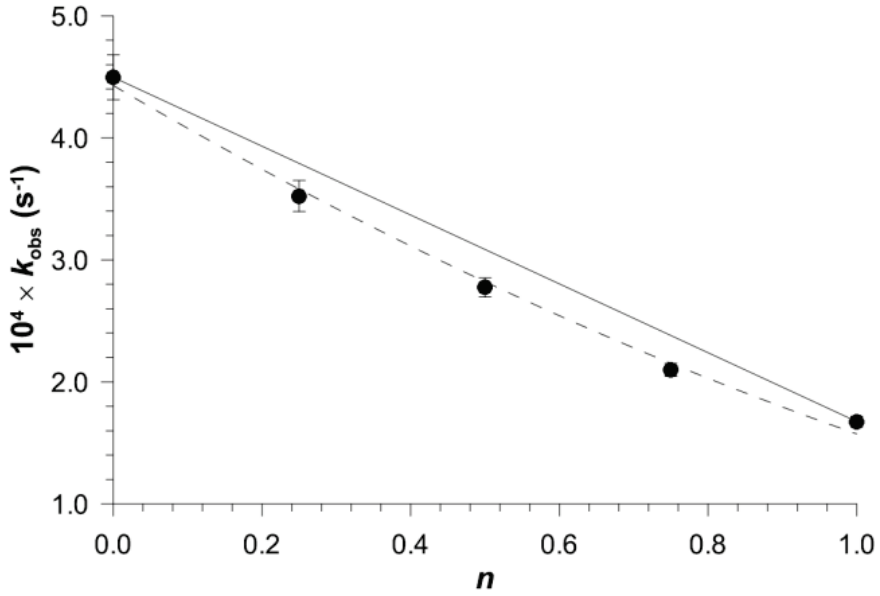

Figure 6-7 Plot of k_{obs} versus the fraction of deuterium, n, in water–deuterium oxide solvent mixtures. The solid line is the linear fit between $n = 0$ and 1 and the dashed line is the best fit for a two proton model.

Presented in Figure 6-7 is the plot of the results from the proton inventory experiment where the fraction of deuterium in the H_2O–D_2O mixtures, n, was systematically varied, in a similar manner to that reported for glucose mutarotation by Lewis *et al*.[128] In both cases a downward curvature results that are consistent with more than a single proton model, a situation that would give a straight line fit. With regard to glucose ring-opening, calculated TSs, which were based on the results from proton-inventory and computational studies, involved a water molecule acting as a general base

en route to an open-chain aldehyde via deprotonation of the anomeric hydroxyl group.[128] Of note, the measured solvent deuterium KIE requires that proton abstraction is nearly complete, that is the TSs are late. The kinetic isotope effect (KIE) for "water-catalyzed" Neu5Ac mutarotation is 4.48 ± 0.74 (cf. k_{H2O}/k_{D2O} = 3.89 for glucose)[21] which provides evidence for a similar transition state where the ketal proton being transferred to the catalytic water is almost complete at the TS. The curvature in the proton inventory results from secondary KIEs from the non-transferring protons.[21]

The KIE for process (ii) is 3.74 ± 0.68, a value which is comparable in magnitude to the water-catalyzed reaction of the carboxylate, and this observation points to the likelihood of a very similar TS for this pathway. Since acid catalysis has been shown to be poor it is likely that this process represents the spontaneous reaction of neutral Neu5Ac rather than acid-catalyzed reaction of the carboxylate anion. Of note, the rate of mutarotation is approximately 10 times faster with the carboxylic acid form than with the carboxylate species, an observation that is consistent with water-catalyzed mutarotation not involving participation of the carboxylate group. Thus, it can be concluded that deprotonation of the anomeric hydroxyl group, which places a partial negative charge adjacent to a negatively charged carboxylate introduces an unfavorable interaction that does not occur during mutarotation of the carboxylic acid species.

With regard to the base-catalyzed reaction, the solvent deuterium KIE is 0.88 ± 0.17. This effect can be dissected in terms of fractionation factor analysis (φ).[122] According to eq. 6.3, the equilibrium isotope effect (EIE) K_D/K_H is equal to the multiple of all product fractionation factors divided by those of the reactant.[122]

Eq 6.3

$$\frac{K_D}{K_H} = \frac{\Pi\phi^{Product}}{\Pi\phi^{Reactant}}$$

Illustrated in Figure 6-8 are the reactant and product states expected for hemi-ketal deprotonation. Displayed in blue are three hydrogenic sites, φ = 0.70, that are hydrogen bonding to a hydroxide ion (φ = 1.25, green),[137] and highlighted in red is the anomeric hydroxyl proton, φ = 1.00. For a fully transferred proton, the resultant anion forms three hydrogen bonds. If this anion is fully solvated, the fractionation factors for each site are expected to be similar to those for *tert*-butoxide (φ = 0.76).[138]

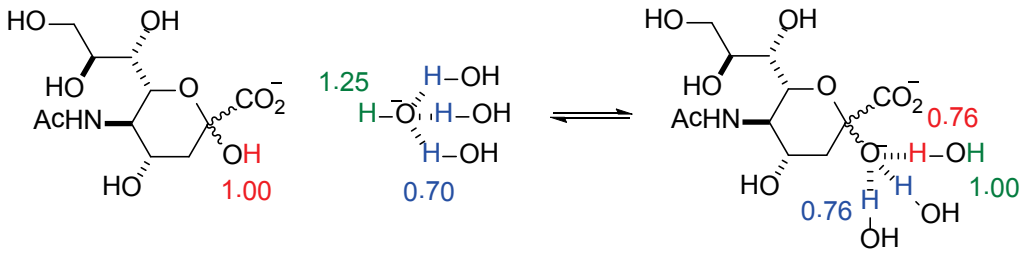

Figure 6-8 Proposed equilibrium formation and fractionation factors for the specific-base promoted formation of the hemi-ketal anion, (coloured H have indicated fractionation factors; all other H are unity).

Thus, the calculated EIE for this deprotonation event is 0.98 (K_D/K_H = $(0.76)^3$/ $(0.70)^3 \times 1.25$). Therefore, the measured solvent deuterium KIE is consistent with a TS for base-catalyzed mutarotation that entails reversible formation of the hemi-ketal anion (specific-base catalysis) followed by a TS that involves ring-opening. However, based on the current kinetic data it is impossible to conclude whether this is an early or late TS.

6.3.2 Implications for Neu5Ac Mutarotase

With regard to the recently discovered β-propeller protein YjhT that displays Neu5Ac mutarotase activity, mutagenesis studies showed that two active site residues, E209A and R215A, displayed a marked decrease in mutarotase activity.[130] Given the conclusion noted above, it is likely that the arginine residue accelerates mutarotation by forming a salt-bridge with the carboxylate group and thus reducing its effective charge (cf. k_o and k_{H2O}, Table 17). In addition, it can be predicted that the glutamate residue facilitates mutarotation by acting as a general-base catalyst by facilitating deprotonation of the anomeric hydroxyl group.

6.4 Conclusions

The work presented in this chapter provides important insight as to how nature evolved a protein that possesses Neu5Ac mutarotase activity. In addition, the data presented can aid in the design of ^{1}H NMR experiments to probe the overall mechanism, whether retaining or inverting, of sialidases. Since the rate of hydrolysis must be greater than the rate of mutarotation, specific conditions can be selected where the activity of the sialidase is maximal while the rate of mutarotation is retarded.

REFERENCE LIST

(1) Blix, G. *Z. Physiol. Chem.* **1936**, *240*, 43-54.

(2) Klenk, E. *Z. Physiol. Chem.* **1941**, *268*, 50-58.

(3) Gottschalk, A.; Whitten, W. K.; Graham, E. R. B. *Biochim. Biophys. Acta.* **1960**, *38*, 183-184.

(4) Blix, F. G.; Gottschalk, A.; Klenk, E. *Nature* **1957**, *179*, 1088.

(5) Angata, T.; Varki, A. *Chem. Rev.* **2002**, *102*, 439-469.

(6) Klepach, T.; Carmichael, I.; Serianni, A. S. *J. Am. Chem. Soc.* **2008**, *130*, 11892-11900.

(7) *Biochemistry and function of sialidases, in Biology of the Sialic Acids*; Saito, M.; Yu, R. K., Eds.; Plenum Press: New York, 1995.

(8) Freiberger, F.; Claus, H.; Gunzel, A.; Oltmann-Norden, I.; Vionnet, J.; Muhlenhoff, M.; Vogel, U.; Vann, W. F.; Gerardy-Schahn, R.; Stummeyer, K. *Mol. Microbiol.* **2007**, *65*, 1258-1275.

(9) Willis, L. M.; Gilbert, M.; Karwaski, M. F.; Blanchard, M. C.; Wakarchuk, W. W. *Glycobiology* **2008**, *18*, 177-186.

(10) Vogel, J.; Bendas, G.; Bakowsky, U.; Hummel, G.; Schmidt, R. R.; Kettmann, U.; Rothe, U. *Biochim. Biophys. Acta.* **1998**, *1372*, 205-215.

(11) Wiley, D. C.; Skehel, J. J. *Annu. Rev. Biochem.* **1987**, *56*, 365-394.

(12) Varki, A. *Trends Mol. Med.* **2008**, *14*, 351-360.

(13) Schwarzer, D.; Stummeyer, K.; Haselhorst, T.; Freiberger, F.; Rode, B.; Grove, M.; Scheper, T.; von Itzstein, M.; Muehlenhoff, M.; Gerardy-Schahn, R. *J. Biol. Chem.* **2009**, *284*, 9465-9474.

(14) Stummeyer, K.; Dickmanns, A.; Muhlenhoff, M.; Gerardy-Schahn, R.; Ficner, R. *Nat. Struct. Mol. Biol.* **2005**, *12*, 90-96.

(15) Miyagi, T. *Trends Glycosci. Glyc.* **2010**, *22*, 162-172.

(16) Corfield, T. *Glycobiology* **1992**, *2*, 509-521.

(17) Warwas, M. L.; Yeung, J. H. F.; Indurugalla, D.; Mooers, A. O.; Bennet, A. J.; Moore, M. M. *Glycoconjugate J.* **2010**, *27*, 533-548.

(18) Telford, J. C.; Yeung, J. H.; Xu, G.; Kiefel, M. J.; Watts, A. G.; Hader, S.; Chan, J.; Bennet, A. J.; Moore, M. M.; Taylor, G. L. *J. Biol. Chem.* **2011**, *286*, 10783-10792.

(19) Kiefel, M. J.; Von Itzstein, M. *Prog. Med. Chem.* **1999**, *36*, 1-28.

(20) Vimr, E. R. *Trends Microbiol.* **1994**, *2*, 271-277.

(21) Henrissat, B.; Bairoch, A. *Biochem. J.* **1996**, *316*, 695-696.

(22) Lentz, M. R.; Webster, R. G.; Air, G. M. *Biochemistry* **1987**, *26*, 5351-5358.

(23) Colman, P. M.; Varghese, J. N.; Laver, W. G. *Nature* **1983**, *303*, 41-44.

(24) Ashwell, M.; Guo, X.; Sinnott, M. L. *J. Am. Chem. Soc.* **1992**, *114*, 10158-10166.

(25) Varghese, J. N.; Colman, P. M. *J. Mol. Biol.* **1991**, *221*, 473-486.

(26) Chong, A. K. J.; Pegg, M. S.; Taylor, N. R.; Vonitzstein, M. *Eur. J. Biochem.* **1992**, *207*, 335-343.

(27) Barnes, J. A.; Williams, I. H. *Biochem. Soc. Trans.* **1996**, *24*, 263-268.

(28) Thomas, A.; Jourand, D.; Bret, C.; Amara, P.; Field, M. J. *J. Am. Chem. Soc.* **1999**, *121*, 9693-9702.

(29) Mader, M. M.; Bartlett, P. A. *Chem. Rev.* **1997**, *97*, 1281-1301.

(30) Withers, S. G.; Rupitz, K.; Street, I. P. *J. Biol. Chem.* **1988**, *263*, 7929-32.

(31) Watts, A. G.; Damager, I.; Amaya, M. L.; Buschiazzo, A.; Alzari, P.; Frasch, A. C.; Withers, S. G. *J. Am. Chem. Soc.* **2003**, *125*, 7532-7533.

(32) Parodi, A. J.; Pollevick, G. D.; Mautner, M.; Buschiazzo, A.; Sanchez, D. O.; Frasch, A. C. C. *EMBO J.* **1992**, *11*, 1705-1710.

(33) Watson, J. N.; Dookhun, V.; Borgford, T. J.; Bennet, A. J. *Biochemistry* **2003**, *42*, 12682-12690.

(34) Newstead, S.; Watson, J. N.; Knoll, T. L.; Bennet, A. J.; Taylor, G. *Biochemistry* **2005**, *44*, 9117-9122.

(35) Guo, X. M.; Laver, W. G.; Vimr, E.; Sinnott, M. L. *J. Am. Chem. Soc.* **1994**, *116*, 5572-5578.

(36) Fersht, A. *Enzyme structure and mechanism*; 2nd ed.; W.H. Freeman: New York, 1985.

(37) Albery, W. J.; Knowles, J. R. *Biochemistry* **1976**, *15*, 5631-5640.

(38) Kohen, A.; Limbach, H.-H. *Isotope effects in chemistry and biology*; Taylor & Francis: Boca Raton, 2006.

(39) Melander, L. C. S.; Saunders, W. H. J. *Reaction rates of isotopic molecules*; Wiley: New York, 1980.

(40) Schramm, V. L. *Annu. Rev. Biochem.* **1998**, *67*, 693-720.

(41) Berti, P. J.; Blanke, S. R.; Schramm, V. L. *J. Am. Chem. Soc.* **1997**, *119*, 12079-12088.

(42) Singleton, D. A.; Thomas, A. A. *J. Am. Chem. Soc.* **1995**, *117*, 9357-9358.

(43) Lee, J. K.; Bain, A. D.; Berti, P. J. *J. Am. Chem. Soc.* **2004**, *126*, 3769-3776.

(44) Schimerlik, M. I.; Rife, J. E.; Cleland, W. W. *Biochemistry* **1975**, *14*, 5347-5354.

(45) Guo, X. M.; Sinnott, M. L. *Biochem. J.* **1993**, *294*, 653-656.

(46) Yan, F. Y.; Wakarchuk, W. W.; Gilbert, M.; Richards, J. C.; Whitfield, D. M. *Carbohydr. Res.* **2000**, *328*, 3-16.

(47) Indurugalla, D.; Bennet, A. J. *Can. J. Chem.* **2008**, *86*, 1005-1009.

(48) Brauman, J. I. *Anal. Chem.* **1966**, ***38***, 607-610.

(49) Findeisen, M.; Brand, T.; Berger, S. *Magn. Reson. Chem.* **2007**, *45*, 175-178.

(50) *200 and more NMR experiments : a practical course*; Berger, S.; Braun, S., Eds.; Wiley-VCH, Weinheim, 2004.

(51) Shaka, A. J.; Keeler, J.; Frenkiel, T.; Freeman, R. *J. Magn. Reson.* **1983**, *52*, 335-338.

(52) Wolfram, S. *The mathematica book*; Cambridge University Press: Cambridge, UK, 2003.

(53) Wilson, J. C.; Angus, D. I.; von Itzstein, M. *J. Am. Chem. Soc.* **1995**, *117*, 4214-4217.

(54) Davies, G.; Sinnott, M. L.; Withers, S. G. *Glycosyl transfer in Comprehensive Biological Catalysis*; Academic: San Diego, 1998.

(55) Friebolin, H.; Supp, M.; Brossmer, R.; Keilich, G.; Ziegler, D. *Angew. Chem.* **1980**, *92*, 200-1.

(56) Koshland Jr., D. E. *Biol. Rev.* **1953**, *28*, 416-436.

(57) Watts, A. G.; Oppezzo, P.; Withers, S. G.; Alzari, P. M.; Buschiazzo, A. *J. Biol. Chem* **2006**, *281*, 4149-4155.

(58) Faruque, S. M.; G., B. N. *Vibrio Cholerae; Genomics and Molecular Biology*; Caister Academic Press, Norwich, Norfolk, UK, 2008.

(59) Hughes, E. *Hist. Med.* **1975**, *6*, 68-74.

(60) Butler, D. *Nature* **2010**, *468*, 483-484.

(61) Enserink, M. *Science* **2010**, *330*, 738-739.

(62) Fishman, P. H. J. *Membr. Biol.* **1982**, *69*, 85-97.

(63) Crennell, S.; Garman, E.; Laver, G.; Vimr, E.; Taylor, G. *Structure* **1994**, *2*, 535-544.

(64) Holmgren, J.; Lonnroth, I.; Mansson, J. E.; Svennerholm, L. *Proc. Natl. Acad. Sci. U.S.A.* **1975**, *72*, 2520-2524.

(65) Galen, J. E.; Ketley, J. M.; Fasano, A.; Richardson, S. H.; Wasserman, S. S.; Kaper, J. B. *Infect. Immun.* **1992**, *60*, 406-415.

(66) Connaris, H.; Crocker, P. R.; Taylor, G. L. *J. Biol. Chem.* **2009**, *284*, 7339-7351.

(67) Moustafa, I.; Connaris, H.; Taylor, M.; Zaitsev, V.; Wilson, J. C.; Kiefel, M. J.;

von Itzstein, M.; Taylor, G. *J. Biol. Chem.* **2004**, *279*, 40819-40826.

(68) Chan, J.; Lewis, A. R.; Gilbert, M.; Karwaski, M.-F.; Bennet, A. J. *Nat. Chem. Biol.* **2010**, *6*, 405-407.

(69) Kim, M. J.; Hennen, W. J.; Sweers, H. M.; Wong, C. H. *J. Am. Chem. Soc.* **1988**, *110*, 6481-6486.

(70) Chokhawala, H. A.; Yu, H.; Chen, X. *ChemBioChem* **2007**, *8*, 194-201.

(71) Sunko, D. E.; Szele, I.; Hehre, W. J. *J. Am. Chem. Soc.* **1977**, *99*, 5000-5005.

(72) Defrees, D. J.; Taagepera, M.; Levi, B. A.; Pollack, S. K.; Summerhays, K. D.; Taft, R. W.; Wolfsberg, M.; Hehre, W. J. *J. Am. Chem. Soc.* **1979**, *101*, 5532-5536.

(73) Chan, J.; Lu, A.; Bennet, A. J. *J. Am. Chem. Soc.* **2011**, *133*, 2989-2997.

(74) Yang, J.; Schenkman, S.; Horenstein, B. A. *Biochemistry* **2000**, *39*, 5902-5910.

(75) Vocadlo, D. J.; Davies, G. J. *Curr. Opin. Chem. Biol.* **2008**, *12*, 539-555.

(76) Bennet, A. J.; Sinnott, M. L. *J. Am. Chem. Soc.* **1986**, *108*, 7287-7294.

(77) Indurugalla, D.; Bennet, A. J. *J. Am. Chem. Soc.* **2001**, *123*, 10889-10898.

(78) Werner, R. M.; Stivers, J. T. *Biochemistry* **2000**, *39*, 14054-14064.

(79) Luo, M.; Schramm, V. L. *Journal of the American Chemical Society* **2008**, *130*, 2649-2655.

(80) Zhang, Y.; Bommuswamy, J.; Sinnott, M. L. *J. Am. Chem. Soc.* **1994**, *116*, 7557-7563.

(81) Mascal, M.; Hafezi, N.; Toney, M. D. *J. Am. Chem. Soc.* **2010**, *132*, 10662-10664.

(82) Kroppenstedt, R. M.; Mayilraj, S.; Wink, J. M.; Kallow, W.; Schumann, P.; Secondini, C.; Stackebrandt, E. *Syst. Appl. Microbiol.* **2005**, *28*, 328-339.

(83) Aisaka, K.; Uwajima, T. *FEMS Microbiol. Lett.* **1987**, *44*, 289-291.

(84) Narine, A. A.; Watson, J. N.; Bennet, A. J. *Biochemistry* **2006**, *45*, 9319-9326.

(85) Watson, J. N.; Newstead, S.; Dookhun, V.; Taylor, G.; Bennet, A. J. *FEBS Lett.* **2004**, *577*, 265-269.

(86) Watson, J. N.; Newstead, S.; Narine, A. A.; Taylor, G.; Bennet, A. J. *ChemBioChem* **2005**, *6*, 1999-2004.

(87) Indurugalla, D.; Watson, J. N.; Bennet, A. J. *Org. Biomol. Chem.* **2006**, *4*, 4453-4459.

(88) Paulsen, H.; Tietz, H. *Carbohydr. Res.* **1985**, *144*, 205-229.

(89) Ogura, H.; Furuhata, K.; Ito, M.; Shitori, Y. *Carbohydr. Res.* **1986**, *158*, 37-51.

(90) Imamura, A.; Ando, H.; Ishida, H.; Kiso, M. *J. Org. Chem.* **2009**, *74*, 3009-3023.

(91) Cook, P. F.; Cleland, W. W. *Enzyme kinetics and mechanism*; Garland Science:

London: New York, 2007.

(92) Taylor, J. R. *An introduction to error analysis: The study of uncertainties in physical measurements*; University Science Books: Mill Valley, Calif., 1982.

(93) Sinnott, M. L.; Guo, X.; Li, S. C.; Li, Y. T. *J. Am. Chem. Soc.* **1993**, *115*, 3334-3345.

(94) Huang, X. C.; Tanaka, K. S. E.; Bennet, A. J. *J. Am. Chem. Soc.* **1997**, *119*, 11147-11154.

(95) Xue, H.; Wu, X.; Huskey, W. P. *J. Am. Chem. Soc.* **1996**, *118*, 5804-5805.

(96) Zhou, X.; Toney, M. D. *J. Am. Chem. Soc.* **1998**, *120*, 13282-13283.

(97) Alon, R.; Bayer, E. A.; Wilchek, M. *J. Biochem. Bioph. Methods* **1991**, *22*, 23-33.

(98) Ziegler, D. W.; Hutchinson, H. D. *Appl. Microbiol.* **1972**, *23*, 1060-1066.

(99) Segel, I. H. *Enzyme kinetics: Behavior and analysis of rapid equilibrium and steady state enzyme systems*; Wiley: New York, 1975.

(100) Schwartz, P. A.; Vetticatt, M. J.; Schramm, V. L. *J. Am. Chem. Soc.* **2010**, *132*, 13425-13433.

(101) Tanaka, Y.; Tao, W.; Blanchard, J. S.; Hehre, E. J. *J. Biol. Chem.* **1994**, *269*, 32306-32312.

(102) Gillard, B. K.; Kurz, J. L. *J. Am. Chem. Soc.* **1972**, *94*, 7199-7201.

(103) Buncel, E.; Lee, C. C. *Secondary and solvent isotope effects*; Elsevier: Amsterdam: New York, 1987.

(104) Palese, P.; Tobita, K.; Ueda, M.; Compans, R. W. *Virology* **1974**, *61*, 397-410.

(105) von Itzstein, M.; Wu, W. Y.; Kok, G. B.; Pegg, M. S.; Dyason, J. C.; Jin, B.; V., P. T.; Smythe, M. L.; White, H. F. *Nature* **1993**, *363*, 418-23.

(106) Billich, A. *Curr. Opin. Invest. Drugs.* **1999**, *1*, 592-601.

(107) Lentz, M. R.; Webster, R. G.; Air, G. M. *Biochemistry* **1987**, *26*, 5351-5358.

(108) Chong, A. K. J.; Pegg, M. S.; Taylor, N. R.; von Itzstein, M. *Eur. J. Biochem.* **1992**, *207*, 335-343.

(109) Ghate, A. A.; Air, G. M. *Eur. J. Biochem.* **1998**, *58*, 320-331.

(110) Watson, J. N.; Newstead, S.; Narine, A.; Taylor, G.; Bennet, A. J. *ChemBioChem* **2005**, *6*, 1999-2004.

(111) Guo, X.; Laver, W. G.; Vimr, E.; Sinnott, M. L. *J. Am. Chem. Soc.* **1994**, *116*, 5572-5578.

(112) Varghese, J. N.; McKimm-Breschkin, J. L.; Caldwell, J. B.; Kortt, A. A.; Colman, P. M. *Proteins: Struct., Funct., Genet.* **1992**, *14*, 327-332.

(113) Amaya, M. F.; Watts, A. G.; Damager, T.; Wehenkel, A.; Nguyen, T.; Buschiazzo, A.; Paris, G.; Frasch, A. C.; Withers, S. G.; Alzari, P. M. *Structure* **2004**, *12*, 775-784.

(114) Varghese, J. N.; Colman, P. M. *J. Mol. Biol.* **1991**, *221*, 473-486.

(115) Chou, D. T. H.; Watson, J. N.; Scholte, A. A.; Borgford, T. J.; Bennet, A. J. *J. Am. Chem. Soc.* **2000**, *122*, 8357-8364.

(116) O'Reilly, D. R.; Miller, L.; Luckow, V. A. *Baculovirus expression vectors : a laboratory manual*; Oxford University Press: New York, 1994.

(117) Ausubel, F. M. *Current protocols in molecular biology*; Greene Publishing Associates; J. Wiley: Brooklyn, N. Y., 1987.

(118) Segel, I. H. *Enzyme kinetics: Behavior and analysis of rapid equilibrium and steady state enzyme systems*; Wiley: New York, 1975.

(119) Watson, J. N.; Dookhun, V.; Borgford, T. J.; Bennet, A. J. *Biochemistry* **2003**, *42*, 12682-12690.

(120) Narine, A. A.; Watson, J. N.; Bennet, A. J. *Biochemistry* **2006**, *45*, 9319-9326.

(121) Shidmoossavee, F. S.; Cheng, L.; Watson, J. N.; Bennet, A. J. *Biochemistry* **2010**, *49*, 6473-6484.

(122) Alvarez, F. J.; Schowen, R. L. In *Secondary and solvent isotope effects: Isotopes in organic chemistry*; Elsevier: Amsterdam ; New York, 1987; Vol. 7, p 1-60.

(123) Dube, D. H.; Bertozzi, C. R. *Nat. Rev. Drug Discovery* **2005**, *4*, 477-488.

(124) Alley, W. R., Jr.; Novotny, M. V. *J. Proteome Res.* **2010**, *9*, 3062-3072.

(125) Dubrunfaut, A. P. *Compt. Rend.* **1846**, *23*, 38.

(126) Lowry, T. M. *J. Chem. Soc. Trans.* **1899**, *75*, 211-244.

(127) Isbell, H. S.; Pigman, W. *Adv. Carbohydr. Chem. Biochem.* **1969**, *24*, 13-65.

(128) Lewis, B. E.; Choytun, N.; Schramm, V. L.; Bennet, A. J. *J. Am. Chem. Soc.* **2006**, *128*, 5049-5058.

(129) Friebolin, H.; Kunzelmann, P.; Supp, M.; Brossmer, R.; Keilich, G.; Ziegler, D. *Tetrahedron Lett.* **1981**, *22*, 1383-1386.

(130) Severi, E.; Mueller, A.; Potts, J. R.; Leech, A.; Williamson, D.; Wilson, K. S.; Thomas, G. H. *J. Biol. Chem.* **2008**, *283*, 4841-4849.

(131) Venkatasubban, K. S.; Schowen, R. L. *Crit. Rev. Biochem.* **1984**, *17*, 1-44.

(132) Glasoe, P. K.; Long, F. A. *J. Phys. Chem.* **1960**, *64*, 188-90.

(133) Serianni, A. S.; Pierce, J.; Huang, S. G.; Barker, R. *J. Am. Chem. Soc.* **1982**, *104*, 4037-44.

(134) Covington, A. K.; Robinson, R. A.; Bates, R. G. *J. Phys. Chem.* **1966**, *70*, 3820-4.

(135) Carey, F. A.; Sundberg, R. J. *Advanced Organic Chemistry, Part A: Structure and Mechanisms*; 5th ed., 2007.

(136) Hudson, C. S. *J. Am. Chem. Soc.* **1908**, *29*, 1571-1576.

(137) Schowen, K. B.; Schowen, R. L. *Methods Enzymol.* **1982**, *87*, 551-606.

(138) Gold, V.; Morris, K. P.; Wilcox, C. F. *J. Chem. Soc., Perkin Trans. 2* **1982**, 1615-1620.